Universität Hamburg
DER FORSCHUNG | DER LEHRE | DER BILDUNG

Phytoplankton in the Elbe estuary:

New insights into community composition and mixotrophy,

from metabarcoding, flow cytometry, and laboratory experiments

Dissertation

zur Erlangung des Doktorgrades Dr. rer. nat. an der

Fakultät für Mathematik, Informatik und Naturwissenschaften im

Fachbereich Biologie der Universität Hamburg

vorgelegt von

Nele Martens

aus Hamburg.

Hamburg

2024

Tag der Disputation:

12.07.2024

Erstgutachterin: Prof. Dr. C.-Elisa Schaum

Zweitgutachter: Prof. Dr. Hans-Peter Grossart

Vorsitz der Prüfungskommission: Prof. Dr. Inga Hense

Weiteres Mitglied der Prüfungskommission: Prof. Dr. Ina Meier

PhD candidate and reviewers

PhD candidate: Nele Martens

First supervisor: Prof. Dr. C.-Elisa Schaum

Second supervisor: Prof. Dr. Hans-Peter Grossart

Panel chair: Prof. Dr. Inga Hense

Publications

Section 2 is a modified version of a manuscript published as: Martens, N., Russnak, V., Woodhouse, J., Grossart, H.-P., Schaum, C.-E., 2024. Metabarcoding reveals potentially mixotrophic flagellates and picophytoplankton as key groups of phytoplankton in the Elbe estuary. *Environmental research.* https://doi.org/10.1016/j.envres.2024.119126

Section 4 is a modified version of a manuscript published as: Martens, N., Ehlert, E., Putri, W., Sibbertsen, M., Schaum, C.-E., 2024. Organic compounds drive growth in phytoplankton taxa from different functional groups. *Proceedings of the Royal Society B* 291: 20232713. https://doi.org/10.1098/rspb.2023.2713

The modifications to the published version concern minor changes to integrate the publication into the thesis (e.g. figure and section numbering).

As the first author of both publications, I carried out the associated literature research, developed the experimental design, contributed to the sample collection, prepared the samples for metabarcoding (e.g. by DNA extraction), isolated the strains needed for the laboratory experiments, carried out pilot studies and part of the final laboratory experiments. I performed the data analysis - e.g. with the help of statistical tests and data visualization. Beyond that, I wrote the first draft of both manuscripts and revised the manuscripts based on the suggestions and requests of the co-authors and the peer-reviewers.

Hamburg, 2024-05-21

_____ _____

Nele Martens (PhD candidate) Prof. Dr. C.-Elisa Schaum (Supervisor)

Dissertation

Phytoplankton in the Elbe estuary:

New insights into community composition and mixotrophy, from metabarcoding, flow cytometry, and laboratory experiments

Project B1

Biota-mediated effects on Carbon cycling in Estuaries

RTG2530

Nele Martens

University of Hamburg

Faculty of Mathematics, Informatics and Natural Sciences

Institute of Marine Ecosystem and Fishery Science

2024

Supervision

Prof. Dr. C.-Elisa Schaum

Prof. Dr. Hans-Peter Grossart

Prof. Dr. Inga Hense

Abstract

Estuaries are centers of human societies, habitats for a specialized flora and fauna and important entities in global carbon cycles. Phytoplankton are the basis of the aquatic food webs in estuaries but here often faced with challenging conditions such as light limitation due to high turbidity and osmotic stress due to salinity gradients. Taxa appearing under such conditions may play a critical role in maintaining primary production and biological carbon pumping, and they may apply specific strategies (e.g. mixotrophy), allowing them to persist. However, knowledge about estuarine biota remains limited. This is also the case in the Elbe estuary, one of Europe's largest estuaries, where the lower ca. 70 km of the water body are largely unexplored. Even in surveyed areas of this habitat, methodological limitations (e.g. of microscopy) may have led to certain groups being previously underrepresented.

In our study, we applied metabarcoding and flow cytometry to assess phytoplankton community composition in the Elbe estuary. Our focus was to identify important groups in the unmonitored mid to lower estuary, to assess the role of picophytoplankton in general, and to compare our results from further upstream with available microscopy data. Further, we carried out laboratory experiments, to assess the abilities of different phytoplankton strains isolated from the Elbe estuary to utilize organic compounds (e.g. sugars).

In compliance with former data from microscopy, phytoplankton communities were overall dominated by diatoms (Mediophyceae) with respect to metabarcoding reads (~ biovolume). However, we found that picophytoplankton and potentially mixotrophic flagellates (e.g. *Cryptomonas*) were more dominant than previously reported. Those groups can be overlooked *via* microscopy, due to their fragile nature and small size. In our laboratory study, we found that all included phytoplankton strains were able to utilize organic compounds. Our results altogether provide support for the significance of mixotrophy in the Elbe estuary.

Further research should address limitations of our study, e.g. concerning the interpretation of metabarcoding results in the context of gene copy numbers, and active mixotrophic behavior of the identified flagellates.

Lay summary

Estuaries, the lower river areas that merge into the oceans, are centers of human lifes, home for a diverse wildlife and important in global carbon cycles. Phytoplankton are the basis of the food chains in estuaries but may suffer from harsh conditions here. For instance, turbidity can darken the water body, but light is needed for photosynthesis. Species that live under such conditions may play an important role because they provide food for zooplankton and take up CO_2. However, there is not much knowledge about estuarine life. This is also the case in the Elbe estuary, one of Europe's largest estuaries, where the lower ca. 70 km are largely unexplored. Even in explored areas of this habitat, certain groups of phytoplankton may have been overlooked so far due to the choice of methods.

In our study, we applied molecular tools (metabarcoding) and automated cell counting techniques (flow cytometry) to assess phytoplankton composition in the Elbe estuary. Our focus was to identify important phytoplankton groups in the unmonitored mid to lower estuary and to compare our results from further upstream with available microscopy data. We also carried out laboratory experiments, to assess the ability of phytoplankton from the Elbe estuary to use organic substances (e.g. sugars), a strategy considered mixotrophy.

In compliance with former knowledge, phytoplankton communities were overall dominated by diatoms. However, we found that the smallest players among the phytoplankton - the picophytoplankton - and potentially mixotrophic flagellates were more dominant than so far reported. Due to their fragile nature and small size, those groups were likely overlooked in former microscopy-based studies. In our laboratory study, we furthermore found that all included phytoplankton species were able to use organic substances. Our results altogether provide support for the importance of mixotrophy in the Elbe estuary.

Zusammenfassung

Ästuare, die unteren Flussbereiche, die in den Ozean übergehen, sind das Zentrum menschlichen Lebens, Zuhause für eine diverse Tier- und Pflanzenwelt und wichtig in globalen Kohlenstoffkreisläufen. Die Basis der Nahrungskette in Ästuaren ist Phytoplankton, welches jedoch unter den harten Bedingungen in diesen Ökosystemen leiden kann. Zum Beispiel kann die Trübung im Wasser dazu führen, dass wenig Licht für die Photosynthese zur Verfügung steht. Arten, die unter solchen Bedingungen leben, sind wichtige Nahrungsquellen für das Zooplankton und sorgen dafür, dass weiterhin CO_2 aufgenommen wird. Dennoch wissen wir wenig über das Leben in Ästuaren. Dies ist auch in der Tideelbe der Fall, eines der größten Ästuare Europas, in der die unteren ca. 70 km weitgehend unerforscht sind. Selbst in den erforschten Bereichen wurden bestimmte Gruppen von Phytoplankton durch die verwendeten Methoden bisher nicht ausreichend berücksichtigt.

In unserer Studie haben wir molekulare Verfahren (Metabarcoding) und automatisierte Zellzählungsmethoden (Durchflusszytometrie) angewendet, um die Zusammensetzung des Phytoplanktons im Elbeästuar zu untersuchen. Unser Fokus lag darauf, herauszustellen, welche Gruppen im weitgehend unerforschten mittleren bis unteren Ästuar wichtig sind, und inwieweit unsere Ergebnisse von weiter stromaufwärts mit hier verfügbaren Mikroskopiedaten übereinstimmen. Weiterhin haben wir Laborexperimente durchgeführt, um zu untersuchen, ob Phytoplankton aus der Elbe organische Substanzen (z.B. Zucker) nutzen kann, eine Strategie, die als Mixotrophie bezeichnet wird.

Diatomeen waren in unserer Studie die dominante Phytoplanktongruppe, was mit dem übereinstimmt, was bereits durch Mikroskopie bekannt war. Wir fanden jedoch heraus, dass die kleinsten Vertreter des Phytoplanktons - das Picophytoplankton - und potentiell mixotrophe Flagellaten eine größere Rolle spielen als bisher angenommen. Diese Gruppen wurden in mikroskopischen Analysen vermutlich z.T. übersehen, da die Zellen fragil bzw. sehr klein sind. In unserer Laborstudie fanden wir zudem heraus, dass alle einbezogenen Phytoplanktonarten organische Substanzen nutzen können. Insgesamt unterstreichen unsere Ergebnisse die Bedeutung mixotropher Lebensstrategien im Elbeästuar.

Eidesstattliche Erklärung/ Statement under oath

Hiermit erkläre ich an Eides statt, dass ich die vorliegende Dissertationsschrift selbst verfasst und keine anderen als die angegebenen Quellen und Hilfsmittel benutzt habe. I hereby declare upon oath that I have written the present dissertation independently and have not used further resources and aids than those stated in the dissertation.

Hamburg, 2024-05-21

_____

Nele Martens

Erklärung Exemplare/ Declaration on copies

Ich versichere, dass das gebundene Exemplar der Dissertation und das in elektronischer Form eingereichte Exemplar identisch sind. I declare that the bound copy of the dissertation and the dissertation submitted in electronic form are identical.

Hamburg, 2024-05-21

_____

Nele Martens

Acknowledgements

I want to thank my first supervisor C.-Elisa Schaum for guiding me through the journey of becoming a PhD. I am also grateful to my second supervisor Hans-Peter Grossart, the chair of my supervision panel Inga Hense, and my institute colleagues, Stefanie Schnell and Luisa Listmann, for their reliable support, to Kai Jensen and Susanne Stirn for organizing the research training group, to Vanessa Russnak, Johanna Biederbick, Elena Hauten, Raphael Koll and the captain and crew of the research and fishing vessels Ludwig Prandtl and Ostetal for providing me with samples and additional environmental data as well as to the responsible persons at the NLWKN and HU for providing me with monitoring data. Lastly, I want to thank my family - my partner Çağıl and my parents, Bärbel and Rainer - for accompanying me through the different steps of my career, and my dog Neo for keeping me grounded.

Funding

This project was funded by the Deutsche Forschungsgemeinschaft (DFG, German Research Foundation) as part of the project 'Biota-mediated effects on Carbon cycling in Estuaries' (407270017/RTG2530).

Statement

Although the work related to my thesis was predominantly planned and executed by myself, science is a group effort and I had help from different people (e.g. by laboratory assistants and co-authors). To acknowledge these contributions, I do use the plural (we, us, our) in this thesis.

Table of contents

1. Introduction 1

   1.1. Study area: The Elbe estuary 1
   1.2. Study project and graduate school: RTG2530 3
   1.3. Study organisms: Phytoplankton 3
   1.4. Knowledge gaps and research approach 7
   1.5. Description of the methods 9

2. Metabarcoding reveals potentially mixotrophic flagellates and picophytoplankton as key groups of phytoplankton in the Elbe estuary 13

3. Picophytoplankton dominate phytoplankton communities in the Elbe estuary in terms of cell counts 44

4. Organic compounds drive growth in phytoplankton taxa from different functional groups 58

5. Discussion 80

1. Introduction

1.1. Study area: The Elbe estuary

In our study we investigated the composition and traits of phytoplankton in the Elbe estuary. Estuaries are transition zones between freshwater, terrestrial and oceanic environments (Levin et al., 2001) and characterized by the mixing of freshwater and seawater, and tidal currents (Tagliapietra et al., 2009). Temporal floodings of the surrounding terrestrial areas (e.g. marshlands) do not only have an impact on the local flora and fauna but might also lead to enhanced matter exchange between the terrestrial and aquatic sites (Levin et al., 2001). Being the interface between substantially different environments, estuaries often feature strong gradients of physico-chemical parameters such as salinity, nutrients and oxygen (Tagliapietra et al., 2009). Interaction of tidal currents and river runoff can result in highly turbid areas, known as maximum turbidity zones (Kappenberg and Fanger, 2007). Estuaries are considered highly productive ecosystems based on high nutrient inputs as well as decomposition of high loads of organic matter (Levin et al., 2001). However, the features mentioned above - e.g. salinity gradients and turbidity - can also be stressors for the local organisms and limit their distribution (see e.g. (Hossain et al., 2016)). Processes in estuaries determine the transfer of materials (e.g. carbon and nutrients) towards the oceans and might have cascading effects on oceanic processes (e.g. oceanic primary production and finally carbon export and storage) (Araujo et al., 2014; Basu and Mackey, 2018; Levin et al., 2001; Subramaniam et al., 2008).

The Elbe estuary is located in a temperate climate zone and one of Europe's largest estuaries. It extends for over 100 km from a weir in Geesthacht to the North Sea (fig. 1.1). The well-mixed mesotidal water body is characterized by areas with high turbidity (Kappenberg and Fanger, 2007) and high nutrient loads that are partially exported to the North Sea (Bergemann and Gaumert, 2010), temporal and local oxygen depletion (Gaumert and Bergemann, 2007) as well as shifts in salinity (FGG Elbe, 2024). The Elbe estuary is a habitat for miscellaneous species and furthermore supplies the local human population with ecosystem services (e.g. port of Hamburg and recreation areas). It has been experiencing

intense anthropogenic pressure for centuries and further changes such as global warming or deepening of shipping channels might have additional impacts on the ecosystem functioning - both for humans and other life forms (see e.g. (Van Maren et al., 2015)).

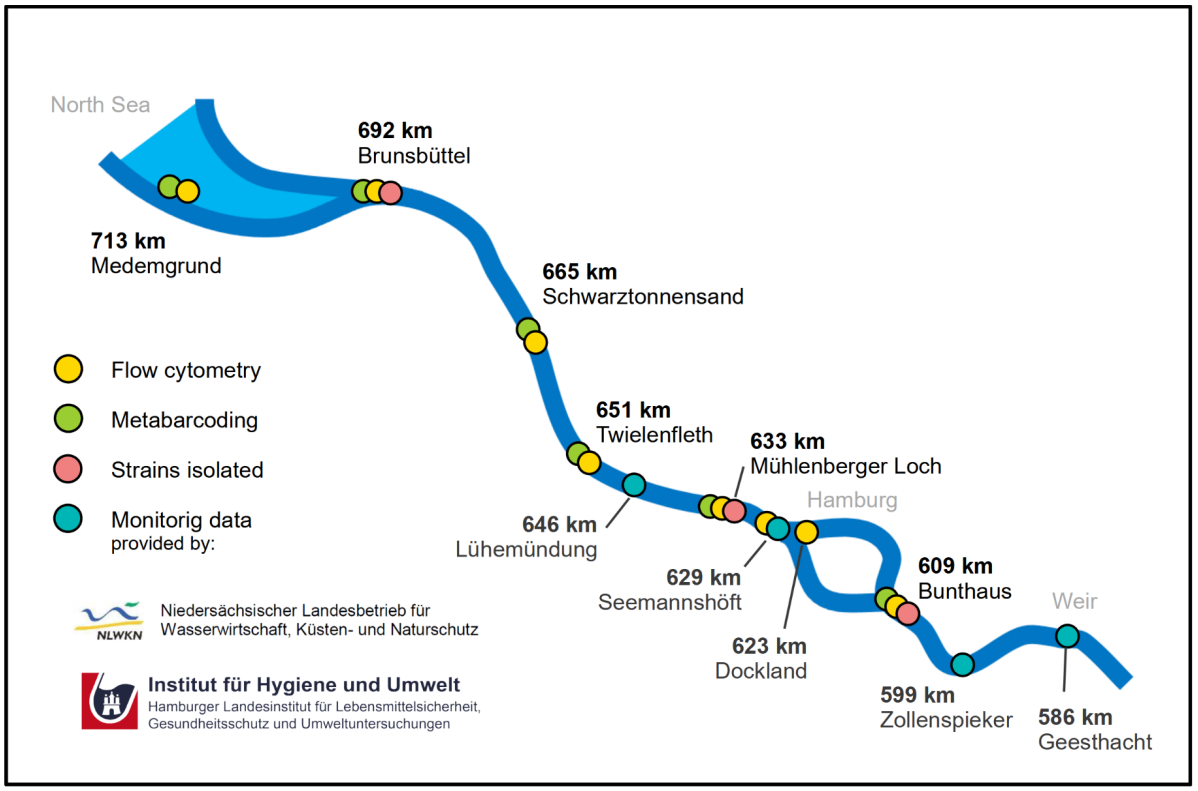

Fig. 1.1: Study area and approximate location of sampling stations along the Elbe estuary included in the different parts of the PhD project. Overlapping circles indicate different methods applied at the same sampling stations (see color scheme in the figure).

In our study, we applied metabarcoding and flow cytometry to analyze phytoplankton communities at different stations along the Elbe estuary (fig. 1.1, green and yellow sampling points) throughout different seasons in 2021 and 2022 (supplementary tab. S2.1). For comparison, we also included microscopy data of phytoplankton communities provided by monitoring facilities (HU, 2023; NLWKN, 2023) (fig. 1.1, blue sampling points). We additionally carried out laboratory experiments on single phytoplankton strains isolated from this ecosystem (fig. 1.1, red sampling points). Further details about the aims and methods are described in the sections below.

1.2. Study project and graduate school: RTG2530

The present project (B1) is part of the DFG-funded project 'Biota-mediated effects on Carbon cycles in Estuaries'. The research training group (RTG2530) altogether investigates how the specific estuarine conditions (e.g. salinity gradients) affect organisms of various trophic levels (i.e. primary producers, consumers and decomposers) and their interactions in and between the estuarine channels and marshlands. Gathering insights into the biological processes in the Elbe estuary provides us better understanding on the functioning of this specific ecosystem and how ecological processes might be affected by environmental change. Beyond that, we want to contribute to the many open research questions about estuaries as carbon sinks or sources in general and their functioning in global carbon cycles in particular. For instance, estuaries have been categorized as CO_2 sources in the past (Borges et al., 2005), however, recent studies indicate that the individual conditions of estuaries such as river runoff, turbidity and anthropogenic influence might have crucial impact on carbon cycles and that estuaries can also be CO_2 sinks (Araujo et al., 2014; Dutta et al., 2021; Hutchings et al., 2020; Kang et al., 2019; Pattanaik et al., 2020). Despite intense research in the last decades in particular many biological processes of estuarine carbon cycling remain cryptic (see also (Ren et al., 2022)).

Though the Elbe estuary has been described as a CO_2 source based on estimates from dissolved inorganic carbon measurements (Amann et al., 2015), we know little about biological processes in this ecosystem - which might also be affected by upcoming changes such as global warming - and most research in this ecosystem has been carried out several decades ago (e.g. (Fast, 1993; Wolfstein, 1996)).

1.3. Study organisms: Phytoplankton

Phytoplankton contribute about 50 % to global primary production (Field et al., 1998). Due to their short generation times and large standing genetic variation, their populations can react quickly to changes in their habitat (Hattich et al., 2017; Stomp et al., 2008). By taking up CO_2 they are the main biological drivers of the CO_2 flux towards aquatic environments

and substantial players in carbon sequestration (Basu and Mackey, 2018). Their performance has cascading effects on the higher trophic levels. Their allocation at the base of the food webs and their fast responses to environmental changes make them important players in terms of a potential feedback of the aquatic ecosystems on climate change (Boscolo-Galazzo et al., 2018). Despite this knowledge, many aspects of the role of phytoplankton in estuaries and similar ecosystems are still largely unexplored.

In the Elbe estuary, phytoplankton have been monitored for decades, providing a large pool of valuable data, but the monitoring is largely limited to the upper 60 km of the water body. It does not cover large parts of the estuary (ca. 70 km) where processes such as formation of turbidity as well as mixing of freshwater and saltwater might make life specifically challenging for phytoplankton and other organisms. Though there is some phytoplankton data from further downstream, these have been obtained several decades ago (e.g. (Fast, 1993; Wolfstein, 1996)) and since then, the ecosystem has experienced vast changes e.g. due to deepening and global warming. Hence, we do not know which are the dominant taxa today that persist under the harsh conditions in the mid to lower Elbe estuary. Moreover, assessment of phytoplankton was so far largely based on microscopy. While this method is very intuitive, it comes with several limitations. Specifically, certain taxa might not be thoroughly covered by microscopy, e.g. the small picophytoplankton, morphologically indistinct taxa and phytoplankton that are sensitive to common methods of fixation or cannot be thoroughly preserved (Altenburger et al., 2020; Bergkemper and Weisse, 2018; Callieri, 2008; Cerino and Zingone, 2006; Estrada et al., 2004; Huo et al., 2020; Medlin et al., 2017; Xia, 2013).

Knowledge about phytoplankton in the Elbe estuary is largely limited to the upper to mid reaches while ca. 70 km of the water body remain largely unexplored. Almost exclusive use of microscopy furthermore restricts our understanding about phytoplankton ecology in this habitat (e.g. with respect to small and cryptic taxa or those sensitive to fixation agents).

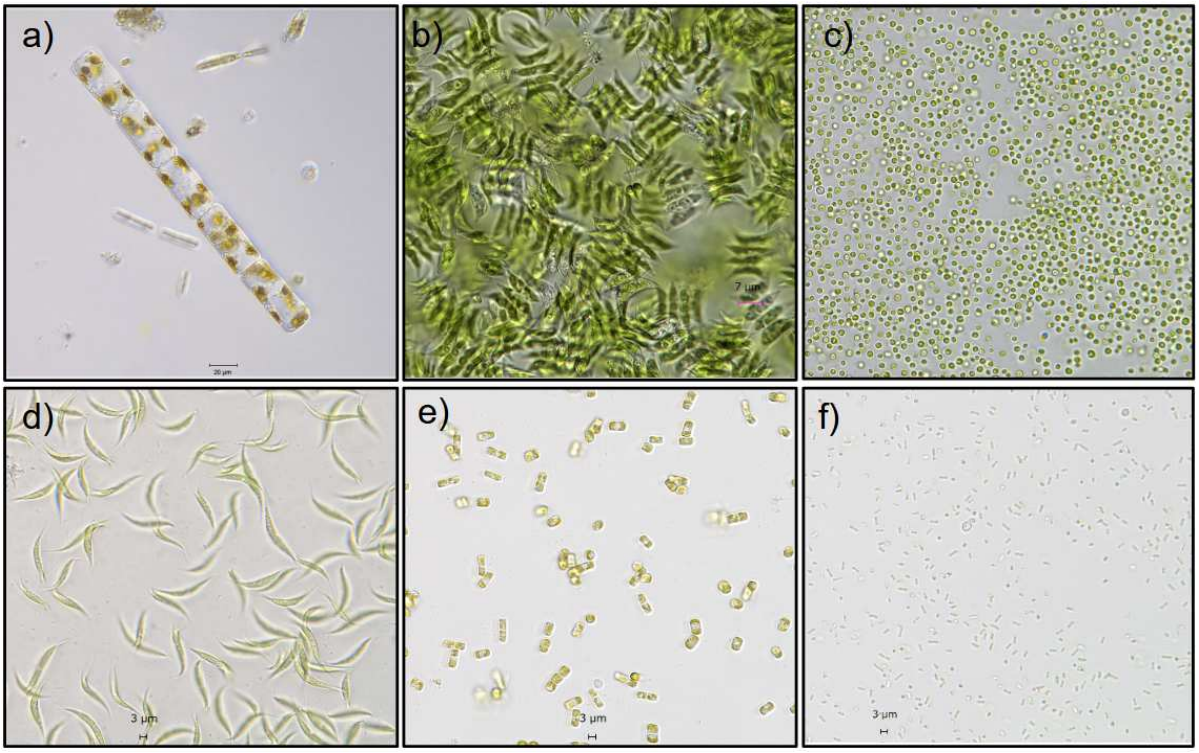

Fig. 1.2: Light microscopic images of different phytoplankton taxa from the Elbe estuary. Photos are selected based on availability. a) shows the diatom *Guinardia* in a community sample from May 2022, where this taxon was particularly dominant in the lower reaches (692 - 713 km) of the Elbe estuary. b) - f) show different phytoplankton strains isolated for the laboratory experiments carried out in this study, with b) *Tetradesmus*, c) *Mychonastes*, d) *Monoraphidium*, e) Thalassiosirales and f) Synechococcales. Note that images have partially different size scales. *Mychonastes* and Synechococcales are considered picophytoplankton.

Those potentially overlooked groups however, might be important entities in estuarine and similar ecosystems. With a cell diameter smaller than 2-3 µm, picophytoplankton, for example, build the smallest known group of phytoplankton (Callieri, 2008; Massana, 2011; Salmi et al., 2021), including picocyanobacteria such as *Synechococcus* and *Cyanobium* and picoeukaryotes such as *Mychonastes* and *Micromonas* (e.g. (Mitbavkar et al., 2021; Somogyi et al., 2020; Tragin and Vaulot, 2019)). Picophytoplankton are crucial for carbon turnover, e.g. as prey for nauplii larvae and filter feeders (Bemal and Anil, 2019; Richard et al., 2022). Despite their small size, picophytoplankton have been found in the guts of mesozooplankton and it has been suggested that they might be consumed indirectly by uptake of aggregates (Stukel et al., 2013; Wilson and Steinberg, 2010). Picophytoplankton are important contributors to primary production in aquatic ecosystems from oligotrophic to eutrophic habitats (Coello-Camba and Agustí, 2021; Moreira-Turcq et al., 2001; Purcell-Meyerink et al.,

2017; Takasu et al., 2023; Zhang et al., 2015) and they contribute to oceanic carbon export (e.g. (Basu and Mackey, 2018; Puigcorbé et al., 2015)). Some picophytoplankton have been shown to survive under extreme conditions, e.g. with respect to temperature, salinity and turbidity (Belkinova et al., 2021; Somogyi et al., 2022). Hence, they might play an essential role in estuaries where living conditions can be challenging for instance with respect to high variability and shifts in environmental parameter values (e.g. salinity, turbidity).

Though picophytoplankton have been found in estuaries (Gaulke et al., 2010; Moreira-Turcq et al., 2001; Purcell-Meyerink et al., 2017; Sathicq et al., 2020), their presence and role in many estuaries - including the Elbe estuary - is still largely unexplored as applied methods (especially light microscopy) are not adequate to detect or classify these small creatures.

Beyond a small cell size, mixotrophy might be a trait that allows phytoplankton to survive and grow in estuaries and deal with the rather inconvenient environment (e.g. with light limitation). Mixotrophy describes the combination of autotrophic and heterotrophic pathways, i.e. the use of organic and inorganic sources of energy and nutrients. Here, the heterotrophic component can include the uptake of particles (e.g. bacteria) *via* phagotrophy (e.g. by cryptophytes, dinoflagellates) (Koppelle et al., 2022; Millette et al., 2023) or the uptake of dissolved compounds (e.g. sugars and amino acids) (Godrijan et al., 2022; Listmann et al., 2021). Mixotrophy has been observed in taxa from various functional groups of phytoplankton, including haptophytes (Anderson et al., 2018; Godrijan et al., 2022; Koppelle et al., 2022), green algae (Azaman et al., 2017; Listmann et al., 2021; Pang et al., 2022), dinoflagellates (Millette et al., 2017), cyanobacteria (Muñoz-Marín et al., 2020), cryptophytes (Ballen-Segura et al., 2017) and diatoms (Villanova and Spetea, 2021) and known mixotrophic taxa were found in various estuarine ecosystems (Hammer and Pitchford, 2006; Lee et al., 2012; Li et al., 2022), including the Elbe estuary (HU, 2023; NLWKN, 2023). It has been suggested that mixotrophy might be a strategy to deal with limited light availability (Calderini et al., 2022; Godrijan et al., 2022; Jones et al., 2009; Millette et al., 2017; Tuchman et al., 2006), hence it might play a significant role in estuaries and similar habitats, where light availability can be highly limited and variable as a

consequence of suspended matter in the water. Other estuarine conditions such as a high content of organic substances and bacteria (see e.g. (Abril et al., 2002; Karrasch et al., 2003)) might additionally promote heterotrophic pathways in phytoplankton (see e.g. (Forsström et al., 2013; Naselli-Flores and Barone, 2019)).

Though some recent studies deal with mixotrophic behavior in estuaries (Dobbertin da Costa et al., 2024; Li et al., 2024; Millette et al., 2021) and it has been addressed before with respect to the Elbe estuary (Wolfstein, 1990) the role of mixotrophy remains cryptic. For instance, we do not know which taxa or functional groups are able to make use of organic carbon and it is ambiguous to us which kinds of organic substances (e.g. amino acids, sugars) can be utilized. With respect to the Elbe estuary, we also lack information about the distribution of potentially mixotrophic taxa along the estuary, especially in the unmonitored reaches where conditions such as turbidity might favor mixotrophic behavior.

1.4. Knowledge gaps and research approach

In our study we address the following knowledge gaps and research questions (RQ):

1) **Composition of phytoplankton in the mid to lower Elbe estuary:**
   RQ1: Which taxa/ groups dominate here?

2) **Picophytoplankton abundance and composition in the Elbe estuary:**
   RQ2: Do picophytoplankton play a specific role?

3) **Insights from applying new methods:**
   RQ3: Do results from this study (RQ1-2) match with known data from microscopy?

4) **Mixotrophy of estuarine phytoplankton:**
   RQ4: Is mixotrophy a strategy to survive in the Elbe estuary?

We here address both ecological and methodological knowledge gaps which are partially intertwined. In particular, we wanted to assess phytoplankton community composition in the mid to lower Elbe estuary in general. As described before, the mid to lower Elbe estuary is characterized by typical estuarine features such as gradients and variations in salinity and turbidity deriving from the mixing of freshwater and saltwater and the tidal currents. Those conditions can challenge phytoplankton and taxa that dominate here might be very resilient and also play a specific role in a changing world. We also tackled methodological knowledge gaps that derive from the so far largely exclusive use of light microscopy by including different methods, namely metabarcoding and flow cytometry. For instance, as described in section 1.3, small-celled taxa such as picophytoplankton might be missed by light microscopy and certain taxa can be destroyed or not thoroughly preserved by fixation methods typically applied on microscopy samples (Bergkemper and Weisse, 2018; Callieri, 2008; Estrada et al., 2004; Markina, 2019). We also wanted to analyze the ability of different taxa to utilize organic carbon. This is a potential strategy for phytoplankton to e.g. deal with light limitation caused by turbidity in the estuarine water, as it has been shown for different taxa (Calderini et al., 2022; Godrijan et al., 2022; Jones et al., 2009; Millette et al., 2017; Tuchman et al., 2006).

A graphical overview of the different methodological components of this study is given in figure 1.3. The study includes three key methods: metabarcoding, flow cytometry and laboratory experiments (see also section 1.5). While the laboratory experiments are directly addressing mixotrophy (RQ4), results from metabarcoding and flow cytometry are combined to answer the research question about community composition, picophytoplankton and the comparability of those results with microscopy data (RQ1-3). Beyond, flow cytometry is used to determine growth of phytoplankton strains in the laboratory study (RQ4). Also, though metabarcoding is not directly related to mixotrophy, this method may identify known mixotrophic taxa and hence add to this topic (RQ4). Sampling, data analysis and comparison with further data is part of all subjects, however, in the metabarcoding study, the comparison with former phytoplankton composition data from microscopy is a more comprehensive component.

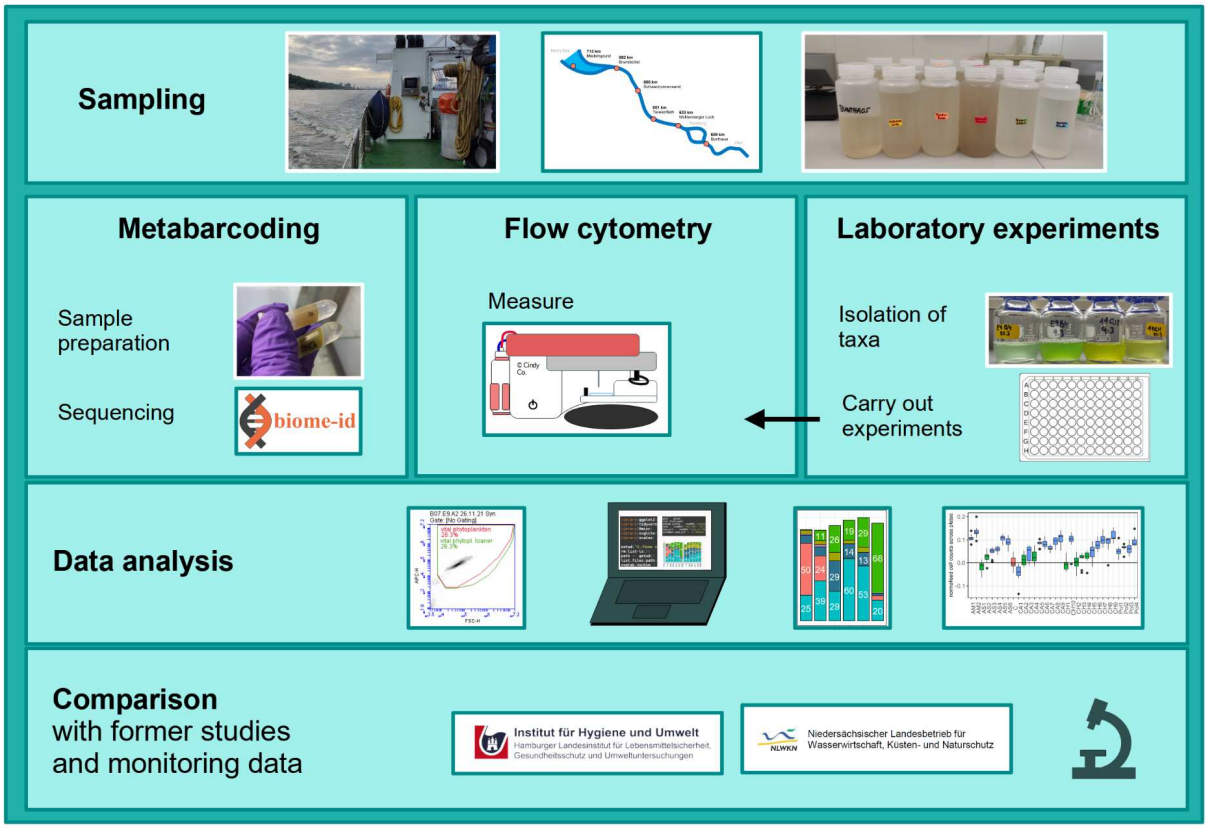

Fig. 1.3: Graphical overview of the different components of this study.

1.5. Description of the methods

In our study, we applied metabarcoding (18S, 16S) to assess phytoplankton community composition throughout seasons in 2021 and 2022 along the Elbe estuary. Metabarcoding is the sequencing of specific target genes (e.g. 18S, ITS, 16S) of the DNA in an environmental sample that contains a mix of different species (e.g. in water sample). In recent years, reams of studies on metabarcoding have been carried out from freshwater to marine sites to identify phytoplankton independently of, e.g., size and morphology (e.g. (Fabrin et al., 2020; Kang et al., 2021; Kolda et al., 2020; Piredda et al., 2018; Rynearson et al., 2020; Stat et al., 2017)). Several studies found that the number of taxa identified with metabarcoding is higher than that identified with microscopy (Chen et al., 2022; Huo et al., 2020; Piredda et al., 2018; Zimmermann et al., 2015). Metabarcoding could furthermore reveal the presence and importance of specific groups in the respective study areas that have been missed before - e.g. parasitic dinoflagellates in the Jiaozhou Bay in China (Chen et al., 2022), harmful cyanobacteria in an urban lake in Brazil (Fabrin et al., 2020), 70 new taxa in the Southern Norwegian coastal waters of the Skagerrak (Gran-Stadniczeñko et al., 2019) - as well as new

taxa of *Thalassiosira* spp. in the Narragansett Bay in the USA (Rynearson et al., 2020). Beyond these findings of so far missed taxa, benefits of metabarcoding include an automated workflow with high throughput and reduced personnel working times (Santi et al., 2021). Hence, including this method in phytoplankton research and on a long-term perspective also in monitoring approaches (e.g. with respect to the European Water Framework Directive) is of significance not only from an ecological but also from an economical perspective. Yet, as a relatively novel method, metabarcoding comes with certain pitfalls. For instance phytoplankton cells contain a certain number of gene 'copies' that are positively correlated with their size (Godhe et al., 2008; Vasselon et al., 2018) (a more detailed description is provided in section 2.1), but might vary and primer mismatch or incomplete databases (Gong and Marchetti, 2019; Kezlya et al., 2023) can impede the assessment of phytoplankton communities. Hence, application of this method does also contribute to the general understanding and implementation of metabarcoding e.g. by comparing results with microscopy data.

Metabarcoding can unveil the importance of taxa that remain underrepresented or undiscovered when applying light microscopy. This can for instance include the small-celled picophytoplankton and taxa that are sensitive to fixation agents commonly used in microscopy (Bergkemper and Weisse, 2018; Callieri, 2008; Estrada et al., 2004; Markina, 2019).

Furthermore, we carried out flow cytometry, mainly with the aim to distinguish and quantify different groups of picophytoplankton. Flow cytometry has been used for decades to characterize phytoplankton communities based on the properties of the single cells (such as autofluorescence, size, granularity) (Dubelaar and Jonker, 2000; Markina, 2019; Paerl et al., 2020; Read et al., 2014; Trask et al., 2005; Veldhuis and Kraay, 1990). It can be used to differentiate between different groups of phytoplankton (e.g. picophytoplankton, phycoerythrin-rich cyanobacteria) (Fragoso et al., 2019; Ning et al., 2021; Read et al., 2014; Thyssen et al., 2022). The great advantage of flow cytometry is a rapid work through of samples that mostly require no preparation (Markina, 2019) and the detection of picophytoplankton (Crosbie et al., 2003; Grob et al., 2007; Ning et al., 2021; Otero-Ferrer et

al., 2018; Paerl et al., 2020) that can be overlooked by conventional methods such as light microscopy (Bergkemper and Weisse, 2018; Callieri, 2008; Estrada et al., 2004; Markina, 2019).

Flow cytometry can be used to distinguish groups of phytoplankton that have common cell characteristics (e.g. picoeukaryotes, phycocyanin-rich picocyanobacteria).

While both metabarcoding and flow cytometry are used to assess community composition they differ in certain ways and have their pros and cons. For instance, metabarcoding provides much more precise information about the entities of a community (e.g. different taxa) while the resolution in flow cytometry is lower and it can only differentiate certain groups that significantly differ in cell traits (e.g. phycocyanin-rich cyanobacteria compared to eukaryotes, picophytoplankton compared to larger phytoplankton). Flow cytometry, on the other hand, provides direct quantitative data (cell counts) while the results from metabarcoding are semi-quantitative (e.g. % of reads). Flow cytometry furthermore provides information about the actual cell size, e.g. with respect to the definition of picophytoplankton, while in metabarcoding assessment of picophytoplankton can only be done based on the usual size range or classification (e.g. *Mychonastes* is considered picophytoplankton but cells *can* sometimes be > 3 µm). Applying both methods together allows us to make use of these different advantages and enables a comprehensive assessment of phytoplankton communities, especially with respect to picophytoplankton.

Flow cytometry is quantitative, but does obtain a lower resolution (e.g. picoeukaryotes), while metabarcoding obtains precise taxa information, but is semi-quantitative. Combining both methods is hence useful to obtain profound results.

Additionally, we carried out laboratory experiments to assess the mixotrophic ability of phytoplankton from the Elbe estuary (fig. 1.3). Though it has been shown before that mixotrophy plays a role in the Elbe estuary (Wolfstein, 1990), the mentioned is community-based, focussing on a narrow spatio-temporal range (summer to fall in 1989

around the area of Brunsbüttel) and on Glucose as a source of organic carbon. We do lack more comprehensive data, e.g. with respect to the abilities of different taxa and the effects of different types of compounds. Understanding which taxa are able to utilize which types of organic compounds is the basis to transfer the results to broader scales, e.g. by combining those results with field data about the composition of phytoplankton and dissolved organic matter. Therefore we isolated different strains of phytoplankton from different stations of the estuary (fig. 1.1). We obtained a total of 17 different strains including seven pico-sized green algae, six nano-sized green algae, one nano-sized cyanobacterium, two pico-sized cyanobacteria and a diatom (tab. 1.1, see also fig. 1.2b-f). Further information about the strains and how they were identified can be obtained from section 4 and the respective supplementary data. We used Biolog Ecoplates™ to expose the taxa to 31 different organic compounds (e.g. amino acids, sugars) in various replicates and assessed if the substances affected their growth (proxied by cell counts measured *via* flow cytometry after approx. 24 h compared to an 'organic-free' control). Ecoplates™ were originally designed as a rapid method to characterized microbial communities, however they have been used to assess the ability of phytoplankton to utilized dissolved organic carbon in different studies (e.g. (Godrijan et al., 2020; Listmann et al., 2021)).

Tab. 1.1: Taxa included in the laboratory experiments. The internal strain ID implies the functional group with N = nano-sized green alga, P = pico-sized green alga, D = diatom, C = cyanobacterium.

Taxa	Strains (Internal ID)	Origin: Station	Origin: Season
Micractinium sp.	N1	609 km	Spring
Monoraphidium sp.	N2, N7, N8	609, 692, 609 km	Spring
Tetradesmus sp.	N3	609 km	Spring
Chlorella-like/ *Chlorella* sp.	N4, P2	609, 692 km	Spring, Winter
Mychonastes sp.	P1, P4, P6	609, 633, 692 km	Spring, Summer
Choricystis sp.	P3	633 km	Winter
unidentified pico green alga	P5, P9	609 km	Winter, Summer
Thalassiosirales sp.	D1	633 km	Winter
Synechococcales sp.	C1, C6, C9	609 km	Summer

2. Metabarcoding reveals potentially mixotrophic flagellates and picophytoplankton as key groups of phytoplankton in the Elbe estuary

This chapter is a modified version of a manuscript published as: Martens, N., Russnak, V., Woodhouse, J., Grossart, H.-P., Schaum, C.-E., 2024. Metabarcoding reveals potentially mixotrophic flagellates and picophytoplankton as key groups of phytoplankton in the Elbe estuary. *Environmental research.* https://doi.org/10.1016/j.envres.2024.119126

The modifications to the published version concern minor changes to integrate the publication into the thesis (e.g. figure and section numbering).

Abstract

In estuaries, phytoplankton are faced with strong environmental forcing (e.g. high turbidity, salinity gradients). Taxa that appear under such conditions may play a critical role in maintaining food webs and biological carbon pumping, but knowledge about estuarine biota remains limited. This is also the case in the Elbe estuary where the lower 70 km of the water body are largely unexplored. In the present study, we investigated the phytoplankton composition in the Elbe estuary *via* metabarcoding. Our aim was to identify key taxa in the unmonitored reaches of this ecosystem and compare our results from the monitored area with available microscopy data. Phytoplankton communities followed distinct seasonal and spatial patterns. Community composition was similar across methods. Contributions of key classes and genera were correlated to each other ($p < 0.05$) when obtained from reads and biovolume ($R^2 = 0.59$ and 0.33, respectively). Centric diatoms (e.g. *Stephanodiscus*) were the dominant group - comprising on average 55 % of the reads and 66 - 69 % of the biovolume. However, results from metabarcoding imply that microscopy underestimates the prevalence of picophytoplankton and flagellates with a potential for mixotrophy (e.g. cryptophytes). This might be due to their small size and sensitivity to fixation agents. We argue that mixotrophic flagellates are ecologically relevant in the mid to lower estuary, where, e.g., high turbidity renders living conditions rather unfavorable, and skills such as phagotrophy provide fundamental advantages. Nevertheless, further findings - e.g. important taxa missing from

the metabarcoding dataset - emphasize potential limitations of this method and quantitative biases can result from varying numbers of gene copies in different taxa. Further research should address these methodological issues but also shed light on the causal relationship of taxa with the environmental conditions, also with respect to active mixotrophic behavior.

2.1. Introduction

Due to their large contribution to global primary production (Field et al., 1998), their role in aquatic carbon sequestration (Basu and Mackey, 2018) and their ability to quickly respond to environmental changes (Hattich et al., 2017; Stomp et al., 2008) phytoplankton play a key role in climate change feedback loops (Basu and Mackey, 2018; Boscolo-Galazzo et al., 2018; Laufkötter et al., 2015). Estuaries, the transient areas between freshwater and marine environments, are hotspots of primary production and substrate turnover, fueled by a high nutrient and carbon availability (Lancelot and Muylaert, 2011). Biota-mediated processes in estuaries have cascading effects on adjacent oceanic ecosystems, e.g. on primary production and carbon export (Araujo et al., 2014; Basu and Mackey, 2018; Lancelot and Muylaert, 2011; Subramaniam et al., 2008). However, biota-mediated processes in estuaries that affect carbon cycling and turnover are complex and still poorly investigated. More fundamentally, we even lack information about which taxa prevail under certain estuarine conditions, such as high turbidity.

In the Elbe estuary, one of Europe's largest estuaries, phytoplankton have been monitored for decades, providing a comprehensive pool of valuable data. However, the monitoring is largely limited to the upper 60 of over 100 km of the estuarine water body. Typical estuarine features such as salinity shifts as a consequence of tidal currents and high turbidity specifically characterize the mid to lower part of the estuary, where phytoplankton have last been investigated in the 1990s (e.g. (Muylaert and Sabbe, 1999; Wolfstein, 1996)). Since then, the ecosystem has changed considerably, e.g. due to dredging, deepening and global warming. Furthermore, the study and analysis methods for classifying phytoplankton have evolved. Analyses of phytoplankton communities, both in monitoring, but also in former literature (e.g. (Wolfstein, 1996)) were primarily based on microscopy, which comes with

some limitations, e.g. a low throughput, restriction to morphology and difficulties to detect picophytoplankton smaller than ca. 2-3 µm (Bergkemper and Weisse, 2018; Callieri, 2008).

In recent years, metabarcoding has been increasingly used as a tool to identify phytoplankton independently of, e.g., size and morphology (e.g. (Fabrin et al., 2020; Kang et al., 2021; Kolda et al., 2020; Piredda et al., 2018; Rynearson et al., 2020)). This method only depends on the DNA - i.e. targeted marker genes such as 18S or ITS - extracted from a water sample. It is a high throughput method with reduced personnel working times (Santi et al., 2021) that allows analyses of, e.g., more or larger samples and consequently has the potential to result in a better representation of the ecosystem. In former studies, metabarcoding revealed the presence of specific taxa, e.g. harmful cyanobacteria, in freshwater, brackish and marine ecosystems (Chen et al., 2022; Fabrin et al., 2020; Rynearson et al., 2020), often resulting in higher diversity estimates compared to microscopy (e.g. (Chen et al., 2022; Huo et al., 2020; Piredda et al., 2018; Zimmermann et al., 2015)).

Metabarcoding can primarily yield information about the genetic setup of phytoplankton communities, as we look at the number of 'copies' of a gene or a combination of specific genes found in the sample that belong to a specific taxon. This does not directly represent the usual measures of phytoplankton abundance, e.g. biovolumes or counts, as copy number can vary even within one species. The tools and methods available to ameliorate this limitation (Gong and Marchetti, 2019; Martin et al., 2022) are not always intuitive for complex samples. However, it has been shown that the number of gene copies held in a phytoplankton cell *can* be positively correlated with its size (Godhe et al., 2008; Vasselon et al., 2018). Hence, metabarcoding reads obtained from a sample might correlate with size dependent values from microscopy (e.g. biovolume), and community composition obtained from both methods might be similar.

In this study, we applied 18S rRNA gene metabarcoding to analyze the community composition of the eukaryotic phytoplankton at different stations along approximately 100 km of the Elbe estuary. Sampling campaigns were carried out in winter, spring and summer in 2021 and 2022. Our aim was to 1) provide phytoplankton data from the unmonitored

reaches of the estuary and set these into context of external forcing (e.g. turbidity, salinity) and 2) to give a rough estimate of the overall comparability of the metabarcoding results with microscopy-based data from local monitoring (HU, 2023; NLWKN, 2023) and previous publications. Assessing the comparability of metabarcoding results with those from microscopy is a prerequisite for the wider use of metabarcoding as an efficient tool to analyze phytoplankton community composition, e.g. in monitoring of estuaries as well as similar ecosystems.

2.2. Methods

Study area & sampling

The Elbe estuary extends for over 100 km from a weir in Geesthacht (ca. 586 km, Germany) to the North Sea (ca. 713 km) (fig. 2.1). Water samples for metabarcoding were taken on the research vessel Ludwig Prandtl by using a flow through system of the ferry box which takes water from the upper water layers. More detailed information is shown in the supplementary data (tab. S2.1). Sampling was conducted at six different stations along the estuary (fig. 2.1) between May and July 2021 as well as February and June 2022. Samples were concentrated on 0.2-0.45 µm filters at about -0.2 bar, resolved in a residue of the sample volume, transferred to tubes and frozen at -26 °C before further processing. Filtration units were rinsed with distilled water between the samples. We extracted DNA using a CTAB protocol (Fawley and Fawley, 2004) (see supplementary data prot. S2.1).

Environmental data (e.g. turbidity, flow rate, salinity) were taken from the on-board ferrybox (Petersen et al., 2011) or obtained from the official database of the FGG Elbe (Flussgebietsgemeinschaft Elbe/ Elbe River Basin Association) (FGG Elbe, 2024) (see also supplementary data tab. 2.1). A missing turbidity value from the pier sampling on 2021-07-29 at 609 km was replaced by a value provided from measurements on 2021-07-26 (from the research vessel) at the same location.

The Elbe estuary was characterized by increasing salinities from upstream towards the North Sea (see also supplementary data fig. S2.1). The salinity in the lower area - especially between 692 km and 713 km - varied drastically, and depended on various factors such as the river flow and the tide. Salinities were specifically low here in winter 2022 and summer 2021 at high river flow (>1000 $m^3 s^{-1}$ and >500 $m^3 s^{-1}$ respectively; (FGG Elbe, 2024)) (see also supplementary data fig. S2.1 and tab. S2.1). In these seasons, sampling in the lower estuary was conducted during decreasing tide, hence, in combination with the high river flow, the surface water current towards the North Sea may have been particularly strong. In other seasons salinities reached up to 10-20 PSU at 713 km. The highest salinity of 20 PSU was achieved in summer 2022 when the river flow was particularly low (< 250 $m^3 s^{-1}$; (FGG Elbe, 2024)) (see also supplementary data fig. S2.1 and tab. S2.1) and sampling was conducted at the peak of the flood. In spring 2021 a flow rate of ca. 462 $m^3 s^{-1}$ combined with a sampling conducted at rising tide added up to a salinity of approximately 10 PSU at the lower station (713 km; see also supplementary data tab. S2.1). The same salinity was measured in spring 2022, when the flow rate was slightly lower (ca. 337 $m^3 s^{-1}$) but sampling was conducted at decreasing tide, which added to the downward current. Notably, in spring 2021, the difference in salinity between 692 km and 713 km was more pronounced than in any other season. Precisely, salinity was eight times higher at 713 km (10.4 PSU) compared to 692 km (1.3 PSU). This might be because the sampling was carried out during rising tide, while river flow was relatively low (462 $m^3 s^{-1}$), which may have resulted in reduced mixing of the different water bodies. The Elbe estuary is furthermore characterized by partially high turbidity especially between the city of Hamburg and the actual river mouth downstream of 700 km (Bergemann, 2004) and in winter ((FGG Elbe, 2024); see also supplementary data fig. S2.1). Those patterns did reflect in our data, where the highest turbidity (>150 NTU) was reached at 713 km in February 2022 (supplementary data fig. S2.1 and tab. S2.1).

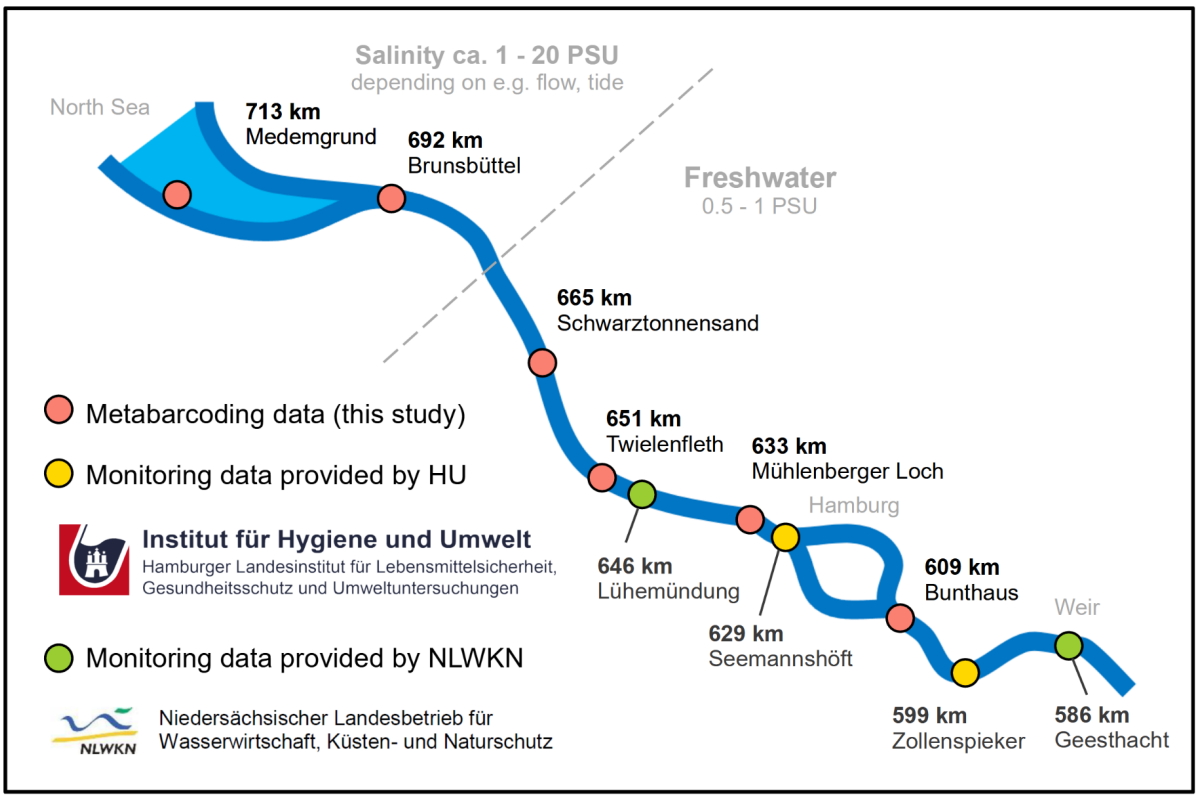

Fig. 2.1: Approximate location of sampling stations along the Elbe estuary referring to the data obtained from metabarcoding in this study (shown in red) and monitoring data provided by (NLWKN, 2023) **(in green) and** (HU, 2023) **(in yellow).** "km" metric indicates the approximate distance from the spring of the Elbe river in the Czech Republic. The discontinuous line indicates the approximate border between freshwater and increased salinities as observed during the sampling campaign.

Metabarcoding & bioinformatics

Metabarcoding was carried out by biome-id (biome-id Dres Barco & Knebelsberger GbR), using 6-12 µL of the total 40 µL of DNA extract and 18S primers 5'-GCTTGTCTCAAAGATTAAGCC-3' (forward) and 5'-GCCTGCTGCCTTCCTTGGA-3' (reverse) targeting the V1-V2 region (supplementary material prot. S2.2). Adapter sequences were removed from demultiplexed paired-end reads using R (version 4.1.3) and the package cutadapt (version 4.7). Additional quality control (removal of reads of low quality containing ambiguous bases), inference and taxonomic assignment was performed using DADA2 (version 1.18) (Callahan et al., 2016). Forward and reverse reads were trimmed to 260 nt and 200 nt, respectively, with maxEE and truncQ cutoffs both equal to two. Taxonomic assignment was made using the assignTaxonomy function with the Silva 18S database

(version 138). We observed a high number of taxa failed to achieve assignment to the genus level. We therefore also assigned the taxonomy of reads to the PR2 18S database (version 4.14) (Guillou et al., 2012). We merged the taxonomy of the two databases, defaulting to PR2 and only referring to the Silva database when reads were unassigned using PR2. We removed reads from non-phytoplankton groups (i.e. groups that are not considered phytoplankton, did not include phytoplankton in our case or did not include any further information if they were phytoplankton or not). When the class was returned as Syndiniales, we re-assigned it to Dinophyceae.

Data analysis

We used R (version 4.1.3) and the packages tidyverse (version 1.3.2) and ggplot2 (version 3.4.0) for data preparation and plotting. We used libreoffice draw for illustrations. Absolute phytoplankton reads were biased by the presence of other non-phytoplankton taxa such as *Eurytemora* and not comparable across samples. Hence, in this study phytoplankton are only included as their relative contributions to the 18S phytoplankton reads, not as absolute abundances. The number of reads found per taxon does furthermore not represent their abundance (i.e. cell counts). This is because eukaryotic cells can hold several gene copies (Santoferrara, 2019). However, as the number of gene copies has been shown to be positively correlated with the cell size (Godhe et al., 2008; Vasselon et al., 2018) our results with respect to phytoplankton composition based on metabarcoding reads might be similar to the community composition based on other size dependent measures, e.g. biovolumes. In this study, we largely focus on key genera (fig. 2.2d), their genotypes (fig. S2.5) and key classes (fig. 2.2b). We define a genotype as a subgroup of a genus that has a unique DNA sequence based on ASV (amplicon sequence variants) in the analyzed gene (18S V1-V2 region). We define key genera and classes as genera respectively classes that contribute at least 10 % respectively 15 % to the eukaryotic phytoplankton reads in at least one sample (i.e. at a station and season). We also calculated the average contribution of genera and classes across seasons and stations (fig. 2.2a, fig. 2.2c). These are calculated from the *relative* contributions at the different stations in the different seasons, i.e. differences in absolute abundances are not included. In the same way we calculated the average

contributions of different genotypes to the key genera (fig. S2.4). We assessed the relationship between the contribution of different key genera, their genotypes and the key classes with station, season and other parameters with a spearman rank correlation using rcorr from the package hmisc (version 5.1-0) in R (fig. 2.3, fig. S2.6, tab. S2.3). For the genotypes (fig. S2.6), we here focussed on those which contributed at least 5 % to the eukaryotic phytoplankton reads in at least one sample (i.e. at a station and season). We additionally used a t-test (t.test from the package stats, version 4.3.1, in R) to calculate if the contributions of the different key classes and genera significantly differed between the upper stations (609 - 633 km), mid stations (651 - 665 km) and lower stations (692 - 713 km) (tab. S2.4). We largely refrain from including species-level data as species assignment is uncertain with the relatively short (ca. 300 - 350 bp) 18S amplicons. However, assignments of possible species to the different key genera and their genotypes is provided in the supplementary material (tab. S2.5) and we do refer to the possibility that certain genotypes *might* represent certain species where reasonable.

Comparative data from microscopy

To obtain a rough overview about the overlap of microscopy and metabarcoding, we included monitoring data provided by the HU (Institut für Hygiene und Umwelt) in Hamburg, Germany and the NLWKN (Niedersächsischer Landesbetrieb für Wasserwirtschaft, Küsten- und Naturschutz) in Lower Saxony, Germany. Monitoring stations are located between 586 km and 646 km, i.e. around the city of Hamburg (fig. 2.1), and we included available samplings from different time points along the years 2021 and 2022 (see supplementary data tab. S2.1, prot. S2.3). Note that due to the different methods, sampling stations and sampling dates, data from metabarcoding and microscopy are not expected to be identical and dissimilarities can have various ecological and methodological reasons that will be addressed exemplarily, but cannot be discussed exhaustively in this study. We removed the cyanobacteria from the microscopy data, as we focus on eukaryotic phytoplankton in this study, and eukaryotic phytoplankton are the dominant type of phytoplankton in the Elbe estuary. Moreover, we removed the choanoflagellate *Desmarella* from the data, as we do not consider this group to be phytoplankton. For the comparison on class level, we added information on class level based on common data bases (see supplementary tab. S2.2).

In the comparison between microscopy and metabarcoding we largely focus on key genera and key classes (fig. 2.4), while also mentioning species level results throughout the text (see also fig. S2.7 and tab. S2.5 for details). If genera or classes accounted for at least 10 % respectively 15 % of the total eukaryotic phytoplankton community at least once, regardless of the method, these were considered key genera respectively classes. For better comparison, we also merged the groups of "unclassified centric diatoms" and "Mediophyceae" into a single group (fig. 2.4). Centric diatoms are not classified by the HU if they are morphologically indistinct. We can assume, also in compliance with the NLWKN data, that those are mostly Mediophyceae. Other types of centric diatoms, e.g. *Aulacoseira* from the class of Coscinodiscophyceae are classified in the HU dataset. As described above, we also calculated the average contribution of genera and classes across seasons and stations (fig. 2.4a, fig. 2.4c). These were obtained from the *relative* contributions at the different stations in the different seasons, without including differences in absolute abundances. This was done to make it comparable with metabarcoding data, where only relative contributions can be obtained. To gain a better understanding about the comparability of the communities described by reads (metabarcoding) and biovolume (microscopy), we calculated the R^2 and p values after pearson using cor.test() and cor() from the package stats in R for the relative contributions of key taxa and classes (see also fig. S2.8a-b). To do so, we pooled the data from closely located stations, e.g. the microscopy sample from 646 km from summer 2022 was compared with the metabarcoding sampled from 651 km from the same season (see also fig. S2.8a-b). We additionally used a t-test (t.test from the package stats in R) to assess whether the contributions of different key classes and genera significantly differed between microscopy and metabarcoding across stations and seasons in the upper to mid estuary (586 - 651 km) (see also fig. S2.9a-b). Note that these statistical tests only included samples from stations where comparative data from the respective other method was available (i.e. data from station 646 km in 2021 and 651 km in winter 2022 is not included, because data from 651 km and 646 was not available in the respective season(s) each; see also fig. 2.4). Lastly, as comparative current monitoring data from downstream of 646 km is not available, we also include a mostly qualitative comparison with microscopy phytoplankton data from former studies that included this area (e.g. (Muylaert and Sabbe, 1999; Wolfstein, 1996)).

2.3. Results

Phytoplankton communities assessed via metabarcoding & relation to abiotic parameters

Concentrations of phytoplankton in terms of chlorophyll *a* were highest at the uppermost station (609 km), with particularly high values from spring (2021 and 2022) to early summer (June 2022) (92.0 - 152.7 µg l^{-1}) (see supplementary data tab. S2.1, fig. S2.1). The eukaryotic phytoplankton communities followed distinct seasonal and spatial patterns (fig. 2.2) according to metabarcoding results.

The overall most dominant group of eukaryotic phytoplankton were centric diatoms from the class Mediophyceae. This group contributed on average 45 % to the eukaryotic phytoplankton in terms of metabarcoding reads (fig. 2.2a) and up to 88 % in single samples (fig. 2.2b). *Stephanodiscus* was the most dominant genus within the Mediophyceae during winter and spring. This taxon represented up to 85 % of the eukaryotic phytoplankton at the upper station (609 km) (fig. 2.2d). *Stephanodiscus* was the most dominant genus across seasons and stations, averaging approximately 16 % of the total phytoplankton (fig. 2.2c). The contributions of *Stephanodiscus* declined from 609 km towards further downstream, resulting in a negative correlation with the stream km ($r = -0.72$, $p = 3.6 \times 10^{-5}$, fig. 2.3). The genus *Stephanodiscus* included 19 genotypes across seasons and stations (fig. S2.4) and the genotype richness of this taxon was particularly high at 609 km in spring 2021 (16 genotypes; fig. S2.5). However, across seasons and stations *Stephanodiscus* was largely (to ca. 98 %) represented by the three most dominant genotypes (genotype 1 - 3; fig. S2.4). Genotype 3 was more dominant from winter to spring than in other seasons and negatively correlated with temperature (fig. S2.5-S2.6, $r = -0.49$, $p = 1.1 \times 10^{-2}$). Our results imply that *Stephanodiscus* was largely represented by the species *S. hantzschii* (genotype 1 and 2; tab. S2.5) but uncertainties in species level identification should be considered (see section 2). Genotype 3 could not be identified to species level. In summer 2021, *Cyclotella* was a dominant taxon at 609 km (fig. 2.2d), contributing 49 % to the eukaryotic phytoplankton and being associated with higher temperatures ($r = 0.92$, $p = 2.3 \times 10^{-11}$, fig. 2.3). *Cyclotella* comprised 24 genotypes across seasons, the highest number among the key genera (fig.

S2.4). Its genotype richness was highest at 609 km in summer 2021 (18 genotypes), but the genus was largely (to ca. 80 %) represented by the three most dominant genotypes (genotype 1 - 3; fig. S4). Genotype 3 was particularly dominant at 609 km and negatively correlated with stream km (fig. S2.5-S2.6, $r = -0.43$, $p = 2.6 \times 10^{-2}$). Genotype 1 and 3 possibly belong to the species *C. meneghiniana*, while genotype 2 could not be identified further (tab. S2.5). *Skeletonema* also played a role, especially at 633 km in summer 2021, where it contributed 35 % to the eukaryotic phytoplankton reads (fig. 2.2d) and was largely represented by a single genotype (fig. S2.4), possibly *S. subsalsum* (tab. S2.5). *Thalassiosira* and *Minidiscus* were important further downstream, mostly downstream of 633 km (fig. 2.2d). Here, *Minidiscus* played a role from spring to summer, contributing up to 17 % to the eukaryotic phytoplankton. This taxon was clearly associated with higher salinities ($r = 0.83$, $p = 1.8 \times 10^{-7}$, fig. 2.3) and was most dominant at around ca. 5-10 PSU, which was also the case for the two most dominant genotypes (genotype 1 and 2, possibly *M. spinulatus*; tab. S2.5, fig. S2.6). However, the genus comprised 8 genotypes across seasons and stations and not all of them were positively correlated with salinity (fig. S2.6). For instance, genotype 3 (possibly *M. comicus*; tab. S2.5) did largely appear at lower salinities (ca. 0-5 PSU, fig. S2.5) and its contributions to the 18S phytoplankton reads were not significantly correlated with salinity or station (fig. S2.6). *Thalassiosira* appeared in all seasons, but was most dominant in winter ($r = -0.71$ with respect to temperature, $p = 5.0 \times 10^{-5}$, fig. 2.3). *Thalassiosira* was the second most dominant genus in our dataset, contributing on average approximately 8 % to the eukaryotic phytoplankton (fig. 2c). The genus comprised 19 genotypes (fig. S2.4). The highest genotype richness of *Thalassiosira* was found at 713 km in spring 2022 (10 genotypes; fig. S2.5). The genotypes of *Thalassiosira* showed strong differences in their relationship with abiotic parameters. Genotype 1 (possibly *T. guillardii*, tab. S2.5) was clearly associated with the winter season and negatively correlated with temperature (fig. S2.5-S2.6, $r = -0.63$, $p = 6.2 \times 10^{-4}$). Two other genotypes of *Thalassiosira* (genotype 3 and 4, not further classified, tab. S2.5) appeared at higher salinities in the lower estuary (e.g. at around 10 PSU) and were positively correlated with this parameter (fig. S2.5-S2.6, genotype 3: $r = 0.84$, $p = 1.0 \times 10^{-7}$, genotype 4: $r = 0.81$, $p = 5.4 \times 10^{-7}$).

Cryptophyceae, the second most dominant class in our dataset, contributed on average 18 % to the communities across seasons and stations (fig. 2.2a). This group appeared in all seasons and areas but was significantly more dominant at the mid stations (651 - 665 km, $p = 5.4 \times 10^{-4}$, tab. S2.4) and lower stations (692 - 713 km, $p = 1.1 \times 10^{-2}$, tab. S2.4) compared to the upper stations (609 - 633 km). The most dominant genus was *Cryptomonas*, the third most dominant taxon in our dataset with an average contribution of approximately 7 % (fig. 2.2c). *Cryptomonas* was particularly dominant in winter, when it contributed up to 26 % of the eukaryotic phytoplankton communities (fig. 2.2d). Moreover, this taxon was quite dominant in the mid area throughout seasons, e.g. contributing > 10 % to the communities at 665 km in spring and summer 2022 (fig. 2.2d). *Cryptomonas* reached significantly higher contributions in the mid area (651 - 665 km) compared to the upper stations (609 - 633 km, $p = 3.1 \times 10^{-2}$, tab. S2.4) and lower stations (692 - 713 km, $p = 1.8 \times 10^{-2}$, tab. S2.4). Though *Cryptomonas* appeared at the mid to lower stations, it was associated with low salinities ($r = -0.58$, $p = 2.0 \times 10^{-3}$, fig. 2.3) and only dominant further downstream when salinities were relatively low (e.g. < 3 PSU). This was for instance the case in winter 2022 (see also supplementary data fig. S2.1, tab. S2.1). *Cryptomonas* comprised 11 genotypes (fig. S2.4). Genotype richness was highest in summer 2021 at 609 km (10 genotypes; fig. S2.5), however, the two most dominant genotypes (genotype 1 and 2, possibly *C. curvata*, tab. S2.5) on average comprised ca. 86 % of the genus reads across seasons and stations (fig. S2.4). Genotype 2 was particularly dominant in winter and negatively correlated with temperature (fig. S2.5-S2.6, $r = -0.58$, $p = 2.1 \times 10^{-3}$), while genotype 1 appeared in similar manners across seasons and expressed no significant relationship to temperature. Both dominant genotypes of *Cryptomonas* were clearly negatively correlated with salinity (fig. S2.5-S2.6, genotype 1: $r = -0.54$, $p = 4 \times 10^{-3}$, genotype 2: $r = -0.44$, $p = 0.02$) but genotype 1 had a stronger affinity to the upper stations, i.e. a significantly negative correlation with stream km ($r = -0.41$, $p = 3.8 \times 10^{-2}$). Another cryptophyte, *Hemiselmis*, appeared nearly exclusively between 692 km and 713 km and was most dominant in summer 2021, when it contributed up to 12 % to the eukaryotic phytoplankton (fig. 2.2d). This taxon was associated with high salinities ($r = 0.75$, $p = 1.1 \times 10^{-5}$, fig. 2.3). However, *Hemiselmis* was most dominant at approximately 5 PSU (at 713 km in summer 2021; fig. 2.2d) and less dominant

in seasons where salinities were higher (up to 20 PSU) in the lower estuary. *Hemiselmis* was largely represented by a single genotype (fig. S2.4), possibly *H. andersenii* (tab. S2.5).

Chlorophyceae were the third most dominant class in the metabarcoding dataset, with an average contribution of 12 % to the eukaryotic phytoplankton reads across seasons and stations (fig. 2.2a). This group was particularly dominant from later spring (end of May 2022) to earlier summer (June 2022) in the upper to mid estuary (approximately 609 km - 665 km), where it achieved a contribution of up to 68 % (fig. 2.2b). Chlorophyceae were largely represented by the genera *Coelastrum* and *Mychonastes* (fig. 2.2c-d). *Coelastrum* was specifically strongly correlated with temperature ($r = 0.78$, $p = 2.3 \times 10^{-6}$, fig. 2.3). This taxon also went along with high chlorophyll *a* values ($r = 0.40$, $p = 0.04$, fig. 2.3), i.e. a high total phytoplankton abundance. *Coelastrum* comprised a single genotype and *Mychonastes* was largely represented by one dominant genotype (fig. S2.4). Both could not be classified beyond genus level (tab. S2.5).

Coscinodiscophyceae - mostly *Guinardia* and largely a single genotype therein, possibly *G. delicatula* (fig. S2.4, tab. S2.5) - and not further identified dinoflagellates (Dinophyceae) played a role downstream (ca. 692 - 713 km) in spring (2021 and 2022) and early summer (June 2022), respectively (fig. 2.2b, fig. 2.2d). *Guinardia* contributed up to 43 % to the eukaryotic phytoplankton reads, and Dinophyceae up to 50 %. Both groups were associated with higher salinities ($r = 0.73$, $p = 2.3 \times 10^{-5}$ for *Guinardia* and $r = 0.51$ and $p = 8.3 \times 10^{-3}$ for Dinophyceae). Precisely, Dinophyceae appeared most dominant in the summer sampling of 2022, when salinity varied between 9.8 PSU (692 km) and 20.0 PSU (713 km) in the lower estuary. *Guinardia* was most dominant at 713 km in spring (2021 and 2022) when salinity was up to approximately 10 PSU. This taxon also appeared at 692 km in spring 2022 when salinity was 4.7 PSU, but did not appear at this station in spring 2021 when salinity was 1.3 PSU.

Not further identified Chrysophyceae were further important parts of the eukaryotic phytoplankton in winter across stations, where they contributed 18-27 % (fig. 2.2b). Chrysophyceae were specifically associated with a high flow rate ($r = 0.65$, $p = 2.9 \times 10^{-4}$, fig.

2.3) and high turbidity ($r = 0.67$, $p = 2.0 \times 10^{-4}$, fig. 2.3), which are typical conditions in winter (see also supplementary data fig. S2.2 and fig. S2.3). Due to their high contributions in winter and minor contributions across seasons (fig. 2.2b), Chrysophyceae achieved an average contribution of nearly 10 % (fig. 2.2a).

Phytoplankton communities in the upper to mid estuary as provided by local monitoring (microscopy) & comparison with the metabarcoding-derived results

In the monitoring data from 2021 and 2022 - covering the area between 586 - 646 km of the Elbe estuary - Mediophyceae and unclassified centric diatoms (that were likely mostly Mediophyceae) were the most dominant groups of phytoplankton in the majority of the included seasons (HU, 2023; NLWKN, 2023) (fig. 2.4b). These groups contributed on average 66 - 69 % to the eukaryotic biovolume obtained from microscopy across seasons and stations (fig. 2.4a). At 586 km and 646 km, diatoms were further identified to genus level. Here *Stephanodiscus* (mostly *S. hantzschii;* fig. S2.7) and *Cyclotella* (mostly *C. meneghiniana*; fig. S2.7) (both Mediophyceae) were the most dominant genera across seasons (fig. 2.4c), contributing on average 23 % and 27 %, respectively. *Stephanodiscus* was particularly dominant in spring, contributing up to 71 % to the eukaryotic phytoplankton biovolume at single stations (fig. 2.4d). *Cyclotella* in contrast was most dominant in summer, with up to 73 % contribution (fig. 2.4d). Other key classes in monitoring were Bacillariophyceae (including, e.g., *Nitzschia*), Coscinodiscophyceae (including, e.g., *Aulacoseira*) and Chlorophyceae (including e.g. *Coleastrum*) (fig. 2.4a; see also species level data in fig. S2.7). Additionally, studies show that diatoms (e.g. *Skeletonema costatum*, *Thalassiosira pseudonana, Cyclotella striata, Guinardia delicatula*) and green algae (e.g. *Coelastrum microporum, Monoraphidium contortum*) played a role further downstream (> 646 km; e.g. at ca. 692 km) (Fast, 1993; Muylaert and Sabbe, 1999; Tillmann et al., 1999; Wolfstein, 1996) where monitoring data is not available.

Community composition was similar across methods. Contributions of key classes and genera were correlated when obtained from reads and biovolume ($R^2 = 0.59$, $p = 6.50 \times 10^{-20}$ and $R^2 = 0.33$, $p = 9.82 \times 10^{-16}$ respectively; see also supplementary fig. S2.8a-b). The overall

dominance of centric diatoms, in particular from the class Mediophyceae, is consistent between the results from microscopy and metabarcoding (fig. 2.4a-b). Between ca. 586 - 651 km *Stephanodiscus* was a key player in spring 2021 and 2022 both with respect to its relative biovolume (NLWKN, 2023) and the relative contribution to 18S reads of the eukaryotic phytoplankton (fig. 2.4d). Both methods imply that *Stephanodicsus* was largely represented by the species *S. hantzchi* (fig. S2.7, tab. S2.5). *Stephanodiscus* achieved similar contributions with microscopy and metabarcoding despite the different stations, sampling dates and methods (fig. 2.4d, fig. S2.9b). For instance, in spring 2021, *Stephanodiscus* contributed 71 % of the eukaryotic biovolume at 586 km on 2021-05-03 and 85 % of the eukaryotic phytoplankton reads at 609 km on 2021-05-07 (fig. 2.4d). Even across seasons, *Stephanodiscus* achieved an average contribution of 23 % in microscopy (NLWKN, 2023) and a comparable number of 29 % in metabarcoding (fig. 2.4c). Some other taxa reached similar contributions in certain seasons at closely related stations, e.g. *Cyclotella* (possibly mostly *C. meneghiniana*; see fig. S2.7, tab. S2.5) at 633 km (metabarcoding; ca. 25 %) and 646 km (microscopy; ca. 18 %) in summer 2021, *Skeletonema* at 609 km (metabarcoding; ca. 11 %) and 586 km (microscopy; ca. 14 %) in summer 2021 and *Coelastrum* at 646 km (microscopy, ca. 3 %) and 633 km (metabarcoding, ca. 4-5 %) in summer 2021 and spring 2022 (fig. 2.4d). Note that in the former examples, species identification differed between the two methods for *Skeletonema* and *Coelastrum* was not identified to species level in metabarcoding (see further information in tab. S2.5, fig. S2.7). Several phytoplankton taxa and groups found *via* metabarcoding in the unmonitored area further downstream, are known for the Elbe estuary from previous studies, e.g. *Thalassiosira* and *Skeletonema* (on genus level), *Guinardia delicatula* and, more vaguely, dinoflagellates (Muylaert and Sabbe, 1999; Tillmann et al., 1999; Wolfstein, 1996).

However, in some cases, the community composition differed between metabarcoding and microscopy. Across seasons and stations, Bacillariophyceae (e.g. *Nitzschia*) were significantly more dominant in the monitoring than metabarcoding ($p = 1.5 \times 10^{-2}$ and 1.1×10^{-2}, respectively; see also fig. S2.9a-b, fig. 2.4a; (HU, 2023; NLWKN, 2023)). The same was the case for Coscinodiscophyceae ($p = 2.9 \times 10^{-2}$, fig. S2.9a, fig. 2.4a), largely represented by *Aulacoseira* and *Triceratium* (fig. 2.4d). Different Mediophyceae, particularly *Cyclotella*,

reached significantly higher contributions with respect to their biovolume compared to their reads ($p = 1.8 \times 10^{-2}$ for Mediophyceae and $p = 5.2 \times 10^{-2}$ for *Cyclotella*, fig. S2.9a-b, fig. 2.4c-d). In metabarcoding, *Chlorophyceae* were significantly more dominant across seasons and stations ($p = 4.5 \times 10^{-2}$, fig. S2.9a, fig. 2.4a). Here *Coelastrum* was particularly dominant in summer 2022 (fig. 2.4d), while in other seasons, contributions of this taxon were more comparable across methods and overall, they were not significantly different (fig. S2.9b).

Chrysophyceae and Cryptophyceae reached significantly higher contributions in metabarcoding across seasons and stations compared to the monitoring data ($p = 3.4 \times 10^{-3}$ and $p = 7.9 \times 10^{-4}$, respectively, fig. S2.9a, fig. 2.4a-b), the latter mostly due to *Cryptomonas* ($p = 1.0 \times 10^{-2}$, fig. S2.9b, fig. 2.4c-d). We do observe enhanced contributions of *Cryptomonas* in winter at the microscopy stations too, but contributions were overall lower in monitoring (up to ca. 3 % in winter but lower in other seasons) than in metabarcoding (e.g. 17 % at 633 km in winter 2022). Beyond, species level identification differed, with *C. curvata* being the dominant *Cryptomonas* species *via* metabarcoding, while in microscopy species level could often not be obtained and otherwise included deviating species e.g. *C. ovata* (fig. S2.7). Some taxa, for instance *Aulacoseira*, *Thalassiocyclus* and *Triceratium* were not found by metabarcoding in any season. Vice versa, various picophytoplankton taxa (< ca. 2-3 µm) that were found *via* metabarcoding along the estuary (*e.g. Mychonastes, Minidiscus, Micromonas, Nannochloris, Ostreococcus*) did neither appear in the monitoring data, nor have they been reported in other literature that include the lower reaches of the Elbe estuary to our knowledge. Of those, *Mychonastes and Minidiscus* appeared particularly dominant (up to 17 % at certain stations during certain seasons) (fig. 2.2d).

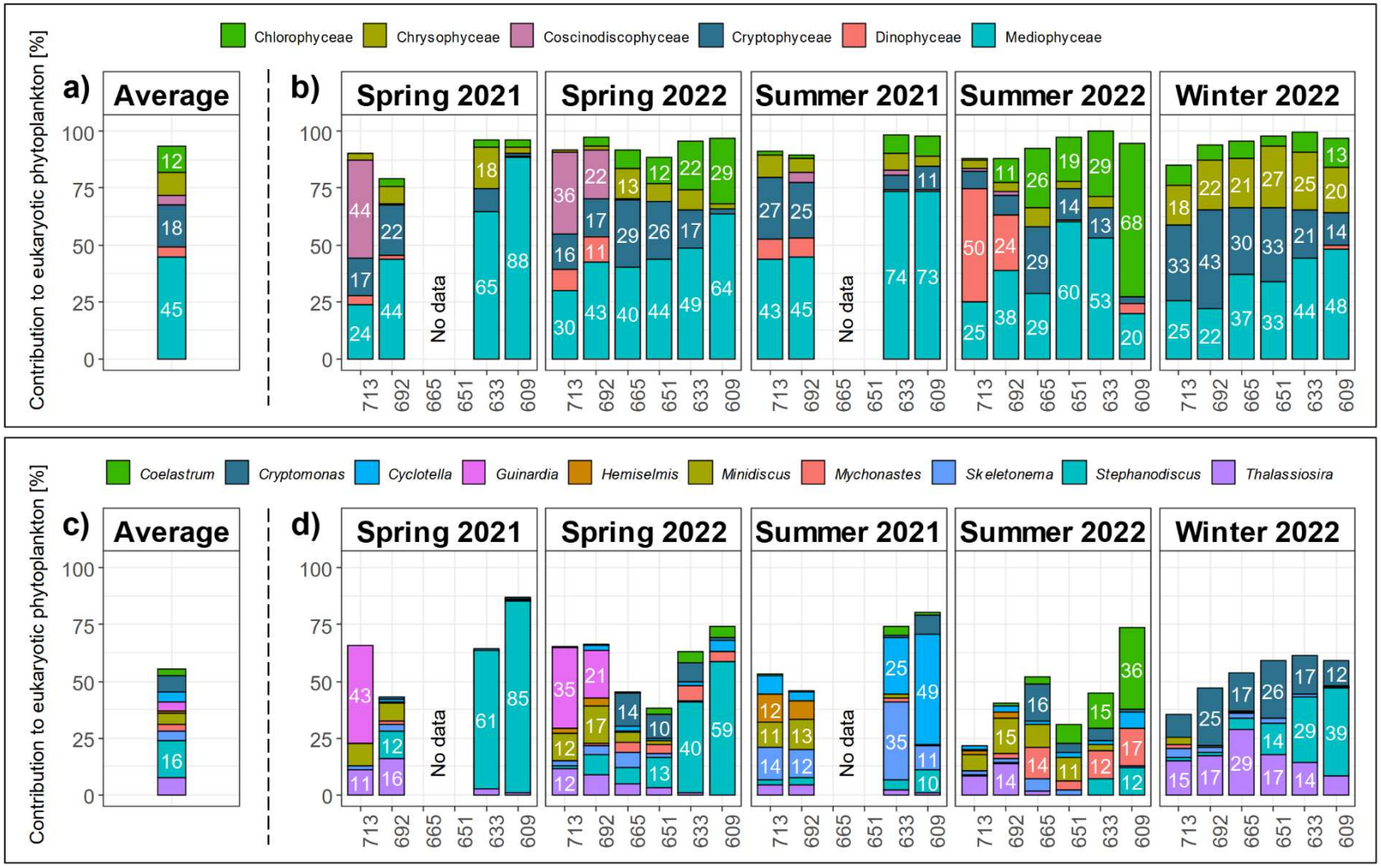

Fig. 2.2: Composition of eukaryotic phytoplankton in the Elbe estuary on class level (a, b) and genus level (c, d) based on metabarcoding reads. a) and c) show the average contributions calculated from the *relative* contributions of classes (a) and genera (c) across all seasons and stations (differences in *absolute* abundances are not included). In b) and d) the horizontal axes show the location in km and the panels show the different seasons (see also table S2.1). Only genera and classes that contributed ≥ 10 % respectively ≥ 15 % at least in one sample are shown. Labels are shown where contribution was ≥ 10 %.

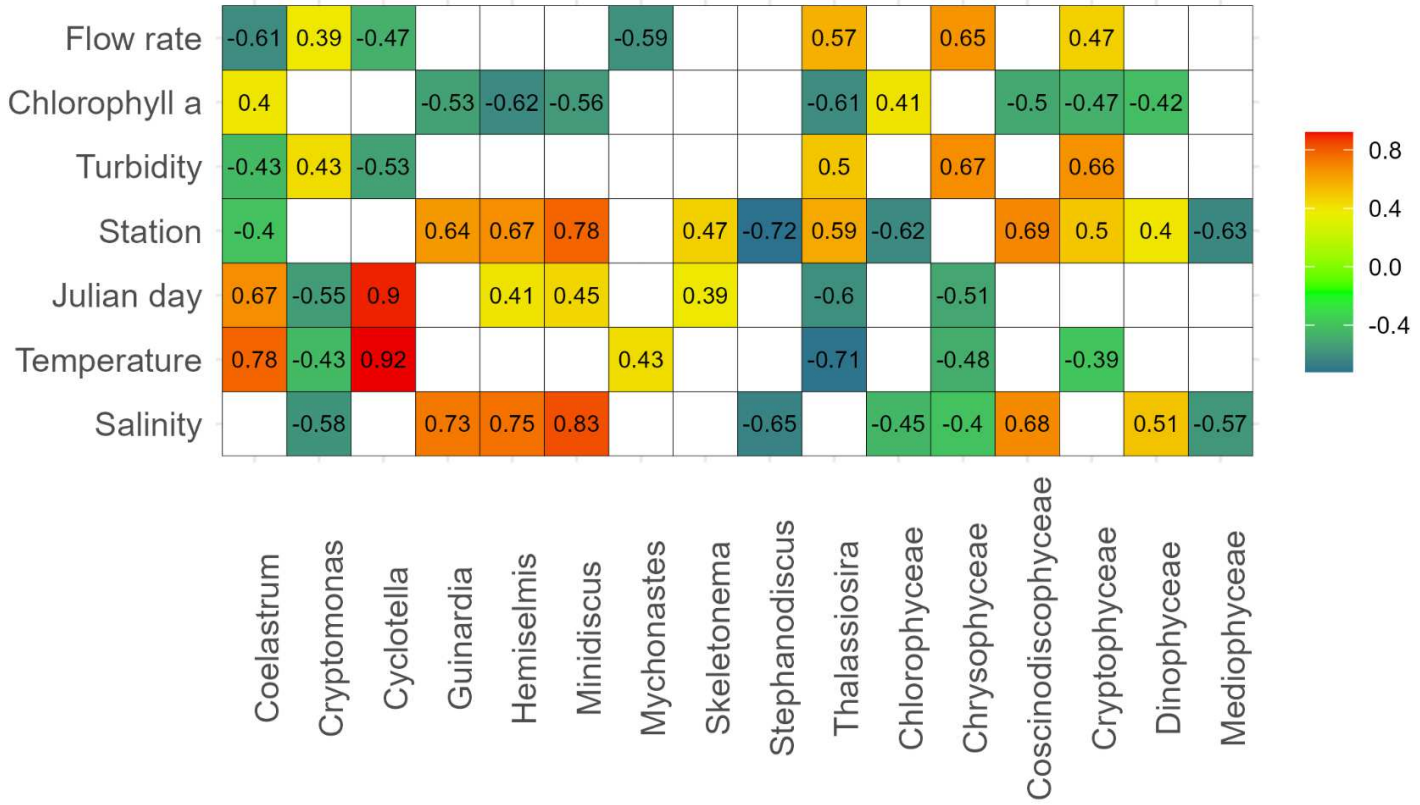

Fig. 2.3: Relationship between the contributions of phytoplankton (key genera and classes) and station, season as well as other environmental parameters. Numbers and color scheme show the correlation coefficient r calculated with spearman rank correlation. Numbers are shown if the relationship is significant ($p \leq 0.05$). All p-values and r-values are shown in the supplementary data (tab. S2.3). Flow rate is obtained from the FGG database (FGG Elbe, 2024) and refers to a fixed station in the upper Elbe (Neu Darchau, at ca. 536 km). Units for environmental parameters are shown in the supplementary material (tab. S2.1).

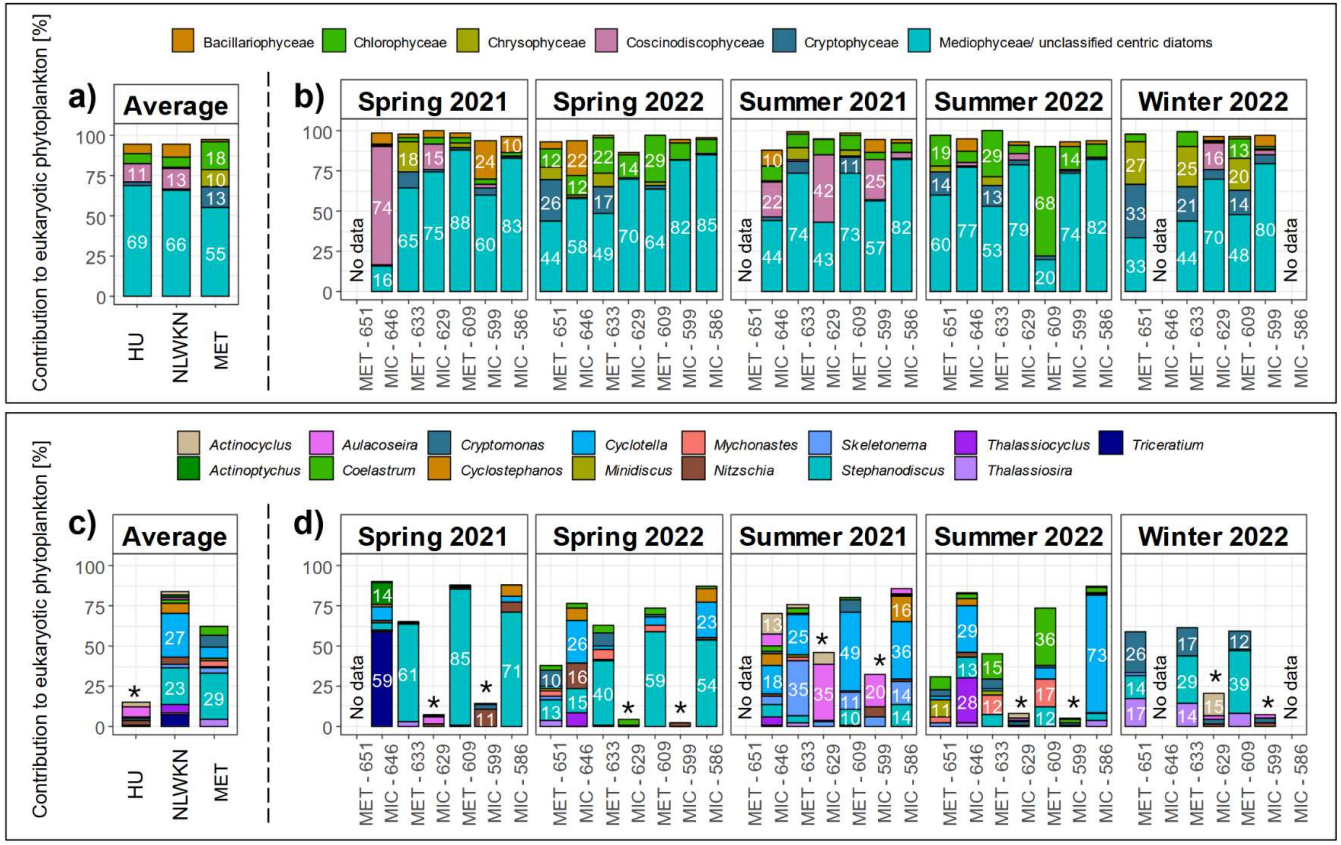

Fig. 2.4: Composition of eukaryotic phytoplankton in the upper to mid Elbe estuary (586 - 651 km) on class level (a, b) and genus level (c, d) with data from microscopy-based monitoring ((HU, 2023; NLWKN, 2023)**; MIC) and metabarcoding (MET; this study).** a) and c) show the average contributions calculated from the *relative* contributions of classes (a) and genera (c) across all seasons and stations (differences in *absolute* abundances are not included) for META and MIC (split by monitoring facilities NLWKN/HU due to non-classification of centric diatoms in HU data; stations per facility see fig. 2.1). In b) and d) horizontal axes show the location in km and give information if data was obtained from microscopy (MIC) or metabarcoding (MET) (see also fig. 2.1). Panels in b) and d) show different seasons, where the exact sampling dates differed between MIC and MET data (see tab. S2.1). Vertical axes show the contributions to biovolume (MIC) and 18S reads (MET). For better comparison, we summarized “unclassified centric diatoms” and “Mediophyceae” into one group in a) and b). In the monitoring from 599 km and 629 km, centric diatoms were not classified any further and hence genera data is missing in c) and d) as indicated by *. Only genera and classes that contributed ≥ 10 %, respectively ≥ 15 % at least in one sample are shown. Labels are shown where contribution was ≥ 10 %.

2.4. Discussion

Parasitic chytrids and nanoflagellates might have affected phytoplankton abundance and community composition

A drop in phytoplankton abundance (chlorophyll *a*) throughout the passage of Hamburg has been observed before and has been associated with strong grazing pressure in this area (Schöl et al., 2009). Selective grazing (see e.g. (Zamora-Terol et al., 2020)) might partially explain shifts in community composition observed between 609 km (upstream of the city of Hamburg) to 633 km (downstream of the city of Hamburg). For instance, in summer 2021, *Cyclotella* was dominant at 609 km and *Skeletonema* at 633 km (fig. 2.4d). In other seasons the shift in composition might not appear as obvious but the decline of the contribution of, e.g., *Stephanodiscus* from 609 km to 633 km does mean that other taxa were affected less by any lethal factors, or growing better. Shifts in community composition around the city of Hamburg appeared in similar manners in the monitoring data (e.g. in spring 2021, where *Stephanodiscus* dominated at 586 km and *Triceratium* at 646 km; (NLWKN, 2023)). However, grazing may not be the only cause of phytoplankton decline and community shifts. Other factors can for instance include the greater water depth in the harbor area compared to the area upstream of Hamburg that can result in light limitation (Wolfstein, 1996) and chytrid infections that have e.g. been observed in *Stephanodiscus* in the Elbe estuary (Muylaert and Sabbe, 1999). Notably, with 18S rRNA marker gene sequencing we identified chytrids from the group *Chytridiomycota* (e.g. *Zygophlyctis* and Rhizophydiales), which infect different types of phytoplankton (Holfeld, 2000; McKindles et al., 2023; Sassenhagen et al., 2023; Seto et al., 2020; Sime-Ngando, 2012), especially at 609 km. Further downstream we found the nanoflagellate *Cryothecomonas* which has been found to feed on *Guinardia* (Drebes et al., 1996; Tillmann et al., 1999). Chytrid-like and nanoflagellate parasites might affect phytoplankton in the Elbe estuary, but due to their sometimes small and inconspicuous appearance, they might be overlooked as a top-down control of community composition and algal biomass. The same applies all the more to viral infections, which have been found for e.g. *Guinardia* (Arsenieff et al., 2019) but are not covered by any of the methods applied in the Elbe estuary so far (e.g. light microscopy and our 18S rRNA sequencing). Viruses are

important entities in aquatic carbon cycles (see e.g. (Kaneko et al., 2021)) and likely also play a role in estuaries (Labbé et al., 2018).

Mixotrophic flagellates might play a larger role in the Elbe estuary than previously assumed

Flagellates from the classes Dinophyceae, Chrysophyceae and Cryptophyceae play a role in various estuaries (Bazin et al., 2014; Kim et al., 2023; Piwosz et al., 2018; Umanskaya et al., 2023; Wu et al., 2022) and are also known from the Elbe estuary (HU, 2023; NLWKN, 2023; Wolfstein, 1996). While the contributions of Dinophyceae in the monitored upper to mid estuary (586 - 651 km) were low (< 5 %) consistent across the methods, Chrysophyceae and Cryptophycae appeared overall more dominant when phytoplankton communities were assessed *via* metabarcoding. Though we lack comparable (and quantitative) data from the mid to lower estuary, this pattern seems to hold here: While dinoflagellates are reported from the lower estuary in former studies, chrysophytes and cryptophytes were either not included or possibly included as vague groups such as 'flagellates' (Muylaert and Sabbe, 1999; Wolfstein, 1996). An underrepresentation of these groups may be related to their fragile nature. Cryptophytes and chrysophytes have been described as sensitive to fixation agents that are commonly used to preserve microscopy samples (Altenburger et al., 2020; Cerino and Zingone, 2006; Medlin et al., 2017; Sonntag et al., 2000; Xia, 2013). Beyond, small-sized taxa such as *Hemiselmis* (ca. 5 µm) might in general be overlooked (Lane and Archibald, 2008). On the other hand, we lack information about the number of 18S gene copies held per cell of chrysophytes and cryptophytes. A high number of gene copies with respect to cell size can render a taxon to appear more dominant when metabarcoding is carried out compared to e.g. biovolumes obtained from microscopy. The available literature is limited and cannot provide clear answers. For instance, some sources report a higher representation of cryptophytes in metabarcoding compared to conventional techniques (Banerji et al., 2018; Hanžek et al., 2023), while others speak of an underrepresentation of cryptophytes based on 18S rRNA marker gene sequencing (Xu et al., 2023) and the cryptophyte *Rhodomonas salina* has an average number of SSU rDNA gene copies per cell with respect to its size (Godhe et al., 2008). Pigment analysis gives further support for the underrepresentation of cryptophytes by microscopy (e.g. (Gieskes and Kraay, 1983; Montoya

et al., 2006)). For chrysophytes, information is even more scarce. However, Charvet el al. found that chrysophytes were more dominant when assessed with microscopy (biomass) compared to metabarcoding reads (Charvet et al., 2012) which rather speaks against a consistent overrepresentation of this group based on sequencing.

While further research is needed to ultimately assess the quantitative relevance of the abovementioned phytoplankton classes in the Elbe estuary, some specific functions of these groups support their importance here and in similar ecosystems. Some taxa such as *Cryptomonas*, the most dominant cryptophyte in our dataset, are able to vertically migrate (deNoyelles et al., 2016), and hence can avoid grazing and support retention in the tidal estuary (Steidle and Vennell, 2024). Moreover, taxa from all three groups, i.e. dinoflagellates (Coyne et al., 2021; Millette et al., 2017), cryptophytes (Ballen-Segura et al., 2017; Princiotta et al., 2019; Urabe et al., 2000) and chrysophytes (Bec et al., 2006) are known for their mixotrophic abilities. Exploiting heterotrophic pathways might help those groups to survive under light limited conditions that typically appear in estuaries due to high turbidity. Transcriptome analyses have revealed that *Cryptomonas* compensates for low light availability in turbid waters by enhanced grazing on bacteria (Calderini et al., 2022). In our data, *Cryptomonas* was particularly dominant in winter, the season when light availability is typically rather low due to low sunlight and high turbidity (fig. 2.2-2.3, fig. S2.1-S2.2). Recent studies have shown that actively mixotrophic flagellates are key components in estuaries (Dobbertin da Costa et al., 2024; Li et al., 2024; Millette et al., 2021).

Their motility and ability to use alternative sources of energy and nutrients might allow mixotrophic flagellates to persist where other phytoplankton taxa are removed by currents or constrained by light limitation. These groups might consequently play a crucial role to maintain primary production and food webs. By incorporating organic carbon (e.g. bacteria) phagotrophic phytoplankton make energy and nutrients available for higher trophic levels. Due to their ability to draw on different sources of nutrients and energy mixotrophs are a more stable food source for higher trophic levels (Katechakis et al., 2005) which is of specific relevance in estuaries and similar ecosystems where phytoplankton abundance can be limited due to environmental forcing (e.g. turbidity, salinity). Simultaneously, by utilizing

heterotrophic pathways, mixotrophic phytoplankton contribute to higher CO_2 production. Considering that phagotrophs might become more reliant on organic prey under warming (Gonzalez et al., 2022; Lepori-Bui et al., 2022), we could head towards a more heterotrophic system that might further negatively affect the oxygen budget of this habitat (Geerts et al., 2017).

Metabarcoding emphasizes the importance of eukaryotic picophytoplankton in estuarine communities

Picophytoplankton are a key component in phytoplankton communities in estuaries (e.g. (Moreira-Turcq et al., 2001; Purcell-Meyerink et al., 2017)). This may be associated with their ability to survive under extreme conditions (Belkinova et al., 2021; Somogyi et al., 2022) and at different light conditions (Callieri, 2017; Tragin and Vaulot, 2019). In a former study, we found that picophytoplankton from the Elbe estuary were able to utilize miscellaneous organic compounds (e.g. sugars, amino acids), which might allow them to maintain growth in the challenging habitat (Martens et al., 2024a). Though there is information about the gene copy numbers of some picophytoplankton taxa (Godhe et al., 2008) and they do have similar gene copies to cell size ratios as larger phytoplankton, we do lack respective data for the most dominant picophytoplankton in our dataset (i.e. *Mychonastes*, *Minidiscus*). Hence, we cannot say if or to what extent picophytoplankton might be overrepresented in our data compared to e.g. biovolume based community assessments. However, picophytoplankton can be difficult to detect and quantify with microscopy due to their small size or sensitivity to fixation agents (see e.g. (Bergkemper and Weisse, 2018; Huo et al., 2020)). In the Elbe estuary, *Minidiscus* and *Mychonastes* were particularly dominant when communities were analyzed *via* metabarcoding (fig. 2.2d). *Mychonastes* has been isolated from the upper Elbe river before (Krienitz et al., 2011) and in a recent study we isolated different strains from the estuarine reaches (Martens et al., 2024a). Both *Minidiscus* and *Mychonastes* underwent changes in taxonomic assignments. *Mychonastes* e.g. might be included as *Dictyosphaerium* in former studies and monitoring data (Krienitz et al., 2011). However, though *Dictyosphaerium* was reported by the monitoring facilities (HU, 2023; NLWKN, 2023) we cannot conclude that it necessarily or exclusively referred to *Mychonastes*. *Dictyosphaerium*

can include colony-forming types that can be more easily detected in microscopy *and* the primarily solitary *Mychonastes* (Krienitz et al., 2011). Notably, both *Dictyosphaerium* and *Mychonastes* were quite dominant in summer 2022, providing up to ca. 9 % of the biovolume (at 629 km; (HU, 2023)) respectively up to 17 % of the metabarcoding reads (at 609 km). This may indicate that they do mean the same group in metabarcoding and microscopy or that those are different taxa that have similar traits with respect to e.g. temperature. Species level identification implies that *Minidiscus* might be largely represented by *M. spinulatus* and *M. comicus*, which have a cell diameter of 2 - 6 µm (Jewson et al., 2016; Park et al., 2017). In the monitoring data, *Minidiscus* might appear as *Thalassiosira* (Park et al., 2017) (e.g. as *Thalassiosira proschkinae*; fig. S2.7) or unidentified centric diatoms < 5 µm but those groups did not express comparable contributions to the eukaryotic phytoplankton. We also lack recent quantitative microscopy data from the mid to lower estuary where *Minidiscus* was particularly dominant but the absence of key species from metabarcoding, such as *M. spinulatus* (also as *Thalassiosira spinulata* (Park et al., 2017)) in former datasets (e.g. (Muylaert and Sabbe, 1999; Wolfstein, 1996)), might imply that *Minidiscus* is not (thoroughly) covered by microscopy. It has been suggested before that small diatoms such as *Minidiscus* are globally overlooked (Leblanc et al., 2018).

By incorporating dissolved organic compounds (Martens et al., 2024a), picophytoplankton may pass on important nutrients along the food webs. Though picophytoplankton may not always be directly consumed by dominant zooplankton groups such as *Eurytemora* (Schöl et al., 2009), it has been suggested that copepods might consume picophytoplankton rather indirectly by uptake of picophytoplankton-containing aggregates (Stukel et al., 2013; Wilson and Steinberg, 2010). Aggregate formation is a typical feature of various aquatic ecosystems including estuaries (Zimmermann-Timm et al., 1998) and estuarine zooplankton might swap to an aggregate diet when phytoplankton availability is low (Modéran et al., 2012). While the nutritional value of aggregates (including e.g. detritus) might be rather low, aggregate-attached phytoplankton (Stukel et al., 2013; Zimmermann-Timm et al., 1998) can add important nutrients such as fatty acids. In areas with low availability of larger-celled taxa such as the mid to lower estuary, zooplankton might be dependent on aggregate-associated

materials, and hence possibly on picophytoplankton. Additionally, picophytoplankton are crucial prey for nauplii larvae and filter feeders (Bemal and Anil, 2019; Richard et al., 2022).

Coastal inputs determine community composition in the lower estuary

The combination of the different currents (river flow, tide) resulted in different salinity conditions in the lower and partially mid estuary (see also further description in the methods and supplementary data fig. S2.1 and tab. S2.1). In winter 2022, when river flow was high (> 1000 m^3 s^{-1}) and sampling was carried out during decreasing tide, salinity rather gradually increased from 665 km (freshwater) to 713 km (2.7 PSU) and the community structure changed in similar manners, i.e. rather moderately. For instance, *Cryptomonas*, which was negatively correlated with salinity (fig. 2.3) contributed similar proportions to the eukaryotic phytoplankton reads in the mid estuary at 651 km (26 %) and in the lower estuary at 692 km (25 %) under freshwater conditions (ca. 0-1 PSU) (fig. 2.2d). In spring 2021, spring 2022 and summer 2022, salinity was higher in the lower estuary (ca. 10 - 20 PSU at 713 km) and there were partially clear boundaries where certain taxa occurred. For example, in spring 2022, *Cryptomonas* contributed ca. 14 % at 665 km at 0.9 PSU, but was practically absent at 692 km where salinity was 4.7 PSU (fig. 2.2d). Similarly, in spring 2021 and spring 2022, *Guinardia*, which was positively correlated with salinity (fig. 2.3), only appeared at stations with salinities above ca. 5 PSU, i.e. at 713 km during both spring samplings and at 692 km only in spring 2022 (fig. 2.2d). Dinoflagellates and *Hemiselmis* were further key groups that appeared overall more dominant at higher salinities. Dinoflagellates were most dominant at ca. 20 PSU in summer 2022, but also appeared at lower salinities, including freshwater, which is reasonable as this group includes various taxa. *Hemiselmis* was most dominant at ca. 1 - 5 PSU in summer 2021. While shifts in salinity can affect phytoplankton, it is likely that movement of the water masses itself had a stronger and more immediate effect on the phytoplankton communities. Marine dinoflagellates (Jansen et al., 2006; Klöpper et al., 2003) and *Guinardia* (Hernández-Fariñas et al., 2014; Schlüter et al., 2012) for instance are important in the North Sea. *Guinardia* is moreover considered an exclusively marine taxon. However, coastal taxa may benefit from river-born materials (see e.g.

(Schlüter et al., 2012; Weston et al., 2008)) and hence their dominance in the lower estuary might not just be coincidental.

In former studies, we find different statements concerning the community composition in the lower Elbe estuary. Muylaert and Sabbe (Muylaert and Sabbe, 1999) speak of in situ production rather than coastal imports, however, it remains unclear which stations they refer to (e.g. rather stations near 713 km or 692 km), but sampling was carried out during rather low salinities. In our data, marine taxa and groups were specifically found at salinities above ca. 5 PSU. Wolfstein (Wolfstein, 1996) found freshwater, brackish and marine taxa at a station near 692 km, but data about their quantity is not available. In the study of Tillmann et al. (Tillmann et al., 1999) the marine taxon *Guinardia delicatula* appeared close to our lower station (713 km) but not further upstream. Altogether, our study provides further understanding about the so far rather limited data on community composition in the lower Elbe estuary.

Broad distribution of certain genera might be explained by different ecotypes

Most of our key genera comprised various genotypes which partially expressed different patterns along space and time respectively abiotic conditions (fig. 2.2, fig. S2.5-S2.6). The different genotypes might represent different ecotypes that inhabit different ecological niches. Combining metabarcoding, microscopy data from the local monitoring (where available) and further literature we find that though some of those potential ecotypes do represent different species (see also tab. S2.5, fig. S2.7) genotypic diversity along environmental conditions appears within species in various cases. This implies that the species alone is not sufficient to explain their distribution.

For instance, *Thalassiosira* and *Stephanodiscus* included one genotype each that was particularly dominant during colder seasons. In the case of *Thalassiosira* this genotype was identified as *T. guillardii*. We lack species identification for the genotype of *Stephanodiscus* associated with lower temperature, but in spring 2021 the genotype appeared to have similar contributions to the eukaryotic phytoplankton as the species *S. minutulus* in

microscopy (fig. S2.7, fig. S2.6, genotype 3), which might imply that the genotype represents this taxon. Both *S. minutulus* and *T. guillardii* are known from other estuaries but not necessarily from the colder seasons (Piwosz et al., 2018; Trigueros, 2000). Similarly, *Minidiscus* seems to divide into different species, with *M. spinulatus* (fig. S2.5, genotype 1 and 2) appearing at higher salinities, while *M. comicus* (genotype 3) was mostly found at 5 PSU or lower salinities, but both taxa appear from brackish to marine habitats (Fernandes and Correr-Da-Silva, 2020; Park et al., 2017). The findings of the same species along different habitat conditions show that the species alone is not sufficient to describe the ecological positioning of these phytoplankton. This is also the case for *Cryptomonas*, where the genotype associated with lower temperatures was assigned to the same species (*C. curvata*) as the other dominant genotype that appeared more important in spring and summer. Genotype diversity of *C. curvata* has been described before (Nishino et al., 2015) and might explain the broad distribution of this species along space and time.

Deviations between microscopy and metabarcoding might be explained by differences in sampling stations and dates and by methodological biases

The correlation between the contributions of various key classes and genera based on reads and biovolumes (fig. S2.8a-b, fig. 2.4) implies a correlation of the number of gene copies per cell with the size of the phytoplankton taxa in the samples, as shown by, e.g., (Godhe et al., 2008; Vasselon et al., 2018). In cases where the results were less similar, those differences can to a certain degree be explained by the different sampling stations and sampling time points (see also supplementary data tab. S2.1). For instance, *Triceratium* (Coscinodiscophyceae) was dominant in spring 2021 at the monitoring station at 646 km (fig. 2.4d). This taxon did not appear in any other microscopy sample from the included dataset, hence, the fact that we did not find this taxon *via* metabarcoding might be due to its narrow spatio-temporal appearance. Similarly, the dominance of *Coelastrum* in metabarcoding in summer 2022 may be an effect of the specific conditions during sampling, as in other seasons, contributions of this taxon were more similar across methods (fig. 2.4d). The metabarcoding sampling in summer 2022 was carried out approximately two weeks earlier than that for monitoring (supplementary data tab. S2.1). During these two weeks, water

temperatures were rising by approximately 2.5 °C ((FGG Elbe, 2024); supplementary data fig. S2.10). This might explain a shift from the dominance of *Coelastrum* (metabarcoding, 2022-06-22) towards higher contributions of *Cyclotella* (monitoring, 2022-07-04). In 2021, when summer sampling was carried out later during the water temperature peak of the year ((FGG Elbe, 2024); supplementary data fig. S2.10), *Cyclotella* was dominant across methods (fig. 2.4d). Ultimately, this might also partially explain why *Cyclotella* appeared on average more dominant in microscopy (fig. 2.4c).

Due to the different sampling stations and dates we cannot completely disentangle where biases were method-related or actual ecological features. However, there is reasonable evidence that some differences cannot be fully explained by spatio-temporal effects. Quantitative differences between the methods - i.e. taxa being differently dominant - can for instance appear when a taxon has a relatively high or low number of 18S gene copies with respect to its size. We might argue that the overall higher contribution of pennate diatoms from the class Bacillariophyceae in microscopy compared to metabarcoding (fig. 2.4a-b) might be caused by such biases. Qualitative differences can appear when taxa are assigned differently or identified only by one of the methods. For instance, we found several picophytoplankton taxa *via* metabarcoding that were so far not reported from the Elbe estuary (e.g. *Minidiscus*, *Mychonastes*). As discussed in a section further above, some of them might be - to a certain extent - included under other names in the monitoring efforts or further literature (e.g. *Mychonastes* as *Dictyosphaerium*; (Krienitz et al., 2011)). However, picophytoplankton appears overall more prominent in metabarcoding (see also section further above) than previously reported in other literature or the monitoring data, which might be related to difficulties in detecting their small mostly solitary cells via microscopy, and due to fixation issues (see e.g. (Bergkemper and Weisse, 2018; Huo et al., 2020)). In turn, in metabarcoding, primer mismatch or incomplete sequencing databases can lead to failure to identify taxa (e.g. (Gran-Stadniczeñko et al., 2019; Huo et al., 2020; Santoferrara, 2019)). This might have been the case for *Aulacoseira*, a genus well known from the Elbe estuary which was especially important in summer 2021 in the monitoring ((HU, 2023), fig. 2.4d, e.g. at 629 km), while not a single read was found *via* metabarcoding of any sample.

Method limitations and need for further research

Both metabarcoding and microscopy do provide valuable insights into the presence of certain taxa in certain areas, which are relevant components in the food webs here. However, when studying community composition, irrespective of the method, certain information remains largely unrevealed. For instance, we know nothing about the actual performance (e.g. growth) of phytoplankton under certain conditions. Do taxa appear more dominant than others because they grow well or just survive better? Do they have specific hydrodynamical traits with respect to cell morphology that make them accumulate in certain areas despite unfavorable environmental conditions? Are potential mixotrophic taxa actively mixotroph in this ecosystem? Beyond those general uncertainties, other factors such as the sampling strategy (e.g. number of samples, locations, dates, and also how sampling is carried out along a moving water body) can affect the results and restrict ecological conclusions.

Further methodological constraints can additionally complicate data interpretation. For instance, primer mismatch, PCR biases and incomplete databases (Kelly et al., 2019; Kezlya et al., 2023; Santoferrara, 2019) can lead to failure to detect or adequately represent taxa and finally affect species composition outputs. The quantitative comparability of metabarcoding with conventional approaches such as microscopy can be affected by the number of gene copies in a cell, which is correlated with cell size but might sometimes experience stronger variations even for strains of the same species (Godhe et al., 2008; Gong and Marchetti, 2019; Vasselon et al., 2018). In microscopy, indistinct morphology, small cell-sizes and effects of fixation agents can affect the accuracy of reported community structures (Bergkemper and Weisse, 2018; Kezlya et al., 2023; Medlin et al., 2017). Identification errors might additionally play a role as sample analysis is not automated but depends on the observer.

By focussing on dominant key taxa, we can largely avoid including artifacts (such as free floating DNA) in our study. The finding of certain groups (e.g. picophytoplankton and Cryptophyceae) along seasons and stations additionally provides certainty about their actual

importance in this ecosystem in quantitative means, and indicate that random process e.g. with respect to PCR amplification did rather not play a significant role. An overlap of key taxa (e.g. *Stephanodiscus hantzchii, Cyclotella meneghiniana*; fig. 2.4, tab. S2.5, fig. S2.7, fig. S2.5) found *via* metabarcoding and microscopy in the upper to mid estuary provides further support about the reliability of the metabarcoding data and their comparability with data from microscopy. However, uncertainties remain from the relatively low number of samples, the missing of replicates and the absence or underrepresentation of certain sampling seasons (fall and winter) and areas (e.g. the mid area which was not sampled in 2021). Moreover, further studies and other research approaches are needed to more thoroughly address how potential drivers such as turbidity and salinity affect the estuarine phytoplankton in causal means (e.g. transcriptome analysis (Calderini et al., 2022) or experimental studies (Sew and Todd, 2020; Wirth et al., 2019)). This is also crucial to differentiate between actual drivers that affect the performance and hydrodynamics (i.e. growth/ survival and current driven distributions of taxa). Also, we suggest determining the actual mixotrophic behavior of potential mixotrophic groups such as cryptophytes, chrysophytes and dinoflagellates (as e.g. in (Dobbertin da Costa et al., 2024; Millette et al., 2021)).

Our study provides first insight in the comparability of microscopy and metabarcoding data from the Elbe estuary. However, as we made use of an available microscopy dataset, samples were not obtained at the same time points or stations, and microscopy data was not available from downstream of 646 km. Differences in the composition of the samples may affect the comparability, and ecological and methodological biases could not be completely disentangled in this study. While we could obtain various valuable information from the comparison, e.g. the missing of certain taxa such as *Aulacoseira* in metabarcoding, but also the complying of different key taxa across methods, comparing metabarcoding and microscopy from the same samples as carried out for other ecosystems (Huo et al., 2020; Mora et al., 2019; Santi et al., 2021) would help to ultimately evaluate the comparability of both approaches in the Elbe estuary and similar ecosystems. As our primer set, which targets the V1-V2 region of the 18S gene, could not amplify certain important taxa (e.g. *Aulacoseira*) we furthermore suggest the use of different more commonly used primers in

further metabarcoding efforts, e.g. 18S primers targeting the V4 or V9 region (Kezlya et al., 2023).

Today, combining metabarcoding and microscopy is the approach of choice to appropriately characterized phytoplankton communities - covering the weaknesses of both methods (Huo et al., 2020; Mora et al., 2019; Santi et al., 2021). However, while further research is needed to eliminate weak points of metabarcoding, its implementation as a standard method to analyze phytoplankton communities appears inevitable due to its benefits especially with respect to automated sample processing, the independence of morphological structures, size and sample fixation. While the desire for comparability and familiar measures such as biovolume appears reasonable, in the discussion about a long-term implementation of metabarcoding, we might also question our current perspectives: Does metabarcoding have to obtain the exact same results as microscopy? Are conventional measures such as cell counts or biovolume the right ones? Are results of metabarcoding, i.e. the detected number of DNA sequences of a taxonomic group, of less ecological relevance?

2.5. Conclusion

We used metabarcoding to identify key taxa along the Elbe estuary, which is characterized by typical estuarine features, such as variations in turbidity and salinity. Results were compared with those available from microscopy-based monitoring and further literature. An overlap in the results from metabarcoding (reads based eukaryotic phytoplankton community composition) and microscopy (biovolume based eukaryotic phytoplankton community composition) indicates that the methods yield comparable results for many key taxa, while certain groups such as picophytoplankton, cryptophytes and chrysophytes appeared underrepresented by microscopy. As phagotrophs, the latter might play a specific role in the turbid light-limited reaches of the estuary. However, further research is needed to ultimately draw conclusions about the role of the abovementioned groups in the Elbe estuary and about the comparability of the results from metabarcoding with those from microscopy (e.g. including larger samples sizes, direct comparison of the methods from the same samples and laboratory experiments aimed at the causal relationship of taxa abundance with environmental conditions).

3. Picophytoplankton dominate phytoplankton communities in the Elbe estuary in terms of cell counts

We plan to publish this chapter in a peer-reviewed journal at a later date.

Abstract

Picophytoplankton are important primary producers, but not always adequately recognized, e.g. due to methodological limitations. In this study, we combined flow cytometry and metabarcoding to investigate seasonal and spatial patterns of picophytoplankton abundance and community composition in the Elbe estuary. Picophytoplankton (mostly picoeukaryotes such as Mychonastes and Minidiscus) contributed on average 70 % (SD = 14 %) to the total phytoplankton counts. In the summer picocyanobacteria (e.g. Synechococcus) played a more significant role. The contributions of picophytoplankton to the total phytoplankton were particularly high from summer to winter as well as in the mid estuary. However, at salinities of around 10 PSU in the mixing area the proportion of picophytoplankton was comparably low (average 49 %, SD = 13 %). Our results indicate that picophytoplankton prevail in the Elbe estuary year-round with respect to cell counts. Picophytoplankton could occupy important niche positions to maintain primary production under extreme conditions where larger phytoplankton might struggle (e.g. at high or low temperature and high turbidity), and also benefit from high nutrient availability here. However, we did not find evidence that they played a particularly significant role at the salinity interface. Our study highlights the importance of including picophytoplankton when assessing estuarine phytoplankton as has been suggested for other ecosystems such as oceans.

3.1. Introduction

Picophytoplankton (< 2-3 µm) are important primary producers in aquatic ecosystems from oligotrophic to eutrophic habitats (Coello-Camba and Agustí, 2021; Moreira-Turcq et al., 2001; Purcell-Meyerink et al., 2017; Takasu et al., 2023; Zhang et al., 2015). These tiny organisms fulfill crucial ecological functions, e.g. as food for nauplii larvae and filter feeders

(Bemal and Anil, 2019; Richard et al., 2022) and in carbon export (Basu and Mackey, 2018; Puigcorbé et al., 2015). The small size of picophytoplankton allows them to occupy specific ecological niches, for example due to the high surface to volume ratio which might facilitate the uptake of required nutrients, and slow sinking velocity that can keep them in the euphotic zone (Massana, 2011; Raven, 1998). Short generation times and high standing genetic variation give picophytoplankton a comparatively high evolutionary potential (e.g. (Barton et al., 2020; Benner et al., 2020; Schaum et al., 2016)). Picophytoplankton are more than likely to prevail in changing environments (see e.g. (Benner et al., 2020; Flombaum and Martiny, 2021a; Tan et al., 2022)). Some picophytoplankton have been shown to appear under extreme conditions e.g. at high or varying salinity, turbidity and temperature (Belkinova et al., 2021; Somogyi et al., 2022).

Extreme living conditions are common across ecosystems, including estuaries. Estuaries are the interfaces between the freshwater and marine world and characterized by gradients and tidal-induced variation of environmental forcing (e.g. salinity, turbidity) and picophytoplankton can be an important group here (Gaulke et al., 2010; Moreira-Turcq et al., 2001; Purcell-Meyerink et al., 2017; Sathicq et al., 2020). However, due to their small size picophytoplankton are still often not adequately recognized. This is largely due to difficulties in detecting and identifying these small-celled organisms with light microscopy, and because they cannot always be thoroughly preserved (Bergkemper and Weisse, 2018; Huo et al., 2020).

Here, we applied flow cytometry and metabarcoding (partially from (Martens et al., 2024b), in the context of new metabarcoding data) to (1) investigate spatial and seasonal patterns in picophytoplankton abundance and composition in the Elbe estuary, (2) identify dominant taxa and (3) assess under which conditions (with respect to abiotic factors, season, location) picophytoplankton and different players within (e.g. picocyanobacteria) might be particularly dominant.

3.2. Material and Methods

The Elbe estuary is located in the North of Germany, passing through the city of Hamburg, and enters the North Sea at Cuxhaven (fig. 3.1a). As one of Europe's largest estuaries it is an important natural habitat and supplies the human population with essential ecosystem services (e.g. *via* port of Hamburg, recreation areas). The Elbe estuary has been experiencing intense anthropogenic pressure for centuries and further changes such as global warming or deepening of shipping channels might have additional impacts on the ecosystem functioning (see e.g. (Van Maren et al., 2015)). The tidal estuarine area is separated from the Elbe river by a weir at 586 km distance from the river source. Here, a total of 50 surface water samples were taken from seven stations along the Elbe estuary during different sampling campaigns (fig. 3.1a, supplementary tab. S3.1). Samples were taken from the upper water layers. Further details about sampling in the different sampling campaigns - e.g. sampling method and sample volume - are given in the supplementary data (tab. S3.1). 25 of the samples were taken around the city of Hamburg (approx. 623 - 633 km) and used as a seasonal dataset (fig. 3.3, fig. S3.4) and 29 samples from longitudinal sampling of six stations (609 - 713 km) covering three different seasons (spring and summer each 2021 and 2022 as well as winter 2022) were used as a spatial dataset (fig. 3.2a-c, fig. S3.2).

Of each sample, 3 to 5 technical replicates à 20 µL were analyzed using flow cytometry (BD accuri C6 plus) with a flow rate of 66 µl min^{-1} and regular cleaning and mixing between the samples. Phytoplankton cells could be distinguished from other suspended matter by their cytometric properties (e.g. fluorescence, size) which were also used to identify different groups of phytoplankton (see e.g. (Ning et al., 2021; Read et al., 2014; Thyssen et al., 2022) and supplementary material fig. S3.1). Picophytoplankton in the included samples from the Elbe estuary could be divided into two major groups: Picoeukaryotes and picocyanobacteria. Picocyanobacteria differed from picoeukaryotes in their fluorescence properties. This group had a higher phycocyanin- and lower chlorophyll-fluorescence (fig. S3.1). Notably, some larger cells might be excluded from our analysis due to detection limits and low sample volume. However, we know from former data (see e.g. (Martens et al., 2024b; NLWKN,

2023)) that taxa < 40 µm (e.g. *Stephanodiscus*, *Cyclotella*) were dominant in most seasons and areas of the Elbe estuary.

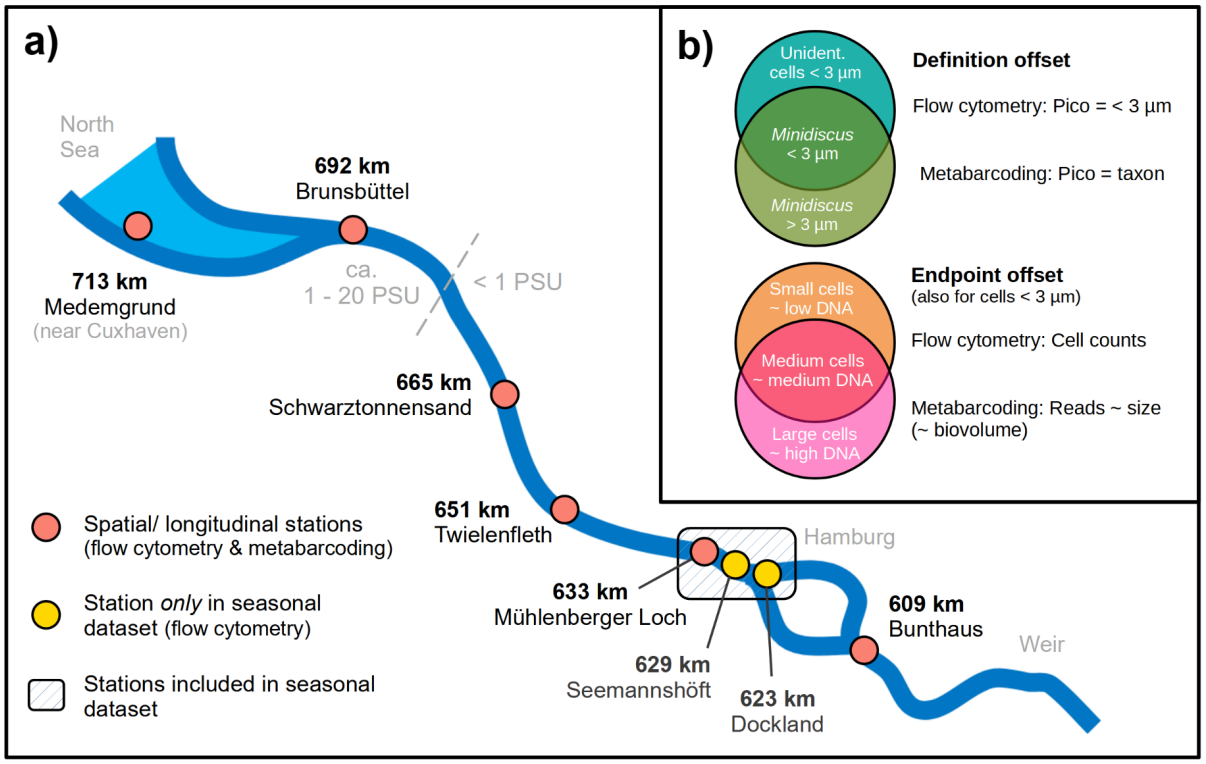

Fig. 3.1: Study area (Elbe estuary) and sampling stations of the seasonal and spatial dataset (a) and schematic overview of the overlap and offset between the measured endpoint and definition of picophytoplankton (Pico) by the different methods (b). In (a) "km" metric indicates the approximate distance from the spring of the Elbe river in the Czech Republic. The discontinuous line shows the approximate border between freshwater and increased salinities during the sampling campaign. In (b) text within the circles are examples.

For the spatial dataset, 16S rRNA metabarcoding as well as 18S rRNA metabarcoding from another study (see further information in (Martens et al., 2024b)) were included to add information about picophytoplankton taxa in the Elbe estuary (fig. 3.2d-e, fig. S3.3). Samples for 16S rRNA sequencing were processed in the same way as shown for the 18S data (Martens et al., 2024b), however, reads were assigned using the BLAST database (carried out by biome-id Dres Barco & Knebelsberger GbR). In both datasets, we selected taxa that are in general considered picophytoplankton or can be < 3 µm (e.g. *Synechococcus*, *Choricystis*, *Mychonastes, Minidiscus*). We kept colony forming taxa that might appear solitary where single cells *can* be < 3 µm (e.g. *Microcystis*) - as well as unidentified cyanobacteria - in the dataset as they might add to the picocyanobacteria counts in the cytometry data. Note that

the definition of picophytoplankton in the metabarcoding data is based on taxa identity and their *usual* size ranges, while in flow cytometry the definition is exclusively based on the *actual* cell size (< 3 µm) (fig. 3.1b). Furthermore, while in flow cytometry we detect abundance, metabarcoding results are rather correlated with biovolume. This is due to the size dependence of DNA copies per cell (Godhe et al., 2008) and as a result, larger (picophytoplankton) taxa might appear more dominant in metabarcoding compared to flow cytometric data without being more abundant in terms of cell counts. Consequently, what is included in "picophytoplankton" and how dominant it is can to some extent differ between the methods (see fig. 3.1b for further examples/ details). We also excluded data from samples with less than 100 picocyanobacteria, respectively picoeukaryotes reads in metabarcoding (fig. S3.3). The number of picophytoplankton reads per sample varied from 147 to 6108 (average 1733) in the 18S dataset and 113 to 5692 (average 2155) in the 16S dataset.

Data were processed in R (version 4.1.3), including the packages tidyverse (version 1.3.2), ggplot2 (version 3.4.0), lubridate (version 1.9.2), scales (version 1.2.1) and MuMIn (version 1.47.5). We also used LibreOffice Draw (version 7.1.2.2) for overview figures and addition of text notes. For spatial analyses, we obtained potentially interesting patterns from the figures showing cell counts and contributions of picophytoplankton groups along stations (fig. 3.2a-c, fig. S3.2) and then carried out an ANOVA aov() and Tukey test TukeyHSD() from the package stats (version 4.3.1) to assess whether the observed patterns were significant. To do so, we partially clustered different stations together, precisely the mid estuary (633 - 692 km) and the mid to lower estuary (633 - 713 km) and compared those with the residue stations, i.e. the uppermost (609 km) and lowermost (713 km) station. In the figures 3.2a-c, 3.3 and S3.4 with used GAMs for curve fitting with geom_smooth() from ggplot2 and the formula y ~ s(x, bs = "cr", k). The k value was determined based on the lowest AIC as obtained from uGamm() from the package MuMIn and AIC() from stats (see tab. S3.3). A spearman rank correlation with the function rcorr() from the package Hmisc() (version 5.1-0) was applied to draw conclusions about the relationship of picophytoplankton groups with abiotic parameters obtained from the samples (precisely water temperature, salinity, turbidity, PO_4 and NO_3; see also supplementary data fig. S3.5-S3.7 and tab. S3.4) (fig. 3.4).

Those data were provided by Helmholtz-Zentrum hereon and obtained from the FGG database (FGG Elbe, 2024).

3.3. Results

Across seasons and methods, flow cytometry detected between 2.3 x 10^3 and 123 x 10^3 picophytoplankton cells mL^{-1} in the samples from the different stations and seasons from the Elbe estuary. On average 70 % (SD = 14 %) and up to 99 % of the detected phytoplankton cells per sample were < 3 µm. Picoeukaryotes were by far the most dominant group with an average contribution of 77 % (SD = 11 %) to the picophytoplankton cell counts, while picocyanobacteria played a role in summer (up to 53 %).

Across seasons, picophytoplankton, picoeukaryotes and picocyanobacteria were overall significantly more abundant at the uppermost station (609 km) than in the area further downstream (633 - 713 km) (fig. 3.2a, ANOVA/ Tukey: p = 6.0 x 10^{-11}, p = 2.1 x 10^{-10} and p = 3.7 x 10^{-6}, respectively; see also tab. S3.2). Contributions of picoeukaryotes to the phytoplankton cell counts were significantly higher in the mid estuary (633 - 692 km) compared to the upper station (609 km) (fig. 3.2c, ANOVA/ Tukey: p = 0.009; tab. S3.2), while they showed no significant differences between the mid and lower, as well as the upper and lower stations (tab. S3.2). As the picophytoplankton fraction was largely represented by picoeukaryotes, those patterns hold for the contributions of picophytoplankton to the phytoplankton cell counts as a whole (fig. 3.2b, ANOVA/ Tukey: p = 0.031 for comparison of the mid (633 - 692 km) and upper area (609 km); tab. S3.2). In contrast, contributions of picocyanobacteria to the picophytoplankton did not express a distinct pattern along space across season (fig. S3.2f).

Minidiscus and *Mychonastes* were the most dominant picoeukaryote taxa across seasons based on 18S rRNA reads (fig. 3.2d). Therein, *Mychonastes* was more dominant in the upper to mid reaches of the estuary (approx. 609 – 665 km), and *Minidiscus* in the mid to lower area (approx. 651 – 713 km). *Nannochloropsis* was prominent at 609 km in early May (spring 2021) and at 692 to 713 km in February (winter 2022) (fig. S3.3a). Here *Choricystis* also

played a role (contributions up to approx. 20 %). Other picoeukaryotes such as *Bathycoccus* and *Picochlorum* were minor contributors to the 18S picophytoplankton reads. Results from 16S sequencing (fig. 3.2e) show that *Synechococcus* and *Microcystis* might be the most relevant contributors to picocyanobacteria in summer 2021, where picocyanobacteria were particularly dominant (up to 53 % of the picophytoplankton cells; see also fig. S3.2f). Here *Microcystis* was more dominant at the upper stations (609 - 633 km) and *Synechococcus* at the lower stations (692 - 713 km). Notably there is some degree of uncertainty to what extent *Microcystis* would fall into the size range of picophytoplankton, due to colony formation and cell size. It is likely that *Synechococcus* reached significantly higher proportions among the cells < 3 µm than suggested in figure 3.2e. Minor contributors to the picocyanobacteria reads were e.g. *Prochlorococcus* and *Cyanobium* ("other" in fig. 3.2e).

In the seasonal dataset from downstream of the city of Hamburg (623 - 633 km), the abundances and contributions of the different picophytoplankton groups expressed distinct patterns along the sampling dates. The complexity is reflected in the high k values (15 - 20) of the fitted GAMs (fig. 3.2, fig. S3.4, tab. S3.3). Picoeukaryotes expressed three seasonal peaks in spring, summer and fall, where the spring peak was most pronounced (fig. 3.3a). Picocyanobacteria reached their maximum abundance around July to August with high abundances extending into October (fig. 3.3b). Picophytoplankton contributions to the total phytoplankton were highest in a single sample from the temperature peak in summer (fig. 3.3c), largely due to picocyanobacteria (fig. 3.3b+d), and across different samples in fall, which is due to low abundance of larger-celled taxa combined with the fall peak of picoeukaryotes and the remains of the fading summer bloom of picocyanobacteria (fig. 3.3a-b, fig. 3.3d). In contrast, picophytoplankton were less dominant within the phytoplankton communities in spring (fig. 3.3c) due to taxa > 3 µm blooming in parallel. Seasonal effects could also be observed in the spatial dataset as longitudinal data was obtained from different seasons (winter, spring and summer). Here, highest absolute abundances of picophytoplankton were observed in summer 2022 (fig. S3.2a). Contributions of picophytoplankton to the total phytoplankton counts were overall highest in summer 2021 and in winter 2022 mostly due to picocyanobacteria as well as picoeukaryotes and low abundance of larger-celled phytoplankton, respectively (fig. S3.2d-f).

Abiotic conditions varied along seasons and stations (see also supplementary fig. S3.5-S3.6). Temperature was highest in July (up to 23 °C in the spatial dataset at 665 km) and low in winter (down to 3 °C). Turbidity, salinity, NO_3 and PO_4 expressed spatial and seasonal patterns (fig. S3.5). Salinity was enhanced at the lowermost stations (692 - 713 km) and highest in summer 2022 and spring of both years (fig. S3.5a). Compared to other seasons, turbidity was enhanced in winter 2022 and spring 2021 (fig. S3.5b), NO_3 in winter 2022 and summer 2021 (fig. S3.5c) and PO_4 in summer 2021 (fig. S3.5d). Note that turbidity was also enhanced in fall 2021 (fig. S3.7; (FGG Elbe, 2024)) where we did not obtain longitudinal samples, but seasonal samples from a fixed area (623 - 633 km). Turbidity, PO_4 and NO_3 concentrations were enhanced downstream of 609 km (fig. S3.5b-d).

Picophytoplankton abundance was positively correlated with temperature (fig.3.4). This was a result of high abundance of picocyanobacteria in summer 2021 (fig. 3.3b, fig. S3.2c, fig. S3.6), high abundance of picoeukaryotes in summer 2022 (fig. S3.2b) and low abundances of both groups in winter (fig. S3.2b-c). Relative contributions of picoeukaryotes to the (pico-)phytoplankton were negatively correlated with temperature (fig. 3.4). Overall this pattern arises from relatively high picoeukaryotes contributions to the phytoplankton in fall and winter (fig. S3.2e, fig. S3.4b) where phytoplankton abundance was generally low, and enhanced picocyanobacteria contributions to the picophytoplankton in summer (fig. 3.3d, fig. S3.2g). Picophytoplankton contributions to the phytoplankton cell counts were negatively correlated with salinity (fig. 3.4), largely due to low contributions at around 10 PSU at 713 km in spring 2021 and 2022 (fig. S3.2d, fig. S3.5a). Cell counts of picophytoplankton were negatively correlated with turbidity and NO_3 (fig. 3.4) due to their high absolute abundance at 609 km - especially in summer - where turbidity and NO_3 concentrations were rather low (fig. S3.2a, fig. S3.5b-c). In contrast, relative contributions of picophytoplankton to the phytoplankton were positively correlated with these parameters and additionally with PO_4 (fig. 3.4). This relationship with PO_4, NO_3 and turbidity is affected by the higher proportions of small cells in the mid to lower estuary compared to 609 km, where these parameters achieved overall higher values and by the seasonal dominance of

picocyanobacteria in summer 2021 (at high PO_4) and picoeukaryotes in winter (at high turbidity and NO_3) (fig. S3.2d-f, fig. S3.5b-d).

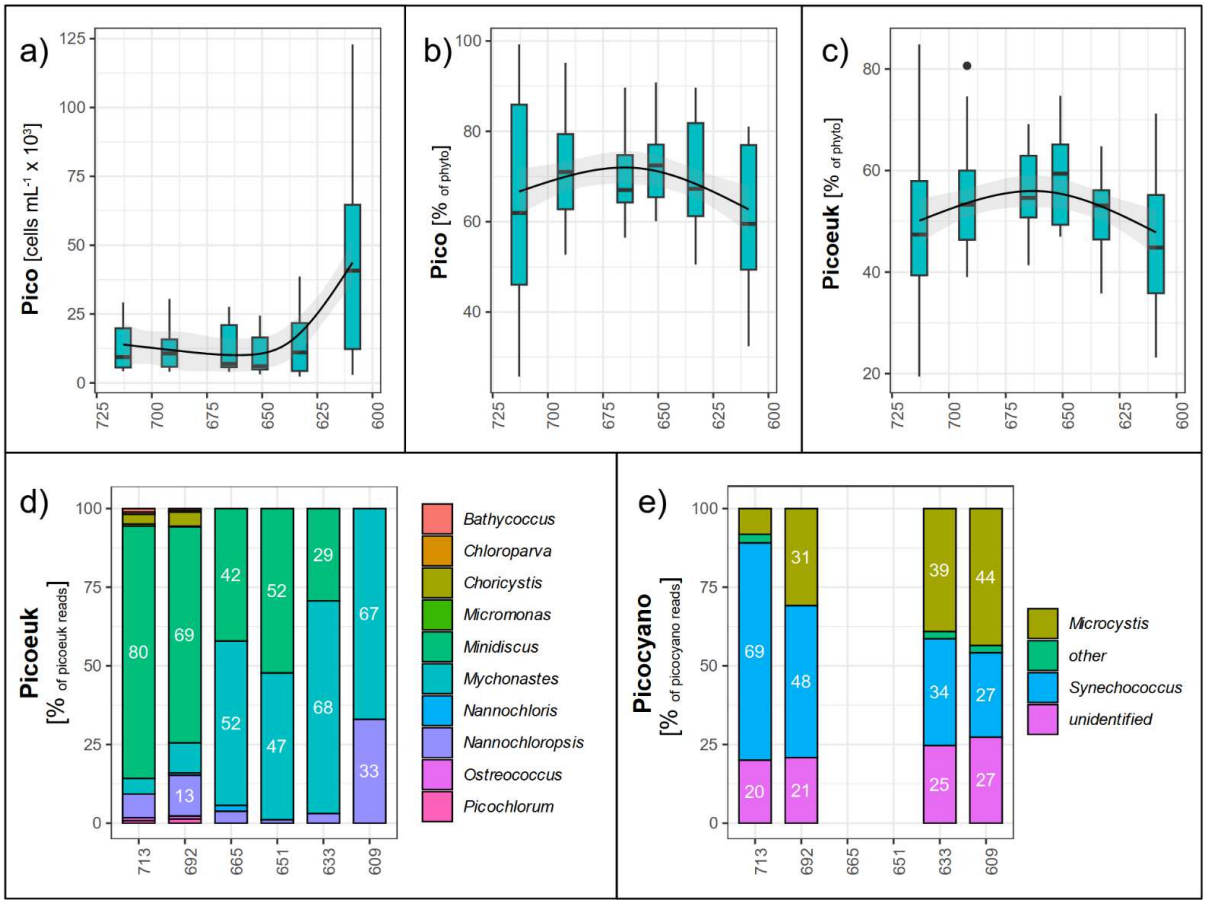

Fig. 3.2: Spatial distribution of different picophytoplankton groups along different stations (stream km) across different seasons. Additional data, also separated by season, can be found in the supplementary material (fig. S3.12, fig. S3.3). Note that the number of samples included per season might differ, especially in d), and e) only shows data from summer 2021 due to lack of sufficient data from other seasons. In a) and e) station is used as a factor for clarity and labels are shown for values >= 10 %. Contributions of cyanobacteria to picophytoplankton can be obtained from c) ("picocyanobacteria = 1 - picoeukaryotes"). Regression lines were added with geom_smooth() from ggplot2 and the method "gam" (see also tab. S3.3). For clarity we use the following abbreviations: Pico = picophytoplankton, picoeuk = picoeukaryotes, phyto = phytoplankton. a) - c) refer to cell counts from flow cytometry, d) - e) to reads from metabarcoding. Data in d) is obtained from a former study (Martens et al., 2024b).

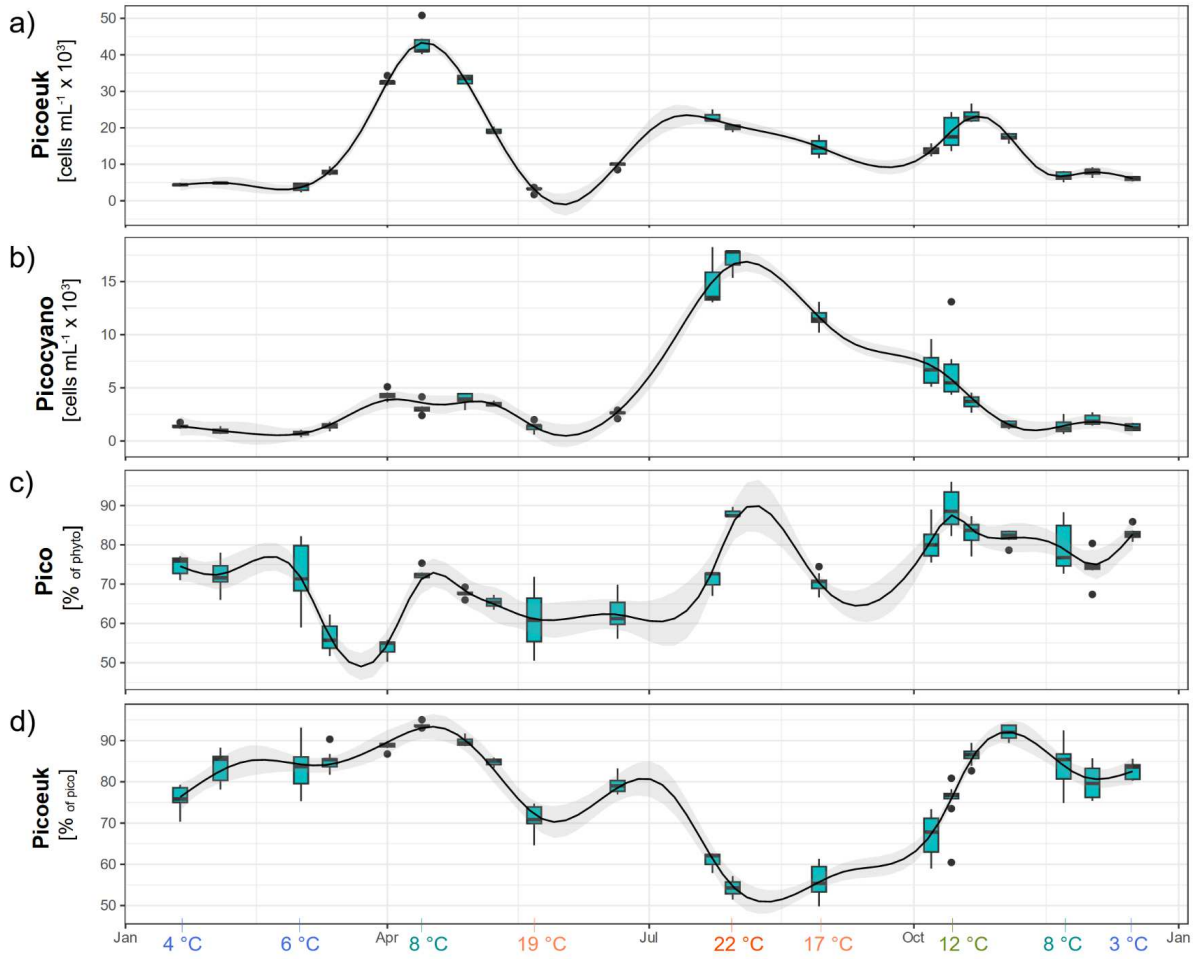

Fig. 3.3: Seasonal distribution of different picophytoplankton groups in the area around Hamburg (approx. 623 - 633 km). Additional data can be found in the supplementary material (fig. S3.4). Horizontal scales show the sampling date independent of the year, i.e. day of the month. Data was merged when sampling was carried out < 5 days apart. Contributions of cyanobacteria to picophytoplankton can be obtained from the picoeukaryotes contribution in c) ("picocyanobacteria = 1 - picoeukaryotes"). Regression lines were added with geom_smooth() from ggplot2 and the method "gam" (see also tab. S3.3). For clarity we use the following abbreviations: Pico = picophytoplankton, picoeuk = eukaryotes, phyto = phytoplankton. On the bottom we show the temperatures at certain time points (see further details in fig. S3.6).

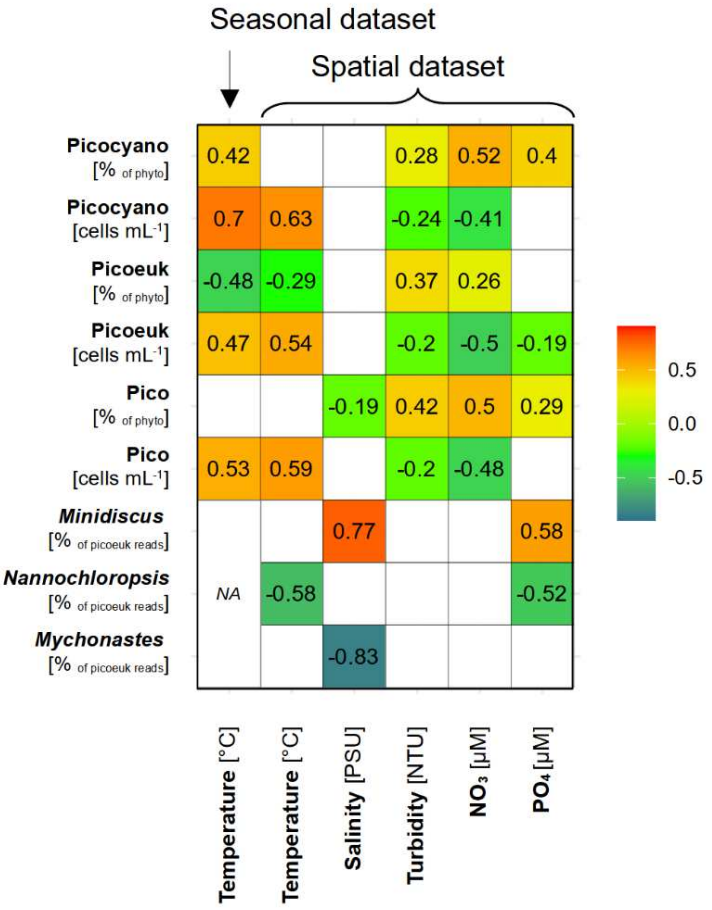

Fig. 3.4: Correlation of different picophytoplankton groups with abiotic conditions in the spatial and seasonal dataset. Numbers and color scheme show the correlation coefficient r calculated with spearman rank correlation for $p \leq 0.05$ (see also tab. S3.4). Salinity, turbidity, NO_3 and PO_4 are shown for the spatial dataset only, as these parameters did either not vary much or were not obtained in the seasonal dataset. Temperature is shown for both datasets separately. 16S data was not included here due to the low number of data points (see methods). For clarity we used the abbreviations picoeuk = picoeukaryotes, picocyano = picocyanobacteria and phyto = phytoplankton.

Due to enhanced contributions to the picoeukaryotes reads from winter to spring compared to the other seasons (fig. S3.3a), *Nannochloropsis* was negatively correlated with temperature (fig. 3.4). The negative relationship with PO_4 can be mainly explained by the high contributions of this taxon at 609 km in spring 2021, where PO_4 was particularly low (precisely below detection limit; fig. S3.5d). *Mychonastes* was clearly associated with the freshwater reaches of the estuary (fig. 3.2d, fig. S3.3a), resulting in negative correlation with salinity (fig. 3.4, fig. S3.5a). In contrast, *Minidiscus* was more dominant further downstream and hence associated with higher salinity and higher PO_4 values (fig. 3.4, fig. 3.2d, fig. S3.3a, fig. S3.5a+d).

3.4. Discussion

We used flow cytometry to quantify picophytoplankton along the Elbe estuary and across seasons, and combined the results with composition data obtained from metabarcoding. Our results indicate that picophytoplankton - and therein picoeukaryotes - were the dominant groups of phytoplankton in the Elbe estuary with respect to abundance in the vast majority of the samples. Notably, different picoeukaryote taxa (precisely *Minidiscus* and *Mychonastes*) could each contribute up to 17 % to the eukaryotic phytoplankton reads, implying that this group was also relevant in terms of biovolume (see also (Martens et al., 2024b) and fig. 3.1b). Considering their ubiquitous appearance throughout water bodies around the world (Coello-Camba and Agustí, 2021; Purcell-Meyerink et al., 2017; Sathicq et al., 2020; Takasu et al., 2023), it is not surprising that picophytoplankton also play an important role in the Elbe estuary, even though empirical evidence has so far been scarce for this ecosystem.

Picophytoplankton have been found to be important at extreme and highly variable salinities, e.g. in hypersaline lakes and in the Black Sea (Belkinova et al., 2021; Somogyi et al., 2022) and at intermediate salinities (e.g. 5 - 10 PSU) in estuaries (Wetz et al., 2011), which are somewhat extreme for both freshwater and saltwater inhabitants. However, our data so far imply that picophytoplankton were overall more abundant and dominant at freshwater and rather high salinity (approx. 20 PSU). Nevertheless, some picophytoplankton taxa, such as certain genotypes of *Minidiscus* (see also (Martens et al., 2024b)) as well as *Ostreococcus*, *Bathycoccus* and *Picochlorum*, which were particularly associated with intermediate salinities (approx. 1 - 10 PSU), have been associated with brackish habitats (e.g. in (Hu et al., 2016; Tragin and Vaulot, 2019)) and high salinity tolerances (Foflonker et al., 2016; Somogyi et al., 2022) before. Those groups might fulfill significant ecological functions at the salinity interface, e.g. as primary producers and as food items for higher trophic levels, the latter regardless of whether they are in particularly good condition.

Distribution patterns in the contributions of picophytoplankton to the total phytoplankton cells - and the relationship of those contributions with abiotic parameters - indicate that

picophytoplankton play a major role under extreme environmental conditions with respect to temperature and turbidity. Picocyanobacteria were associated with high water temperatures in summer (e.g. up to 22 °C; see also temperatures along seasons in fig. S3.6), as observed for picocyanobacteria in other studies (Alegria Zufia et al., 2021; Murrell and Lores, 2004). This group may become more dominant in the Elbe estuary under global warming (see also (Flombaum and Martiny, 2021b)), which might affect food webs due to the relatively low nutritional value and possible toxicity of cyanobacteria (Ger et al., 2016; Sim et al., 2023). Picoeukaryotes were most abundant in spring, but their relative contributions to the phytoplankton communities were overall highest in fall and winter, as well as in the middle reaches of the estuary, i.e. at a combination of low temperature and low light availability (due to turbidity and sunlight). While further research is needed to disentangle the effects of temperature and turbidity, picoeukaryotes have been associated with the colder seasons in other studies (Alegria Zufia et al., 2021; Vörös et al., 2009) and a positive relationship between turbidity and picophytoplankton as a whole has been observed before. Those studies argue that picophytoplankton might have specific strategies in light harvesting (Coe et al., 2021; Malinsky-Rushansky, 2002; Somogyi et al., 2022, 2017; Soulier et al., 2022). Additionally, we found that picoeukaryotes from the Elbe estuary were particularly skilled in utilizing organic compounds (Martens et al., 2024a) which might give them advantages over other phytoplankton groups. The positive relationship of the contributions of different picophytoplankton groups with nutrients (NO_3 and PO_4) furthermore imply that those groups benefit from high nutrient availability, e.g. in areas with otherall low phytoplankton concentrations such as the mid to lower estuary (633 - 713 km).

Phytoplankton concentrations are known to decline along the Elbe estuary, especially through the city of Hamburg. This is partially explained by local grazing effects (Schöl et al., 2009) but may also be affected by e.g. sinking in the current-calmed harbor basins (Wolfstein, 1996). Picophytoplankton abundance followed this pattern in our study. However, due to their small size, they might be less affected by those factors than larger-sized taxa, which can beyond the aforementioned ones contribute to the elevated contributions in the mid estuary compared to the station upstream of Hamburg (609 km). For instance, small picophytoplankton cells have a reduced sinking velocity compared to

larger-celled phytoplankton. Moreover, while one of the key zooplankton taxa - *Eurytemora* (Schöl et al., 2009) - may utilize picophytoplankton e.g. as part of aggregates (Modéran et al., 2012; Wilson and Steinberg, 2010) - they likely prefer to consume larger-celled phytoplankton, and hence, picophytoplankton might be removed less rapidly by grazing.

Methodological limitations - such as an underrepresentation of samples with intermediate to higher salinities - might have affected some of our interpretations, however, consistent findings across a high number of samples included, e.g. with respect to the picophytoplankton dominance in terms of cell counts, make it inevitable to conclude that picophytoplankton play a key role in the Elbe estuary. Their high contributions under extreme conditions - e.g. high temperatures and low light availability - implies that they occupy ecological niches to maintain primary production where larger phytoplankton might struggle, and their small nature might protect them from rapidly being removed from the water body. In contrast, in microscopic data from the Elbe estuary, larger-celled phytoplankton taxa dominate. For instance, in our flow cytometric data, picoeukaryotes < 3 µm made on average 51 % (ranging from 12 - 74 %) in the different samples in the upper to mid estuary (precisely 609 - 651 km) in spring and summer 2021. At close by monitoring stations in these seasons (568 km and 646 km; see also (Martens et al., 2024b; NLWKN, 2023)), groups described as < 5 µm (small representatives of *Dictyosphaerium* and centric diatoms) made on average only ca. 8 % (ranging from 1 - 23 %) of the microscopic cell counts. Our results emphasize the importance to include the so far underrated group of picophytoplankton in (estuarine) research and provide insights into the comparability of techniques (e.g. flow cytometry, metabarcoding) for detecting (pico)phytoplankton communities.

4. Organic compounds drive growth in phytoplankton taxa from different functional groups

This chapter is a modified version of a manuscript published as: Martens, N., Ehlert, E., Putri, W., Sibbertsen, M., Schaum, C.-E., 2024. Organic compounds drive growth in phytoplankton taxa from different functional groups. *Proceedings of the Royal Society B* 291: 20232713. https://doi.org/10.1098/rspb.2023.2713

The modifications to the published version concern minor changes to integrate the publication into the thesis (e.g. figure and section numbering).

Abstract

Phytoplankton are usually considered autotrophs, but an increasing number of studies shows that many taxa are able to also utilize organic carbon. Acquiring nutrients and energy from different sources might enable an efficient uptake of required substances and provide a strategy to deal with varying resource availability, especially in highly dynamic ecosystems such as estuaries. In our study we investigated the effects of 31 organic carbon sources on the growth (proxied by differences in cell counts after 24 h exposure) of 17 phytoplankton strains from the Elbe estuary spanning four functional groups. All of our strains were able to make use of at least 1 and up to 26 organic compounds for growth. Pico-sized green algae such as *Mychonastes*, as well as the nano-sized green alga *Monoraphidium* in particular were positively affected by a high variety of substances. Reduced light availability, typically appearing in turbid estuaries and similar habitats, resulted in an overall poorer ability to utilize organic substances for growth, indicating that organic carbon acquisition was not primarily a strategy to deal with darkness. Our results give further evidence for mixotrophy being a ubiquitous ability of phytoplankton and highlight the importance to consider this trophic strategy in research.

4.1. Introduction

Phytoplankton may play a more complex role in the carbon cycle than previously assumed. While one of their main roles is fixing CO_2 through photosynthesis - which is the basis of carbon sequestration (Basu and Mackey, 2018) - various studies now provide evidence that many taxa are actually able to acquire organic carbon from their environment, either by phagotrophy (Koppelle et al., 2022; Millette et al., 2023) or by uptake of dissolved compounds (Godrijan et al., 2022; Listmann et al., 2021). Mixotrophy appears for taxa from miscellaneous functional groups of phytoplankton, including haptophytes (Anderson et al., 2018; Godrijan et al., 2022; Koppelle et al., 2022), green algae (Azaman et al., 2017; Listmann et al., 2021; Pang et al., 2022), dinoflagellates (Millette et al., 2017), cyanobacteria (Muñoz-Marín et al., 2020), cryptophytes (Ballen-Segura et al., 2017) and diatoms (Villanova and Spetea, 2021).

Combining autotrophic and heterotrophic mechanisms might enable an efficient uptake of carbon and required nutrients such as N, P or amino acids (Foresi et al., 2022; Reinl et al., 2022). Mixotrophic phytoplankton can achieve higher biomass yields in the presence of organic carbon compared with autotrophic conditions (Kang et al., 2004; Liu et al., 2009), which is made use of in bioengineering (Chu et al., 2022). The availability of different pathways of energy and nutrient acquisition might also have substantial benefits in highly dynamic ecosystems, e.g. when light, prey or nutrient availability vary (Anderson et al., 2018; Godrijan et al., 2022; Millette et al., 2017; Naselli-Flores and Barone, 2019), and allow phytoplankton to be a stable food source for zooplankton (Katechakis et al., 2005).

In tidal estuaries water masses are constantly reshuffled while phytoplankton drift between freshwater and saltwater ecosystems. Here phytoplankton are exposed to high variations in environmental conditions such as salinity and turbidity (Tagliapietra et al., 2009), as well as a high number of organic substances such as amino acids (Kerner and Yasseri, 1997) or fatty acids (Franke et al., 1995). The utilization of organic compounds in such ecosystems might be critical for phytoplankton to maintain growth, especially where light is limited as a consequence of high loads of suspended matter. Different phytoplankton taxa have been

shown to survive and grow based on organic carbon in the dark and at reduced light levels (Calderini et al., 2022; Godrijan et al., 2022; Jones et al., 2009; Millette et al., 2017; Tuchman et al., 2006). Hence, unsurprisingly, the importance of mixotrophic taxa in estuarine ecosystems has been reported in several studies (Hammer and Pitchford, 2006; Lee et al., 2012; Li et al., 2022; Wolfstein, 1990).

There is an increasing awareness that mixotrophy of phytoplankton might be the norm rather than the exception (Flynn et al., 2013; Reinl et al., 2022). This alters our understanding of food webs and substrate cycles. As part of the microbial loop as well as by grazing on bacteria and other small organisms, mixotrophic phytoplankton contribute to trophic upgrading (Principiotta et al., 2019). Here, trophic upgrading means that they do not only pass on energy and nutrients as such, but might also alter them towards a higher nutritional value for zooplankton (Traboni et al., 2021), e.g. by providing high lipid and protein contents (Naselli-Flores and Barone, 2019). By incorporating both organic and inorganic matter, biomass of mixotrophic phytoplankton becomes decoupled from the actual primary production. Mixotrophic phytoplankton can have a reduced chlorophyll content (Azaman et al., 2017; Liu et al., 2009; Znachor and Nedoma, 2010) and might therefore be underrepresented quantitatively with conventional measuring techniques that make use of pigment concentrations. Ultimately, recent studies show that integrating mixotrophy in climate change research is crucial for understanding carbon dynamics (Ward and Follows, 2016; Wieczynski et al., 2023).

Here, we investigated the effects of 31 dissolved organic compounds on the growth of 17 phytoplankton strains isolated from the Elbe estuary by using Biolog EcoPlates™. Our aim was to compare the potential of different phytoplankton taxa from different functional groups to utilize dissolved organic carbon for growth, as proxied by differences in cell counts after 24 h exposure. We moreover wanted to investigate the effects of reduced light availability that might occur frequently in the turbid estuary on organic carbon source uptake.

4.2. Methods

Isolation and cultivation of phytoplankton

Water samples for the isolation of phytoplankton were collected in March (2021-03-12), May (2021-05-07/08) and February (2022-02-28) on the research vessel *Ludwig Prandtl* (LP210308, LP210503, LP220228) as well as during one sampling from the pier in July (2021-07-21). The sampling stations were located at 609 km (Bunthäuser Spitze), 633 km (Mühlenberger Loch) and 692 km (Brunsbüttel) distance from the spring of the Elbe river in the Czech Republic. Station coordinates are given in the supplementary material in addition to information about abiotic parameters during sampling (tab. S4.1).

We used a dilution approach to isolate the phytoplankton strains. This was conducted either in 96 well plates, where samples were diluted to contain on average 0.5 cells per well or on agarose by picking colonies grown from single cells. Each strain went through this process at least twice to ensure clonality on the level of the focal species. We obtained 17 clonal phytoplankton strains (fig. 4.2, tab. S4.1). Note that isolation success is biased by the abundance of taxa but also by their viability in the laboratory and does not necessarily reflect the natural communities. We did not remove the microbiome, as former studies have shown that phytoplankton can depend on bacteria in their environment (Pang et al., 2022; Yao et al., 2019). Moreover, co-occurrence and interactions with bacteria reflect the natural conditions in the field.

All strains were maintained in WHM freshwater medium to which silicate was added (0.11 mol l^{-1} Na_2SiO_3). The pH of the media was approximately 7. In a common garden approach, winter strains were kept at 12 °C (respectively 15 °C) and summer strains at 18 °C. Strains were held at a 12 h: 12 h light: dark cycle at approximately 150 µmol photons s^{-1} m^{-2} in the light phase. Cultures were gently mixed at 60 r.p.m. on a horizontal shaker.

All included strains are shown in fig. 4.2 as well as in the supplementary data (tab. S4.1) together with further information (e.g. origin, abiotics).

Identification of the strains

DNA was extracted using a CTAB protocol (Fawley and Fawley, 2004). Cyanobacteria were identified by 16S sequencing (27F forward 5'-AGAGTTTGATCCTGGCTCAG-3', 1429R reverse 5'-GGTTACCTTGTTACGACTT-3') and eukaryotes were identified by 18S sequencing (5'-GCTTGTCTCAAAGATTAAGCC-3' forward, 5'-GCCTGCTGCCTTCCTTGGA-3' reverse) using the ncbi BLAST database. Additionally, morphological criteria from microscopy (Keyence BZ-X800) and flow cytometry (BD accuri C6 plus) were included to characterize the different strains. Green algae were assigned to the pico green or nano green fraction based on their size represented by their flow cytometric characteristics (see supplementary data tab. S4.1).

Our strains were identified as seven pico-sized green algae, six nano-sized green algae, three cyanobacteria and one diatom (tab. S4.1). All strains differed from each other either morphologically, with respect to their origin and sampling season and/ or genetically, hence representing unique geno- or ecotypes. Further information about how we assigned the taxa to the different strains is provided in the supplementary data (tab. S4.1).

Experimental setup

An overview of the experimental setup is given in fig. 4.1a. We used Biolog EcoPlates™ to analyze the effects of organic carbon sources on the growth of the phytoplankton strains. The plates contained 31 organic substances, as well as a control without an organic compound, in triplicates. Organic compounds included 10 carbohydrates, nine carboxylic acids, six amino acids, four polymers and two amines. We added 100 µL aliquots of samples with known cell count to each well of the EcoPlates™.

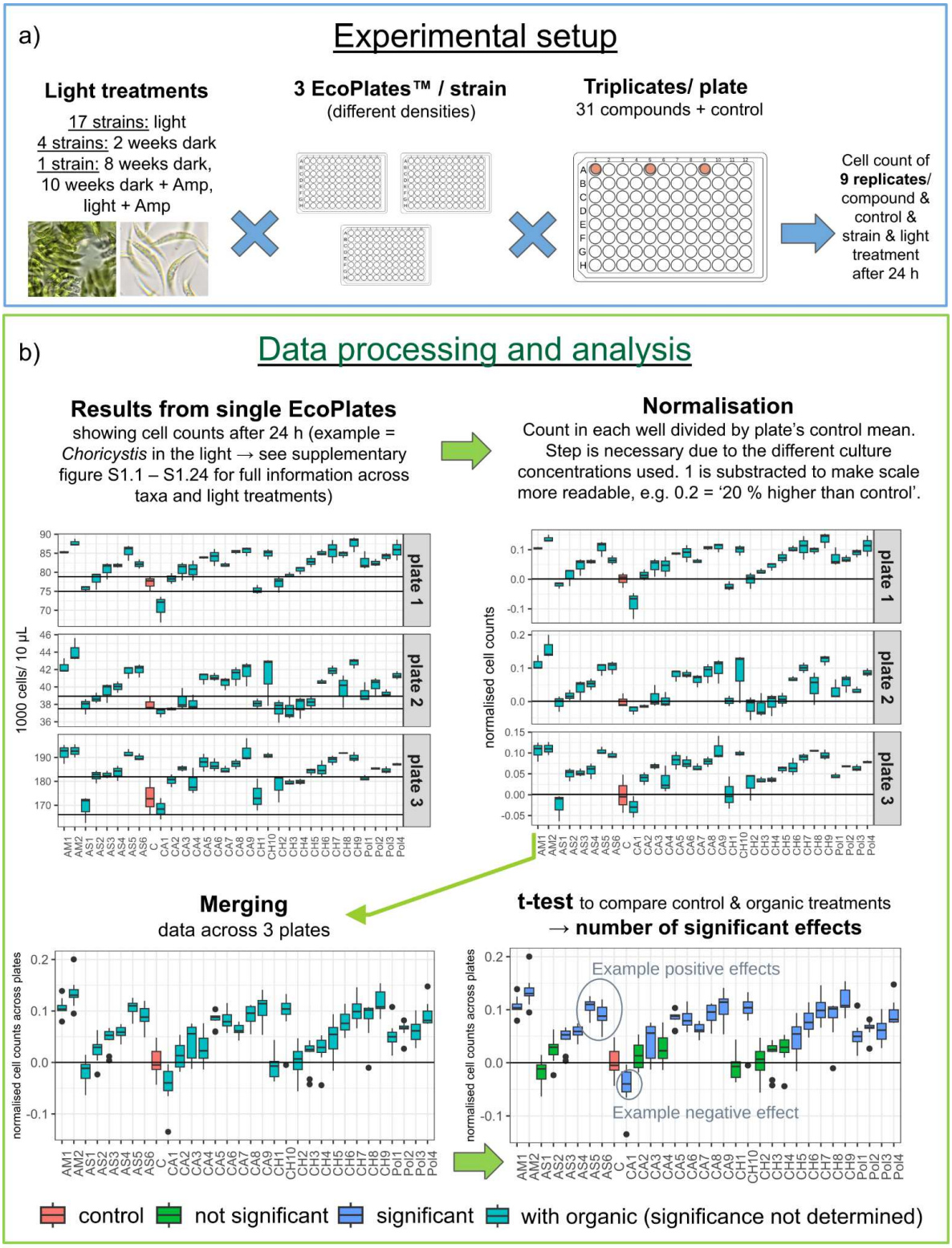

Fig. 4.1: Experimental setup (a) and data processing and analysis (b). 'Light' and 'dark' refer to the condition of the light phase of the 12 h:12 h light: dark cycle, which were ca. 150 µmol photons s^{-1} m^{-2} in the light treatment and ca. 75% reduced in the dark treatment. Amp = ampicillin (100 µg ml^{-1}) added ca. five days prior to measurements. The horizontal axes in (b) show the control and different organic compounds, as can be obtained from the supplementary information (fig. S4.1.1-S4.1.24). Significance refers to the comparison of an organic treatment with the control without added organic compounds.

After approximately 24 hours, we used flow cytometry (BD accuri C6 plus) to determine the number of cells in each well. To do so, the cultures were resuspended by pipetting and transferred from the EcoPlates™ to regular 96 well plates suitable for the flow cytometer. Here, we measured 10 µL per well with a flow rate of 66 µl min^{-1}, regular cleaning and mixing between the samples. Small volumes have been shown to be overall sufficient to accurately determine cell numbers of homogeneous phytoplankton monocultures, such as the strains included in this study (see example data in the supplementary data tab. S4.4). The average control variation on the plates was 5.8 %. Gating was conducted optically based on the obvious phytoplankton clusters. The cell count after ca. 24 h incubation in the plates was used as a proxy for growth (see further explanations in the section "determination of growth"). More precisely, we compare the cell counts in the organic treatment wells with those in the control wells, and describe the *relative* growth, i.e. were cultures growing *better* or *worse* in the presence of organic than in the control? While this is not a growth rate *per se*, and not a perfect proxy for growth, we refer to it as 'growth' throughout the text for better readability.

All 17 strains were grown under standard light incubation, i.e. 12 h: 12 h light: dark cycle, where the photon flux in the light phase was ca. 150 µmol photons s^{-1} m^{-2}. We refer to this setup as 'light' throughout the study. In the strains' habitat, light availability quickly declines along the water column due to high turbidity (Fast, 1993). We therefore wanted to also investigate the effects of reduced light availability on the use of organic carbon for growth. For practical reasons, we selected a subset of four strains that particularly covered the largest groups of our pool of strains - i.e. nano and pico green algae. Those included one strain each of *Mychonastes* (strain P4), *Choricystis*, *Tetradesmus* as well as one strain of *Monoraphidium* (strain N7). Light reduction across wavelengths was achieved by semi-transparent foil (Lee Zirkon Filter, type 210), while running the standard 12 h: 12 h light: dark conditions of the incubators as described above. We refer to the ca. 75 % light reduction as 'dark' or 'darkness' throughout the text. The strains were kept in culture flasks in the dark for two weeks prior to the measurements, then transferred to the EcoPlates™ and incubated in the dark in the presence of the organic compounds for approximately 24 h. One strain, *Mychonastes* (strain P4) was grown under reduced light availability with a longer

dark acclimation time of eight weeks in order to assess the effect of acclimation time. To test for potential effects of the microbiome on the results the same strain was also included in an ampicillin treatment, both under standard light conditions and after dark acclimation of 10 weeks. Here, ampicillin was added as 100 µg ml^{-1} ca. five days prior to the measurement. During the longer phases in the dark, i.e. more than two weeks, cultures were regularly transferred into fresh medium.

To be able to account for potential plate effects, we repeated the experiment three times for every strain and light treatment, thereby including different densities within the exponential growth phase. This resulted in a total of ca. 70 plates included in this study. Exponential growth was ensured by tracking of the cell counts in various different samples prior to the transfer of the cultures to the EcoPlates™ (see supplementary data fig. S4.2).

Metadata for the measurements - e.g. exact incubation times - can be found in the supplementary data (tab. S4.2).

Data processing and analysis

Cytometric data (cell counts) were processed and analyzed in R (version 4.1.3), including the packages Tidyverse (version 1.3.2) and stats (version 4.1.3). We used ggplot2 (version 3.4.0) for graphical presentation of data and LibreOffice Draw (version 7.1.2.2) for overview figures and addition of text notes.

An overview of the data processing is shown in fig. 4.1b. Results of the plate replicates were similar despite different cell densities (see supplementary data fig. S4.1.1-S4.1.24) across a wide range of taxa and compounds, allowing us to merge data across plates for every strain and light treatment. To do so, we first normalize the data of each plate by the plate's control mean (fig. 4.1b, upper right panel). For clarity we subtracted 1 from all ratios so that negative effects are represented by negative values and positive effects by positive values. The normalization step was necessary, as strains were included at different densities in the different plates. We then merged the datasets (fig. 4.1b, lower left panel), resulting in nine

replicates per strain, light treatment and organic compound respectively control. We then used the t-test (R, package stats version 4.1.3) to assess whether there were significant differences between each treatment with different organic compounds and the control ($p \leq 0.05$) (fig. 4.1b, lower right panel, see also supplementary data tab. S4.3 and fig. S4.1.1-S4.1.24 lower panel). This gave us the number of significant positive and negative effects per strain and light condition across organic compounds, i.e. how many compounds positively or negatively affected our strains (fig. 4.2a, b). The normalized cell counts i.e. ratios of organic treatments vs. controls were moreover used to describe the strength of the effects on the strains, i.e. how much higher or lower cell counts were compared to the control (fig. 4.2c).

In the same way as described, we calculated the number of significant effects and the effect strength per type of organic compound (e.g. carbohydrate, amino acids) summarized across all different strains in the standard light treatment (fig. 4.3a-c). We indicated by '+' and '-' how the number of significant effects changed from light to the two weeks dark treatment with respect to the four strains included in that part of the experiment, i.e. *Mychonastes* (strain P4), *Tetradesmus*, *Choricystis* and *Monoraphidium* (strain N7) (fig. 4.3a, b).

Lastly, we used the t-test (R package stats version 4.1.3) to assess if the ratio was different between the different light treatments for the respective selection of strains (fig. 4.2c) ($p \leq 0.05$, see supplementary data tab. S4.3).

Determination of growth

As described in the section "experimental setup", our assessment of growth was based on the cell counts after 24 h in the EcoPlates™ exclusively. Here we understand growth relatively, i.e. did cultures grow better or worse in the organic treatment wells compared to the control wells? Cell count was not determined in the wells of the EcoPlates™ prior to the 24 h incubation i.e. at day 0. This is because the small volume in the wells does not allow a sampling of aliquots sufficient for flow cytometry, as ca. 100 µL are needed in the wells during measurement to avoid air entering the system, and sampling directly from the

EcoPlates™ is not possible. Due to the general homogeneous character of the samples (see supplementary data tab. S4.4), gentle mixing prior plating and rapid transfer to the wells of the EcoPlates™, we can assume, from cell count measurements using aliquots from the samples growing in flasks, that the cell count was equal when transferred to the wells. Only the *Chlorella*-like strain had a slightly less homogeneous character, resulting in higher variation among technical replicates (see supplementary data tab. S4.4), which is also reflected in enhanced control variation in the EcoPlates™ (on average 12 % and up to 24 % on a single plate). However, any variation would be covered within the variation of the replicates on the plates. This means that even an inhomogeneous distribution of cells in the wells is very unlikely to affect the plate results significantly in terms of false positive effects. All our strains were able to grow within the time frame of a single day (see also example cell counts in the supplementary fig. S4.2). Hence, the relatively short period of 24 h was sufficient to draw conclusions about relative effects of growth on the included strains.

4.3. Results

Organic carbon drives growth in phytoplankton in the light

In the light, growth, as proxied by differences in cell counts, was significantly positively affected by different organic compounds in all 17 strains and significantly negatively affected in 13 strains (fig. 4.2a, b, tab. S4.3). While most strains experienced both positive and negative effects depending on the organic compound, the vast majority of effects were positive.

Overall, the highest number of significantly positive effects in the light treatment - up to 25 out of 31 - appeared for the pico green algae strains, particularly the three *Mychonastes* strains, *Chlorella*, *Choricystis* and one of the unidentified pico green algae strains (fig. 4.2b, tab. S4.3). In the group of nano green algae results varied, with a low number of significantly positive effects in *Tetradesmus*, the *Chlorella*-like strain and *Micractinium* and higher numbers of 14 - 23 significantly positive effects in the three *Monoraphidium* strains. The number of significantly positive effects on our diatom and the cyanobacteria was overall rather low. Strongest positive effects in the light treatment appeared for *Mychonastes* with

up to 90 % increased cell numbers, followed by the Synechococcales with up to 70 % increased cell numbers compared to the control (fig. 4.2c).

The number of significantly negative effects was overall low compared with the number of significantly positive effects under the standard light conditions (fig. 4.2a, b, tab. S4.3). The highest number of significantly negative effects here was found for *Tetradesmus* which was negatively affected by nine organic compounds. Strongest negative effects in the light appeared for the *Monoraphidium* strain N7, as well as different *Mychonastes* strains where cell counts were diminished by up to over 90 % and up to over 70 % respectively (fig. 4.2c, see also supplementary data fig. S4.1.6, S4.1.9, S4.1.13) compared with the control without organic compounds.

Effects of different compounds can be taxa-specific

While the majority of compounds had positive effects across a wide range of taxa, we found a few taxa-specific differences (supplementary fig. S4.1.1-S4.1.24). For instance, Tween 40 and Tween 80 significantly negatively affected many different taxa, including e.g. *Mychonastes* (e.g. fig. S4.1.9, S4.1.13, S4.1.19), *Monoraphidium* (fig. S4.1.7) and *Tetradesmus* (fig. S4.1.3). In contrast *Choricystis* was significantly positively affected by these polymers (fig. S4.1.11). All three cyanobacteria and the diatom included in this study were significantly negatively affected by D-xylose (fig. S4.1.20-S4.1.23). In other taxa, specifically *Mychonastes* (fig. S4.1.9, S4.1.13, S4.1.19) D-xylose had significantly positive effects on growth. This highlights that different taxa can be affected in different ways by the same organic compounds.

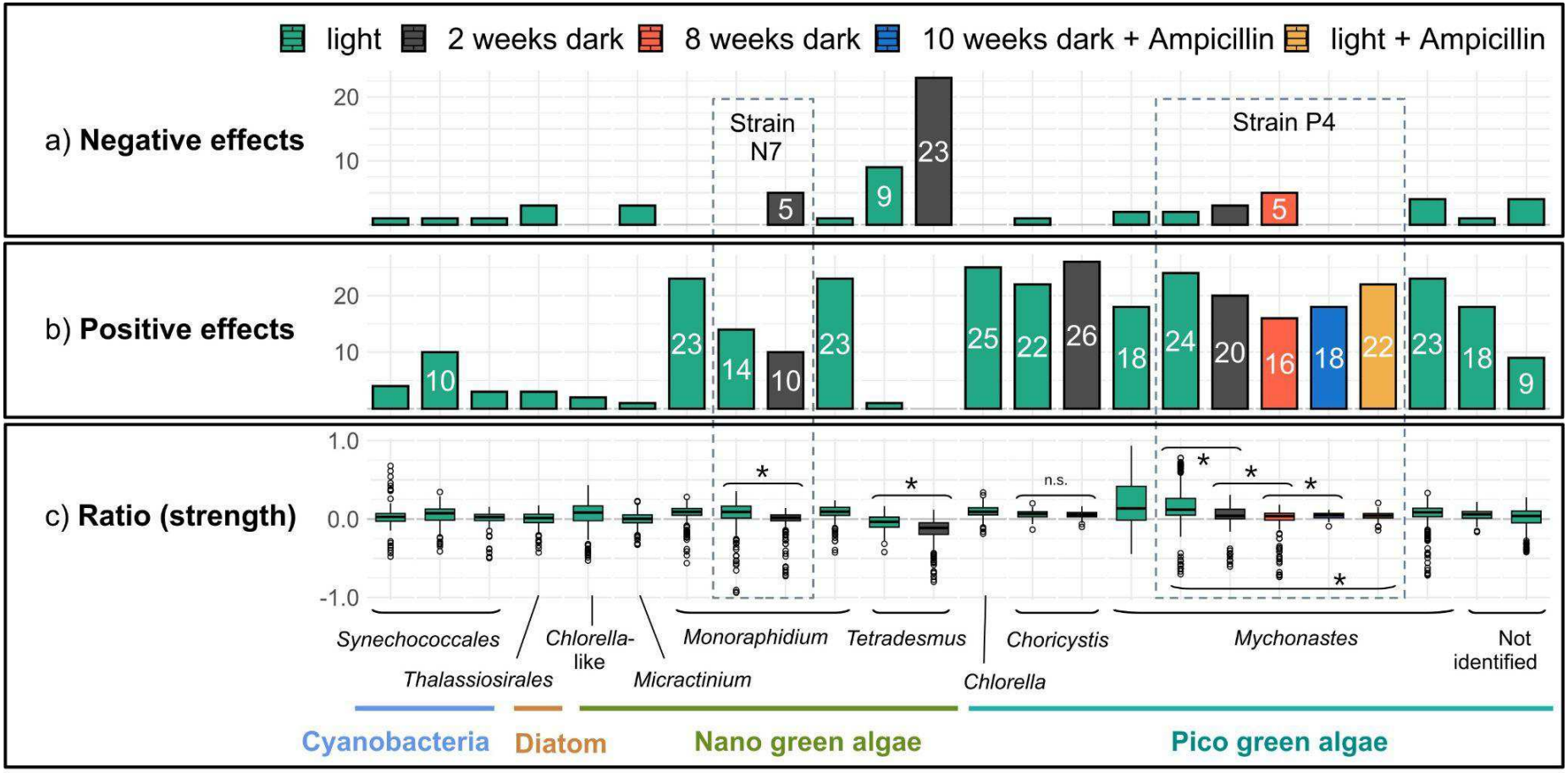

Fig. 4.2: Number of significantly negative (a) and positive (b) effects (t-test, p ≤ 0.05, tab. S4.3) of organic compounds on the growth of phytoplankton and effect ratio (strength) (c) across three plate replicates per strain and light treatment. The x-axis shows the taxa, including various strains in some cases, and light treatment (indicated by color). E.g. we included three different strains of *Mychonastes*, while one of them – P4 – was included with different light treatments. Strain names N7 and P4 are shown explicitly as needed for the further description. In (a) labels with less than five significant effects were removed for clarity. (c) includes all effects independent of their significance per strain and light treatment, i.e. every single measurement normalized by the control of the respective plate. This is presented by relative values around 0. Each boxplot consists of 279 values (31 substances x 3 well replicates x 3 plate replicates). Where relevant, we highlighted where the ratios of the different light treatment groups were significantly different (t-test, p ≤ 0.05, indicated by *; n.s. = not significant) in (c).

Darkness downgrades effects of organic carbon

Incubation in the dark had largely negative effects on the use of organic compounds for growth compared to the standard light conditions (fig. 4.2). Precisely, *Mychonastes* (strain P4), *Tetradesmus* and *Monoraphidium* (strain N7) had more significantly negative and fewer significantly positive effects after two weeks in the dark (fig. 4.2a, b, tab. S4.3). In the three strains, the overall ratio between organic treatments and controls was significantly lower after two weeks in the dark than in the light (fig. 4.2c, tab. S4.3). *Tetradesmus* was significantly negatively affected by 23 compounds in the dark (fig. 4.2a, tab. S4.3, see also supplementary data fig. S4.1.4), which was the highest number of negative effects achieved by a single strain in the whole experiment. The taxon also achieved the strongest negative effects in the dark, with up to 80 % reduced cell counts compared to the control (fig. 4.2c, see also supplementary data fig. S4.1.4).
Choricystis achieved a higher number of significantly positive and lower number of significantly negative effects in the dark compared to the standard light conditions (fig. 4.2a+b, tab. S4.3). The overall ratio between organic treatments and the control across compounds remained identical (fig. 4.2c, tab. S4.3) indicating that there was a shift in how different substances affected the strain.

A longer dark acclimation time of eight weeks tested on *Mychonastes* (strain P4) did not positively affect the ability to use organic carbon for growth compared to the two weeks acclimation in the dark (fig. 4.2). Indeed, the longer acclimation time resulted in even fewer significantly positive and more significantly negative effects (fig. 4.2a, b, tab. S4.3) and the overall ratio between organic treatments and controls was significantly lower (fig. 4.2c, tab. S4.3).

Ampicillin removes negative effects in both light treatments and reduces the strength of positive effects in the light

The treatment of *Mychonastes* (strain P4) with ampicillin affected the overall outcome compared to the respective references without ampicillin in the light (standard light treatment) and in the dark (eight weeks dark treatment). Consistently, both in the light and in the dark, the addition of ampicillin removed all negative effects (fig. 4.2a, tab. S4.3), specifically the strong growth inhibition that appeared in the treatments with Tween 40 and Tween 80 in the absence of ampicillin (see also supplementary material fig. S4.1.13, S4.1.14, S4.1.16, S4.1.17). Both in the light and in the dark, there was a net loss of two significantly positive effects in the ampicillin treatment. This net loss was a result of some additional significantly positive effects and the removal of some significantly positive effects in the ampicillin treatment (see also supplementary material fig. S4.1.13, S4.1.14, S4.1.16, S4.1.17). This largely concerned different substances in the light and in the dark. In the dark, the overall ratio between the organic treatments and the control increased in the presence of ampicillin, mostly due to the removal of negative effects (fig. 4.2c, tab S4.3). In contrast, in the light, the overall ratio was reduced in the presence of ampicillin (fig. 4.2c, tab S4.3). While negative effects were removed by ampicillin, the effect strength of positive effects was reduced in the light: Without ampicillin, significantly positive effects went along with an average cell count increase of 22.7 %. In the ampicillin treatment, the average increase was only 5.6 %.

Positive effects are caused by a high variety of different compounds

In the light, the highest number of significantly positive effects across strains was achieved by different carboxylic acids and carbohydrates, which are also the two groups with the most substrates included (fig. 4.3b, tab. S4.3). Strongest positive effects were achieved by carboxylic acids, specifically 2-hydroxy benzoic acid as well as itaconic acid, with up to 90 % increased cell numbers (fig. 4.3c).

Significantly negative effects were often associated with the polymers Tween 40 and Tween 80, as well as the carboxylic acid D-galactonic acid g-lactone and the carbohydrate D-xylose

(fig. 4.3a, tab. S4.3). Strongest negative effects appeared for Tween 80 where cell count was up to ca. 94 % lower than in the control (fig. 4.3c).

In the dark, the number of significantly negative effects overall increased for all types of compounds (fig. 4.3a) for the subset of strains included, i.e. *Mychonastes* (strain P4), *Tetradesmus*, *Monoraphidium* (strain N7) and *Choricystis*. On average, it increased by about four significantly negative effects. The change was remarkably strong for carbohydrates, where 10 times more significantly negative effects appeared in the dark compared to light, mostly associated with *Tetradesmus*. The number of significantly positive effects declined for all types of compounds except carbohydrates (fig. 4.3b), where it increased from 17 to 19. This was associated with more significantly positive effects by carbohydrates on the growth of *Mychonastes* and *Choricystis* in the dark.

4.4. Discussion

Pico green algae and Monoraphidium particularly benefit from organic carbon

In our study, we investigated the ability of 17 phytoplankton strains to use 31 dissolved organic carbon sources for growth. All of our strains took advantage of the presence of certain organic compounds (fig. 4.2b). This is in compliance with former studies conducted with phytoplankton strains from the same or related taxonomic groups both from natural habitats and from culture collections, including e.g. *Mychonastes* (Abdullin and Bagmet, 2015), *Choricystis* (Oliveira et al., 2022), *Monoraphidium* (Zhao et al., 2013), *Tetradesmus* (Patnaik and Mallick, 2020) and *Micractinium* (Smith et al., 2015). Our results support the idea that mixotrophy might be a default strategy in phytoplankton rather than an exceptional ability. Strains that were positively affected by a high number of different compounds, i.e. more than 10 to more than 20, moreover originated from all different sampling stations and seasons included (see also supplementary data tab. S4.1). Hence, mixotrophy seems to appear across seasons and space in the Elbe estuary.

Pico-sized green algae such as *Mychonastes, Choricystis* and *Chlorella* were significantly positively affected by a high variety of organic substances, and included some of the strongest effects (fig. 4.2b,c, tab. S4.3, see also supplementary data fig. S4.1.10, S4.1.11, S4.1.13). Their small size allows for rapid uptake of dissolved compounds. Moreover, these fast-living creatures might be able to more quickly adjust to the availability of organic compounds than larger taxa, and show their full potential within the relatively short 24 h experiments. However, the results show that size was not necessarily the only key driver, as the larger *Monoraphidium* taxa experienced similar effects on growth to the pico green algae, while the small cyanobacteria did not.

Poor positive effects of organic carbon on the growth of some taxa does not necessarily imply that there were no effects at all. Other studies have shown that organic carbon can alter traits beyond growth, such as cell size (Azaman et al., 2017) that were not determined in our study. The results of the *Chlorella*-like strain - i.e. a low number of effects - might have been related to its less homogeneous character (see also section "determination of growth" in the methods and supplementary data tab. S4.4), resulting in higher variation and lower probability to become significant in the t-test. Ultimately, some of the strains with a rather low number of less than 5 significantly positive effects (fig. 4.2b) had more significant effects on single plates which did not re-appear in the other plate replicates and were therefore not significant when the plate data were merged. This was for instance the case in *Micractinium* (see supplementary fig. S4.3.3) and Thalassiosirales (see supplementary fig. S4.3.5). Those strains seem to use more organic carbon sources under certain conditions, in this case mostly in the later exponential phase (see also examples in supplementary data fig. S4.3.3-S4.3.7). In the later exponential phase, nutrient limitation and remineralisation of compounds by bacteria could play a role. However, effects appearing in the late exponential phase were to large extent reflected on the plates with less dense cultures (supplementary data fig. S4.3.3-S4.3.10, see also section "*Inorganic nutrient limitation and remineralisation by bacteria did likely not affect the results" below*). Hence nutrient limitation appears to not be the primary driver for the effects observed. The role of the growth phases for organic carbon acquisition has rarely been discussed to our knowledge (Listmann et al., 2021). Our

results highlight the necessity to integrate the life cycle into mixotrophy related research, especially taking into account that in the field taxa might often not grow exponentially.

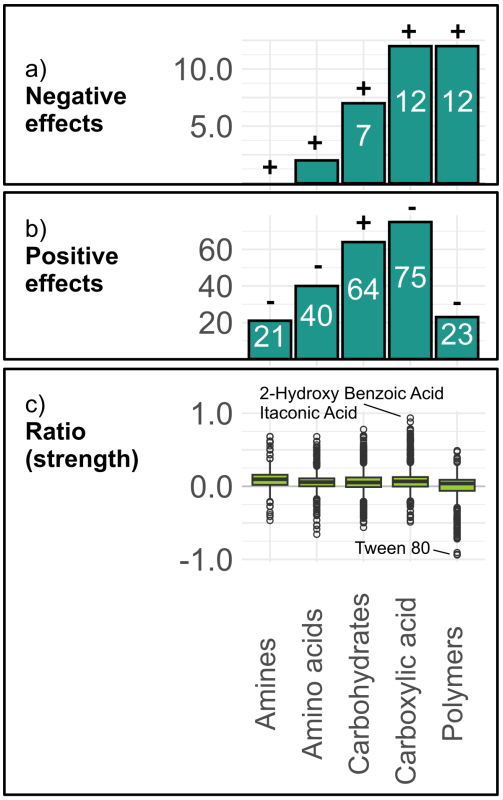

Fig. 4.3: Number of significantly negative (a) and positive (b) effects (t-test, p ≤ 0.05, tab. S4.3) of different types of organic compounds on the growth of the 17 phytoplankton strains in the light (three plates per strain) and effect ratio (strength) (c). The '+' and '-' indicate how the number of significant effects changed from light to dark (two weeks incubation), referring to the four strains included in the dark experiment, namely *Mychonastes* (strain P4), *Tetradesmus*, *Choricystis* and *Monoraphidium* (strain N7). Precisely, '+' indicates an increase of significant effects from light to dark and '-' indicates a decrease of significant effects from light to dark. Note the varying numbers of compounds included per substrate type described in the methods. (c) includes all effects, independent of their significance per strain and light treatment, i.e. every single measurement normalized by the control of the respective plate. This is presented by relative values around 0. The number of data points included in the box plots varied from ca. 300 to ca. 1500 depending on the number of substrates included per substrate type.

Organic carbon acquisition is not primarily a strategy to deal with darkness

Combining autotrophic and heterotrophic mechanisms might enable phytoplankton to maintain growth, especially under highly variable and partially stressful conditions such as light limitation, which is common in estuaries and similar habitats (Tagliapietra et al., 2009).

Different studies have found mixotrophy to be associated with reduced light availability, which has largely been investigated for phagotrophs (Calderini et al., 2022; Millette et al., 2017) and benthic diatoms (Tuchman et al., 2006). Some phytoplankton taxa have been shown even to survive complete darkness on the basis of organic carbon (Godrijan et al., 2022; Jones et al., 2009).

However, for the strains included in our dark experiment, we found overall fewer significant and weaker positive and more significant and partially stronger negative effects in the dark than in the light (fig. 4.2a-c, tab. S4.3). While significantly negative effects could be removed by addition of ampicillin, indicating bacteria played a role here, positive effects remained constrained both in the ampicillin treatment and with enhanced dark acclimation time.

This indicates that the poorer ability to utilize organic carbon for growth was an effect of the reduced light availability. Light dependence of organic carbon uptake and utilization has been observed before (Beamud et al., 2014; Muñoz-Marín et al., 2020). Though many of our strains would certainly benefit from different organic compounds in their natural habitat also at reduced light availability, our results indicate that organic carbon acquisition was not primarily a strategy to maintain growth in the dark. Factors beyond growth however, such as accumulation of storage substrates (e.g. polyglucans and lipids) that could ensure longer term survival have not been investigated in this study and could play a role. A shift in the use of different types of compounds for growth towards a higher number of significantly positive effects of carbohydrates in the dark - specifically in *Choricystis* and *Mychonastes* - might show the effort of phytoplankton to acquire an alternative source of energy where light is limited (fig. 4.3b, tab. S4.3). We should furthermore consider that our dark acclimation study only included four taxa - all green algae - that do neither represent the full range of phytoplankton taxa nor that of ecotypes of taxa in the Elbe estuary and we cannot extrapolate our results on other taxa and functional groups. Also, there is to our knowledge no study available dealing with the uptake of organic compounds under light limitation by green algae in particular, hence, we lack comparable data to confirm if the observed behavior is typical for green algae in general or only for the small number of taxa or strains included in our study.

Inorganic nutrient limitation and remineralisation by bacteria likely did not affect the results

As we worked with non-axenic cultures, bacterial activity can to a certain extent affect the results. Particularly, there might be concerns that abiotic nutrient limitation could play a role in denser cultures, and that remineralisation of the organic compounds by bacteria might promote phytoplankton growth and cause false positive effects. While we cannot completely avoid effects of bacterial supply of inorganic nutrients, we made sure to minimize effects on the study outcome by experimental design, data assessment and processing. First of all, by tracking the cell counts in various different samples prior to the transfer to the EcoPlates™, we ensured that growth was exponential at the beginning of the 24 h incubation window. Second, cultures were included at different densities along the exponential growth phase: at early, mid and late exponential phase. Cultures were grown in enrichment medium (WHM), and at densities below the late exponential phase we can be very certain that abiotic nutrient limitation did not play a role. By comparing the data of the different EcoPlates™, we found that there was no overall trend of more significant positive effects appearing at higher densities, which would be implied, if nutrient limitation and remineralisation played a dominant role (supplementary data fig. S4.3.1). To assess this, we applied the t-test per EcoPlate™ and compared the number of significant effects achieved on the different plates of a strain and light treatment (fig. S4.3.1-S4.3.2). In 83 and 96 % of the cases, significantly positive respectively negative effects, did not exclusively appear at the densest plate, but also at lower cell concentrations proxied by the plate's control mean. Moreover, in 61 and 83 % of the cases, a higher or equal number of significantly positive respectively negative effects was found at lower to mid densities compared to the highest density included. In a few cases, where significant effects only appeared in the densest plates, this had no apparent effect on the overall results merged across plates, as discussed in detail in den supplementary material (fig. S4.3.3-S4.3.7). Lastly, we do know from a former study (Listmann et al., 2021) that use of organic carbon might be growth phase dependent, hence, nutrient limitation alone might not explain why we see more effects in denser plates in some cases.

Negative effects of organic carbon might have been promoted by bacteria

Though in an overwhelming amount of cases organic compounds had positive effects on the growth of our taxa, significantly negative effects appeared for various strains. While the positive effects appeared evenly distributed across various different compounds, a high number of negative effects were associated with the polymers Tween 40 and Tween 80 as well as the carboxylic acid D-galactonic acid g-lactone. The number of significant negative effects overall increased when strains were held in darkness (fig. 4.2a, fig. 4.3a). A specifically high number of significantly negative effects appeared for *Tetradesmus* (fig. 4.2a). Similar results were obtained in former studies with another *Tetradesmus* strain under heterotrophic conditions (Sutherland and Ralph, 2021). The results of the Ampicillin treatment on *Mychonastes* (strain P4) in the dark and in the light, where all significantly negative effects were removed, gives indications that the negative effects might be largely explained by microbial processes. Such processes might play a role in hindering phytoplankton growth in the estuary. Phytoplankton strongly decline along the estuary especially during the passage through the city of Hamburg and so far this has been led back to grazing (Schöl et al., 2009; Walter, 2017). Potential negative effects of bacterial processes should be considered.

The microbiome might reinforce the utilization of organic carbon by phytoplankton

In the Ampicillin treatment of *Mychonastes* (strain P4) the strength of positive effects was diminished in the light, and in both the light and dark, the number of significantly positive effects was slightly lower compared to the samples that had not received an Ampicillin treatment. We can largely rule out that inorganic nutrient limitation and remineralisation by bacteria played a role here, as especially the very strong positive effects of up to ca. 80 % increased cell numbers in the light appeared in the plate with the lowest concentration of the culture (see also supplementary data fig. S4.1.13), where inorganic nutrients were surely not a limiting factor. However, bacteria that live in a symbiosis-like relationship with phytoplankton might benefit from the organic sources present and in turn provide other substances, e.g. essential vitamins (Amin et al., 2012), that drive the growth of

phytoplankton. Our results emphasize that the microbiome might be important for phytoplankton to make use of organic substances in their environment.

Data processing might have led to covering of effects

As mentioned in the section "data processing and analysis", data was merged across plates as results were mostly similar in the different plate replicates (see also supplementary fig. S4.1.1-S4.1.24). In a few cases, results were less similar across plates, e.g. for *Micractinium* in general (supplementary fig. S4.1.1), and in case of single compounds across different taxa (supplementary fig. S4.1.1-S4.1.24). This can lead to covering of potential significant effects that appeared only on single plates, but not repeatedly across plate replicates (also shown exemplarily for some strains in fig. S4.3.3-S4.3.10). However, this is an acceptable trade-off with giving the data more power by including more replicates, i.e. making it far less likely that identified significant effects are based on random variation.

Culture handling and plate life might have affected phytoplankton, but are unlikely to have affected the overall results

We tracked the cell counts prior to plating. By comparing those counts with the results of the experiments - i.e. cell counts after 24 h in the EcoPlates™ (day 1) - we found that in some taxa cell counts declined from day 0 (culture flasks) to day 1 (EcoPlates™), or increased less than expected. A decrease was observed in ca. 35 % of the plates (see also supplementary fig. S4.2), and an increase of less than 5 % in 8 % of the plates. It appears that this phenomenon was randomly distributed across different taxa. It might be either explained by the culture handling (e.g. mixing and transfer to the plate) or by the difficulties associated with life in the plates (e.g. sticking to cell walls). As culture handling, and plate effects in general, should be identical for the controls and treatments on the same plates, this is unlikely to affect the overall outcome of this study. Higher cell numbers in the treatment wells after 24 h compared to the control would still indicate higher growth caused by the compounds in the treatment wells. This is because the organic compound included is the only difference between the control and treatment wells. Hence, there is no mechanistic

indication that positive effects of organic compounds found on growth in this study could be reinforced by such plate effects. Additionally, due to the inclusion of 9 replicates per organic treatment and control, and the significance calculated, random false identification of effects in general should not appear. However, where compounds had negative effects on the growth of phytoplankton, this could exacerbate effects introduced by culture handling and growth in well plates with comparatively low medium volumes. As a result, there is a chance that negative effects of organic compounds could in some cases be reinforced, while still only appearing if there were negative effects of the compounds in the first place.

4.5. Conclusion

Organic compounds promoted the growth of phytoplankton taxa from the Elbe estuary across functional groups, season and origin. The role of phytoplankton as partial heterotrophs - e.g. in trophic upgrading - should be considered in upcoming research. Our results moreover indicate that organic carbon acquisition is not primarily a strategy to deal with reduced light availability. However, effects beyond growth, e.g. use of organic compounds to accumulate storage substrates for longer-term survival in the dark, could play a role and have not been included in this study. Bacteria might promote negative effects of organic carbon on the growth of phytoplankton. Those should be considered in further research and discussions about phytoplankton abundance in the Elbe estuary and similar habitats.

5. Discussion

In the present study, we applied metabarcoding and flow cytometry to analyze community composition in the Elbe estuary. We emphasized the knowledge gaps deriving from the lack of monitoring and research in the mid to lower estuary, so far largely exclusive use of microscopy, and specifically with respect to picophytoplankton. We further carried out laboratory experiments to assess the ability of phytoplankton taxa from the Elbe estuary to utilize dissolved organic compounds. Below we address the research questions indicated in section 1.4 by pointing out key findings of our study. We also highlight further ecological implications from our results and provide suggestions for further research. An overview of the key findings along space and seasons is provided in figure 5.1.

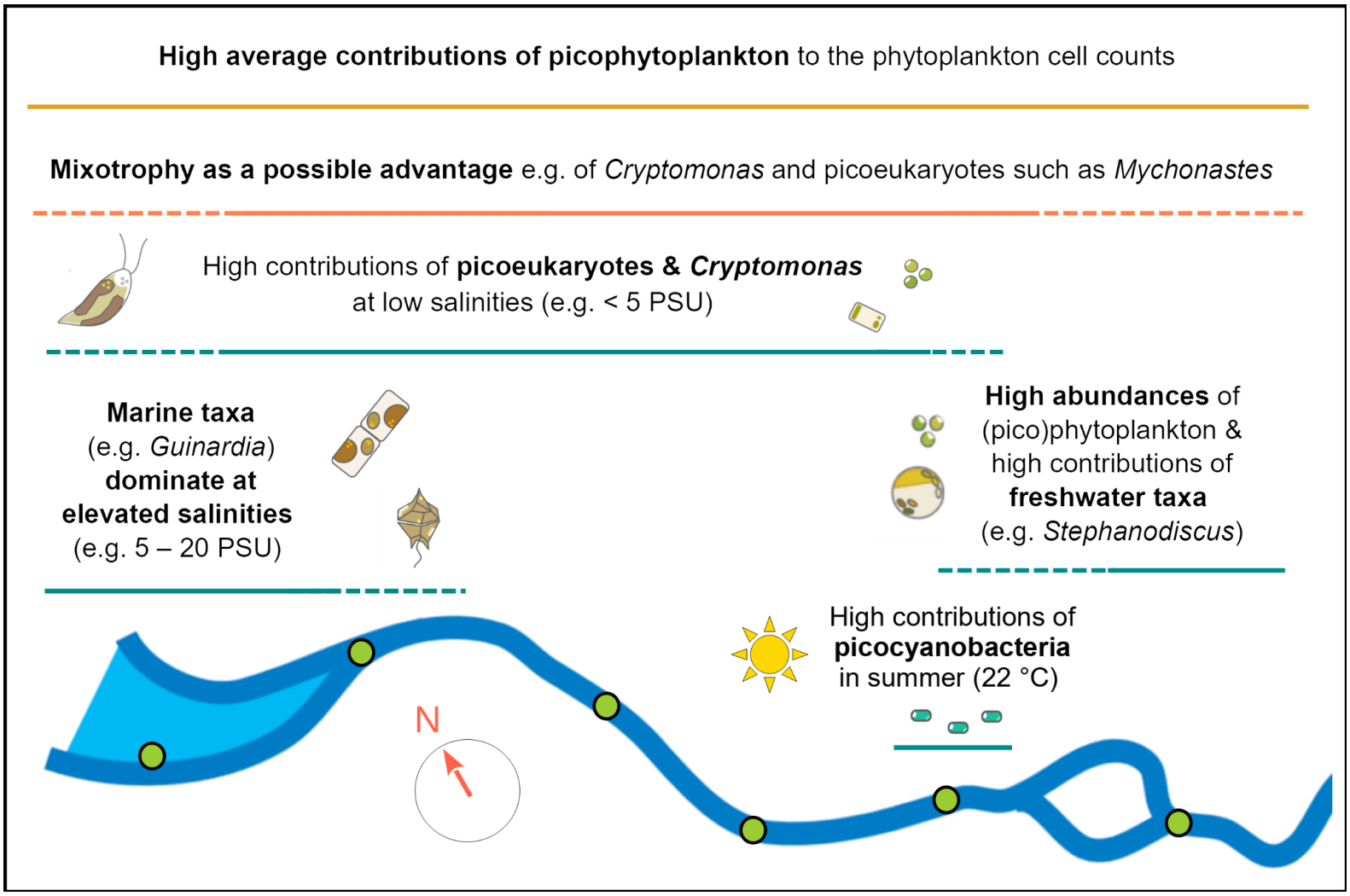

Fig. 5.1: Overview of key findings. Horizontal lines indicate the approximate area where a finding was most relevant (continuous line) or also relevant to some degree (discontinuous lines) along the estuary referring to the respective sampling stations included (see also fig. 1.1 for details). Icons are added to support the information transferred in the respective text notes. Note that the figure is highly simplified for clarity.

RQ1: Which phytoplankton taxa and groups dominate in the mid to lower Elbe estuary?

The mid to lower Elbe estuary is particularly characterized by typical estuarine features such as gradients and variations in salinity and high turbidity in response to river flow and tidal currents (section 2.2, fig. S2.1). Taxa that appear under such conditions may play a critical role in maintaining food webs and biological carbon pumping, but knowledge about phytoplankton in this area is limited to a few studies from decades ago (e.g. (Muylaert and Sabbe, 1999; Wolfstein, 1996)). Since then, the ecosystem has furthermore considerably changed, e.g. due to dredging and global warming.

We applied metabarcoding and flow cytometry to assess community composition along the Elbe estuary (section 1.5). The former is suitable to identify key taxa (e.g. on genus level, and even different species and genotypes within) while the latter can be used to distinguish between phytoplankton groups with certain cell traits (e.g. size). As the number of gene copies per cell is correlated with cell size in phytoplankton (Godhe et al., 2008), composition based on metabarcoding can be understood as a proxy for composition based on size dependent measures (e.g. biovolume). In contrast, flow cytometric data provides abundance i.e. cell counts, e.g. of size groups such as picophytoplankton.

While residues of freshwater taxa from upstream (e.g. *Stephanodiscus*, *Skeletonema*, *Mychonastes*; section 2.3, fig. 2.2d) could be found in the mid to lower estuary, we identified further taxa and groups which were in particular associated with this area (651 - 713 km), as key groups in the mid to lower estuary. These included *Thalassiosira*, *Minidiscus*, *Hemiselmis*, *Cryptomonas* and *Guinardia* as well as not further identified dinoflagellates (fig. 2.2, section 2.3 - 2.4). Therein, *Hemiselmis*, *Minidiscus, Guinardia* and the group of dinoflagellates - partially known from the North Sea (Klöpper et al., 2003; Schlüter et al., 2012) - appeared particularly dominant in the lower estuary (692 - 713 km) and were associated with elevated salinities (e.g. 5 - 20 PSU), indicating that these phytoplankton were pushed into the estuary by the flood stream. Those phytoplankton can however benefit from river-born materials in the river plume (see e.g. (Schlüter et al., 2012; Weston et al., 2008)) and hence their dominance in the lower estuary may not just be coincidental.

Notably, *Minidiscus* was represented by different genotypes and species and not all of them were correlated with salinity (fig. S2.5 - S2.6, tab. S2.5). Diversity within this genus might explain its rather broad distribution along the mid to lower estuary (section 2.4, fig. 2.2d). Similarly, certain genotypes of *Thalassiosira* were positively correlated with salinity (fig. S2.5 - S2.6) though the genus as a whole was not (fig. 2.3).

Cryptomonas was the only dominant genus of phytoplankton that was particularly associated with the mid estuary (651 - 665 km). This group reached significantly higher contributions to the eukaryotic phytoplankton reads in this area compared to both the upper stations (609 - 633 km) and the lower stations (692 - 713 km) (tab. S2.4). *Cryptomonas* was clearly associated with low salinities (section 2.3 - 2.4, fig. 2.3), and did only appear downstream of 665 km when salinity was below 5 PSU as e.g. in winter (fig. S2.5). We conclude that *Cryptomonas* is not forced into the estuary by currents, but rather has specific strategies to retain, survive and/ or grow in this area. This taxon is known for its mixotrophic ability (Ballen-Segura et al., 2017; Princiotta et al., 2019; Urabe et al., 2000) and may obtain additional energy by grazing on bacteria. Transcriptome analyses show that *Cryptomonas* can compensate for low light availability in turbid waters by enhanced phagotrophy (Calderini et al., 2022). Additionally, *Cryptomonas* can vertically migrate (deNoyelles et al., 2016). This can help them to avoid grazing but also support their retention in the estuary (Steidle and Vennell, 2024). The described skills may allow *Cryptomonas* to persist in the mid to lower Elbe estuary, while other taxa are removed by currents or constrained by light limitation (due to high turbidity).

Results from flow cytometry furthermore imply that picophytoplankton - mostly picoeukaryotes - were the dominant group of phytoplankton in the mid estuary with respect to cell counts. This group reached significantly higher contributions between 633 and 692 km compared to the upper station (609 km) across seasons (section 3.3, fig 3.2b-c, tab. S3.2). While results from flow cytometry and metabarcoding are not directly comparable (see details in section 3.2 and fig. 3.1b), we can argue that *Mychonastes* and *Minidiscus* were the dominant taxa of this group (fig. 3.2d). Similar to *Cryptomonas*, certain traits might help picophytoplankton to retain, survive and/ or grow in this area. For instance, due to their

small size, picophytoplankton might be less affected by elimination factors around the city of Hamburg, such as grazing by the key zooplankton *Eurytemora* (Schöl et al., 2009). Their smallness can also support retention in the surface layers where light is more available and hence avoid losses by sinking and promote photosynthetic growth. Beyond, it has been suggested that picophytoplankton in general might prevail in turbid waters - such as those found in the mid to lower Elbe estuary - which is attributed to specific advantages in light harvesting (Coe et al., 2021; Gaulke et al., 2010; Malinsky-Rushansky, 2002; Somogyi et al., 2022, 2017; Soulier et al., 2022). Mixotrophy in terms of acquisition of dissolved organic carbon can furthermore support the growth and competitive advantage of picoeukaryotes in particular in the Elbe estuary (see also discussion about RQ4).

Coastal taxa such as *Guinardia* can dominate the lower Elbe estuary during floods. *Cryptomonas* (*via* metabarcoding) and picoeukaryotes (*via* flow cytometry) appeared particularly dominant in the mid estuary. The presence of these groups here appears not primarily to be based on currents, but they may have certain strategies to thrive in this area (e.g. mixotrophy).

RQ2: Do picophytoplankton play a specific role in the Elbe estuary?

Picophytoplankton have cell sizes smaller than 2-3 µm and can easily be missed when phytoplankton communities are analyzed with the standard method of light microscopy (Bergkemper and Weisse, 2018; Callieri, 2008). In the last decades, the importance of picophytoplankton has found more and more attention in research. Their ubiquitous appearance throughout different water bodies around the world (Coello-Camba and Agustí, 2021; Moreira-Turcq et al., 2001; Purcell-Meyerink et al., 2017; Takasu et al., 2023; Zhang et al., 2015) might be associated with specific features of picophytoplankton going along with their small size and simplicity (e.g. low sinking velocity, high relative surface to take up nutrients) (Massana, 2011; Raven, 1998). These traits allow them to coexist with and sometimes even outcompete larger-celled phytoplankton.

In our study, we analyzed picophytoplankton (< 3 µm) abundance, their contributions to the total phytoplankton cell counts and the proportions of picoeukaryotes and picocyanobacteria *via* flow cytometry (see also section 1.5, section 3). We additionally included information about picophytoplankton taxa from metabarcoding (18S and 16S sequencing) (section 1.5, section 3).

Picophytoplankton contributed on average approximately 70 % (SD = 14 %) to the phytoplankton cell counts in the different samples and were the dominant type of phytoplankton in the Elbe estuary in the majority of the seasons and areas (see also section 3). Though picophytoplankton (and especially picoeukaryotes) were more important in the mid to lower estuary with respect to relative contributions to the phytoplankton (see discussion about RQ1), they achieved overall highest abundances upstream of Hamburg where they could also reach high contributions (average 61 %, SD = 16 %). This indicates that picophytoplankton were not exclusively associated with specific estuarine conditions such as salinity gradients and turbidity that rather appear further downstream, but played a general role and may also be of significance in the riverine areas of the Elbe upstream of the weir. While picoeukaryotes were the dominant type of picophytoplankton throughout most

seasons, picocyanobacteria dominated at high water temperatures in summer (e.g. 22°C) where they could make up to 43 % of the phytoplankton cell counts.

In our metabarcoding data, single taxa of picophytoplankton (namely *Mychonastes* and *Minidiscus*) did furthermore each contribute up to 17 % to the eukaryotic phytoplankton reads, which can be understood as a proxy for relative biovolume (see also (Godhe et al., 2008) and section 2.1 - 2.2). This indicates that picophytoplankton are also relevant in terms of biovolume. Considering their global importance, it is not surprising that picophytoplankton play an important role in the Elbe estuary.

Picophytoplankton are overall the dominant group of phytoplankton in the Elbe estuary with respect to cell counts, capturing particularly large proportions in the middle reaches of the water body. Therein picoeukaryotes were the dominant group in most seasons, while picocyanobacteria played a dominant role in summer. Certain picophytoplankton taxa (especially *Mychonastes* and *Minidiscus*) were additionally important in terms of metabarcoding reads which can be understood as a proxy for relative biovolume.

RQ3: Do results from this study (RQ1-2) match with known data from microscopy?

Phytoplankton communities in the Elbe estuary were so far largely analyzed with light microscopy, and data are limited to current monitoring from the upper to mid reaches (586 - 646 km) (HU, 2023; NLWKN, 2023) and less recent studies from the mid to lower area (e.g. 692 km) (Muylaert and Sabbe, 1999; Wolfstein, 1996). While applying light microscopy to assess phytoplankton community structures appears intuitive, this method comes with some limitations, e.g. a low throughput, restriction to morphology and difficulties to detect picophytoplankton smaller than ca. 2-3 µm (Bergkemper and Weisse, 2018; Callieri, 2008).

Hence, in our study, we applied other methods to analyze phytoplankton communities, mostly metabarcoding, as well as flow cytometry with respect to picophytoplankton in particular. Flow cytometry is a rapid and simple method to provide cell count based data and can e.g. be used to determine the proportion of picophytoplankton in a community (section 1.5). Metabarcoding can obtain more precise information (e.g. genera) (section 1.5). As the number of gene copies per cell is correlated with cell size in phytoplankton (see also (Godhe et al., 2008) and section 2.1 - 2.2), composition based on metabarcoding can be compared with composition based on microscopy-based biovolumes. Yet, differences in the results might sometimes result from the different measurement endpoints. For instance, a high gene copy number can make certain taxa appear more dominant *via* metabarcoding compared to microscopy.

Our results show that the composition of eukaryotic phytoplankton based on 18S reads was similar to the composition of eukaryotic phytoplankton based on microscopy-based biovolume from monitoring in the upper to mid estuary (586 - 651 km) (HU, 2023; NLWKN, 2023) (section 2.3 - 2.4, fig. S2.8). For instance, centric diatoms from the group Mediophyceae and therein *Stephanodiscus* were dominant players in both datasets (fig. 2.4, section 2.3 - 2.4). Furthermore, taxa identified in the lower estuary *via* metabarcoding partially match with those from former literature. For instance, *Guinardia* has been observed in the lower Elbe estuary before *via* microscopy (Tillmann et al., 1999; Wolfstein, 1996).

However, we also found differences between the results from metabarcoding and microscopy. Some taxa (e.g. *Aulacoseira*, *Nitzschia*) appeared not thoroughly covered by metabarcoding. This can be related to different factors, including e.g. primer mismatch or a relatively low number of gene copies with respect to cell size.

In the upper to mid estuary, where monitoring data is available (586 - 651 km), picophytoplankton appeared more dominant both in terms of 18S reads in metabarcoding (section 2.3 - 2.4) as well as in terms of cell counts from flow cytometry (section 3.4) compared to the microscopy-based biovolumes and cell counts, respectively. Beyond, potentially mixotrophic flagellates from the classes Cryptophyceae (especially *Cryptomonas*) and Chrysophyceae were more dominant *via* metabarcoding compared to microscopy here (section 2.3 - 2.4, fig. S2.9). For all mentioned groups, there is no indication that this was caused by differences in sampling time points and stations between the microscopy and metabarcoding datasets (see details in section 2.3 - 2.4, tab. 2.1), and they appear furthermore underrepresented or even absent in former literature from the lower reaches of the estuary (Muylaert and Sabbe, 1999; Wolfstein, 1996).

We conclude that these deviations were based on methodological differences with respect to metabarcoding and microscopy. While we cannot completely exclude such effects, we did not find evidence that these groups, i.e. picoeukaryotes, cryptophytes and chrysophytes - have a particularly high gene copy number that would make them appear more dominant in metabarcoding data. In microscopy however, these groups can be underrepresented due to their small size and because cells are often fragile and can be destroyed by fixation agents or not thoroughly preserved (Bergkemper and Weisse, 2018; Cerino and Zingone, 2006; Lane and Archibald, 2008; Medlin et al., 2017; Sonntag et al., 2000; Xia, 2013).

Our study implies that metabarcoding and microscopy overall yield comparably results, but certain groups can be underrepresented by the one or other method: Picophytoplankton and certain flagellates (e.g. cryptophytes) appeared underestimated in microscopy data, likely due to their small and fragile nature (Bergkemper and Weisse, 2018; Cerino and Zingone, 2006; Lane and Archibald, 2008; Medlin et al., 2017; Xia, 2013). In turn, metabarcoding seems to not (adequately) cover certain key taxa from microscopy (e.g. *Aulacoseira*, *Nitzschia*), possibly due to primer mismatch or low number of gene copies.

RQ4: Is mixotrophy a strategy to survive in the Elbe estuary?

Mixotrophy is the ability of phytoplankton to utilize organic carbon sources, which can be divided into the uptake of dissolved compounds and phagotrophy, i.e. the uptake of particles such as bacteria (section 1.3). A flexible acquisition of energy and nutrients from different available sources appears a reasonable life strategy to efficiently acquire resources (see e.g. (Muñoz-Marín et al., 2020; Reinl et al., 2022)), especially in ecosystems such as estuaries where organic material is fairly available (see e.g. (Abril et al., 2002; Karrasch et al., 2003)) while light for photosynthesis can be limited due to turbidity (fig. S2.1).

In our experimental study (section 4) we assessed the ability of different phytoplankton strains isolated from the Elbe estuary to utilize dissolved organic compounds for growth. Though phagotrophy was not directly addressed in our study, results from metabarcoding can provide further evidence about the importance of potentially phagotrophic taxa (section 3). Lastly, combining the results from our laboratory study - i.e. the ability of different taxa to utilize organic carbon - with community data from metabarcoding and flow cytometry can help understanding the impact of mixotrophic behavior on community structures.

Though in our laboratory study (section 4) all included phytoplankton strains were able to utilize certain organic compounds for growth, we found distinct differences between the taxa and functional groups. The majority of the included pico green algae strains (e.g. *Mychonastes*, *Choricystis*) as well as all three nano green algae strains of *Monoraphidium* could utilize a high number of organic compounds (e.g. > 20) while some other taxa showed a rather poor ability to utilize organic substances (e.g. *Tetradesmus* and picocyanobacteria from the group Synechococcales) (see also fig. 4.2).

The ability to utilize organic carbon did not automatically result in high contributions of the taxa in the field (e.g. in case of *Monoraphidium*), and vice versa, picocyanobacteria which achieved high contributions to cell counts in summer, did have a rather poor ability to utilize organic carbon in our experiments. These results show that organic carbon acquisition is certainly not the only factor shaping phytoplankton communities, and others such as

selective grazing or temperature tolerance were additionally important. However, the apparent success of picoeukaryotes in the Elbe estuary according to metabarcoding and flow cytometry (see also discussion about RQ2) might be partially explained by their mixotrophic abilities.

In our metabarcoding data, we additionally found evidence for the importance of potentially phagotrophic groups such as dinoflagellates, cryptophytes and chrysophytes (Ballen-Segura et al., 2017; Bec et al., 2006; Millette et al., 2017) in the Elbe estuary (see also section 2.4). Low light availability - paired with high prey availability - might support the importance of these groups in estuaries. *Cryptomonas* for instance, which was particularly dominant at high turbidity in the Elbe estuary (fig. 2.2 - 2.3), has been found to compensate for low light availability by enhanced grazing (Calderini et al., 2022).

Though picoeukaryotes were also associated with high turbidity i.e. low light availability, especially in our flow cytometry dataset (fig. 3.4), we could not prove in our experiments that mixotrophy was a specific strategy to deal with darkness. Indeed, included taxa could overall utilize organic compounds more thoroughly at standard light conditions and it has been shown before that the uptake and utilization of organic compounds *can* depend on light availability (Beamud et al., 2014; Muñoz-Marín et al., 2020).

However, only four strains - all green algae - were included in the dark experiment - and results should not be transferred to other taxa and groups. Especially diatoms - a dominant group in the Elbe estuary (fig. 2.2, fig. 2.4) - were underrepresented in our data, and it has been shown before that benthic representatives of this group can increase the use of organic compounds in the dark (Tuchman et al., 2006). Moreover, it should be considered that the ability of mixotrophy still provides certain groups such as picoeukaryotes a relative advantage over others, even when not being a specific strategy to deal with darkness and elevated numbers of positive effects caused by carbohydrates in the dark might moreover show the effort to exploit alternative sources of energy (see also fig. 4.3).

Combined, our results from the laboratory experiments and the community data obtained *via* metabarcoding and flow cytometry provide strong evidence for mixotrophy playing a crucial role in phytoplankton in the Elbe estuary as implied in former research (Wolfstein, 1990).

Though mixotrophy might play a specific role under typical estuarine conditions (e.g. light limitation, high availability of organic matter) we should not conclude that this feature is limited to estuaries. Mixotrophy has been found in numerous phytoplankton taxa from miscellaneous habitats (Anderson et al., 2018; Azaman et al., 2017; Ballen-Segura et al., 2017; Godrijan et al., 2020; Koppelle et al., 2022; Listmann et al., 2021; Millette et al., 2017; Muñoz-Marín et al., 2020; Pang et al., 2022; Villanova and Spetea, 2021) and the finding from our laboratory experiments, where all 17 strains across functional groups were able to utilize certain organic compounds, provides further support for mixotrophy being the norm rather than the exception in phytoplankton (see also (Flynn et al., 2013; Mitra et al., 2014).

Ecological significance

The findings of our study altogether provide new insights into the biotic structures of the Elbe estuary.

Phytoplankton in the mid to lower estuary, including those that are forced into this area by tidal currents (e.g. *Guinardia*) or by the river stream (e.g *Stephanodiscus*) and specifically those who appear more autochthonous (e.g. *Cryptomonas*, picoeukaryotes) might occupy specific ecological niches in this area, where phytoplankton abundance is overall low and maintain a certain level of primary production here.

Though, due to their size, picoeukaryotes are not a preferred food item for dominant taxa such as *Eurytemora* (Schöl et al., 2009), they might be important e.g. as food for nauplii larvae and filter feeders (Bemal and Anil, 2019; Richard et al., 2022). Moreover, it has been suggested that *Eurytemora* can swap to an aggregate diet when phytoplankton availability is low (Modéran et al., 2012). Aggregate formation is a typical feature of various aquatic ecosystems including estuaries (see e.g. (Zimmermann-Timm et al., 1998)). While the nutritional value of aggregates (including e.g. detritus) can be rather low, aggregate-attached phytoplankton (Stukel et al., 2013; Zimmermann-Timm et al., 1998) could add important nutrients such as fatty acids. In areas with low availability of larger-celled taxa such as the mid to lower Elbe estuary, zooplankton might be largely dependent on aggregate-associated materials, and hence possibly on picophytoplankton.

Mixotrophy has cascading effects along the food chains. It has been shown that mixotrophically grown phytoplankton can be of higher nutritional value for zooplankton (Traboni et al., 2021). More generally, by incorporating organic carbon (e.g. bacteria, dissolved compounds) phytoplankton make energy and nutrients (more) available for higher trophic levels. Due to their ability to draw on different sources of nutrients and energy, phytoplankton with a high mixotrophic ability are moreover a more stable food source for zooplankton (Katechakis et al., 2005). Altogether, these factors make mixotrophy appear

critical in areas such as the mid to lower Elbe estuary where food availability for zooplankton is overall low.

Conversely, exploiting heterotrophic pathways places mixotrophic phytoplankton into a more heterotrophic state compared to the assumption of purely autotrophic behavior. Phytoplankton that do use organic substances to gain energy have been shown to have increased respiration rates (Liu et al., 2009; Smith et al., 2015) and downregulate photosynthesis by reducing their chlorophyll a content (Liu et al., 2009; Smith et al., 2015; Znachor and Nedoma, 2010). Where respiration exceeds photosynthesis phytoplankton tip over to become net heterotrophs, i.e. CO_2 producers. This might particularly be the case when habitat conditions such as those in the mid to lower Elbe estuary (e.g. low light availability and high prey availability) favor heterotrophic pathways and when other conditions such as high temperatures additionally fuel respiration (Barton et al., 2020; Padfield et al., 2016).

Method limitations and need for further research

By including various samples along space and time, focussing on dominant groups and setting our results in the context of further literature and monitoring data (e.g. (Calderini et al., 2022; Dobbertin da Costa et al., 2024; NLWKN, 2023)) we can be largely certain about the plausibility of our conclusions. Yet, experimental design and methodological pitfalls (see also section 2.4) can always affect interpretations.

For example, due to the relatively low number of samples analyzed and the underrepresentation of certain areas and seasons (e.g. fall, winter, mid stations; see also section 2.4), especially in the metabarcoding dataset, uncertainties remain e.g. with respect to the relationship of taxa to environmental conditions. For instance, *Cryptomonas* was associated with elevated turbidity, but turbidity was also specifically high in winter, where this taxon prevailed, and temperature might have affected these results. To disentangle the effects of different drivers, further research should address the direct causal relationship of *Cryptomonas* and other important groups with environmental conditions, e.g. in the context

of mesocosm or more simple laboratory experiments. Such experiments can also give insights about the well-being of those phytoplankton under the typical estuarine conditions, rather than just evaluating their appearance as it is the case in e.g. metabarcoding and microscopy-based field surveys.

Beyond that, variations in gene copy numbers (Gong and Marchetti, 2019) might alter the comparability of metabarcoding and microscopy data. While our findings about the quantitative importance of picophytoplankton could be backed up by flow cytometric results, we do miss further support concerning the importance of e.g. *Cryptomonas* and its potential underrepresentation in the microscopy data. We hence supposed that further research should address these limitations, e.g. by obtaining the size-normalized number of 18S gene copies of *Cryptomonas* isolated from the Elbe estuary *via* qPCR (see e.g. (Vasselon et al., 2018)).

In our experimental study, we could prove that several phytoplankton taxa from the Elbe estuary exploit dissolved organic compounds for growth (section 4). Results from metabarcoding provide additional support that potentially phagotrophic taxa (e.g. *Cryptomonas*) play a role in the Elbe estuary (section 2), however, further studies should address to what extent those express actively mixotrophic behavior in the Elbe estuary (as e.g. in (Dobbertin da Costa et al., 2024; Millette et al., 2021)). Moreover, the mixotrophic ability of diatoms from the Elbe estuary (e.g. *Stephanodiscus*, *Thalassiosira*) should be approached in further research as this group is a dominant group in the Elbe estuary, but could not thoroughly be included in our laboratory experiments. Lastly, the role of the microbiome in relation to the utilization of organic compounds by phytoplankton should also be investigated in more detail.

Conclusion

By applying metabarcoding and flow cytometry - and including the unmonitored mid to lower reaches of the study area - we provide new insights into phytoplankton communities along the Elbe estuary. We postulate, that picophytoplankton and potentially mixotrophic groups of phytoplankton such as *Cryptomonas* might play a key role, especially in the mid estuary, but have so far been underrated when communities were assessed *via* microscopy, possibly due to their small size and fragile nature. Our laboratory experiments furthermore provide further evidence for mixotrophy being a key function in phytoplankton from the Elbe estuary - and more broadly spoken in phytoplankton in general. High contributions of various potentially phagotrophic flagellates (e.g. *Cryptomonas*) identified in the phytoplankton communities of the Elbe estuary analyzed *via* metabarcoding give further support for the importance of a mixotrophic life strategy in this habitat. However, further research should address the weak points of our research, e.g. with respect to a relatively low number of samples and underrepresentation of certain areas and seasons in the metabarcoding dataset and the interpretation of metabarcoding results in the context of gene copy numbers. Moreover, active mixotrophic behavior of the identified potentially mixotrophic flagellates (e.g. *Cryptomonas*) in the Elbe estuary should be investigated, and diatoms from this habitat should be more thoroughly included into considerations about mixotrophic behavior.

Literature

Abdullin, Sh.R., Bagmet, V.B., 2015. Experimental analysis for the possibility of heterotrophy in algae: The example of some strains from the Propashchaya Yama Cave. Russ J Ecol 46, 481–482. https://doi.org/10.1134/S1067413615050033

Abril, G., Nogueira, M., Etcheber, H., Cabeçadas, G., Lemaire, E., Brogueira, M.J., 2002. Behaviour of Organic Carbon in Nine Contrasting European Estuaries. Estuarine, Coastal and Shelf Science 54, 241–262. https://doi.org/10.1006/ecss.2001.0844

Alegria Zufia, J., Farnelid, H., Legrand, C., 2021. Seasonality of Coastal Picophytoplankton Growth, Nutrient Limitation, and Biomass Contribution. Front. Microbiol. 12, 786590. https://doi.org/10.3389/fmicb.2021.786590

Altenburger, A., Blossom, H.E., Garcia-Cuetos, L., Jakobsen, H.H., Carstensen, J., Lundholm, N., Hansen, P.J., Moestrup, Ø., Haraguchi, L., 2020. Dimorphism in cryptophytes - The case of Teleaulax amphioxeia/Plagioselmis prolonga and its ecological implications. Science Advances 6.

Amann, T., Weiss, A., Hartmann, J., 2015. Inorganic Carbon Fluxes in the Inner Elbe Estuary, Germany. Estuaries and Coasts 38, 192–210. https://doi.org/10.1007/s12237-014-9785-6

Amin, S.A., Parker, M.S., Armbrust, E.V., 2012. Interactions between Diatoms and Bacteria. Microbiol Mol Biol Rev 76, 667–684. https://doi.org/10.1128/MMBR.00007-12

Anderson, R., Charvet, S., Hansen, P.J., 2018. Mixotrophy in Chlorophytes and Haptophytes—Effect of Irradiance, Macronutrient, Micronutrient and Vitamin Limitation. Front. Microbiol. 9, 1704. https://doi.org/10.3389/fmicb.2018.01704

Araujo, M., Noriega, C., Lefèvre, N., 2014. Nutrients and carbon fluxes in the estuaries of major rivers flowing into the tropical Atlantic. Front. Mar. Sci. 1. https://doi.org/10.3389/fmars.2014.00010

Arsenieff, L., Simon, N., Rigaut-Jalabert, F., Le Gall, F., Chaffron, S., Corre, E., Com, E., Bigeard, E., Baudoux, A.-C., 2019. First Viruses Infecting the Marine Diatom Guinardia delicatula. Front. Microbiol. 9, 3235. https://doi.org/10.3389/fmicb.2018.03235

Azaman, S.N.A., Nagao, N., Yusoff, F.M., Tan, S.W., Yeap, S.K., 2017. A comparison of the morphological and biochemical characteristics of *Chlorella sorokiniana* and *Chlorella zofingiensis* cultured under photoautotrophic and mixotrophic conditions. PeerJ 5, e3473. https://doi.org/10.7717/peerj.3473

Ballen-Segura, M., Felip, M., Catalan, J., 2017. Some Mixotrophic Flagellate Species Selectively Graze on Archaea. Appl Environ Microbiol 83, e02317-16. https://doi.org/10.1128/AEM.02317-16

Banerji, A., Bagley, M., Elk, M., Pilgrim, E., Martinson, J., Santo Domingo, J., 2018. Spatial and temporal dynamics of a freshwater eukaryotic plankton community revealed via 18S rRNA gene metabarcoding. Hydrobiologia 818, 71–86. https://doi.org/10.1007/s10750-018-3593-0

Barton, S., Jenkins, J., Buckling, A., Schaum, C.-E., Smirnoff, N., Raven, J.A., Yvon-Durocher, G., 2020. Evolutionary temperature compensation of carbon fixation in marine phytoplankton. Ecology Letters 23, 722–733. https://doi.org/10.1111/ele.13469

Basu, S., Mackey, K., 2018. Phytoplankton as Key Mediators of the Biological Carbon Pump: Their Responses to a Changing Climate. Sustainability 10, 869. https://doi.org/10.3390/su10030869

Bazin, P., Jouenne, F., Friedl, T., Deton-Cabanillas, A.-F., Le Roy, B., Véron, B., 2014. Phytoplankton Diversity and Community Composition along the Estuarine Gradient of a Temperate Macrotidal Ecosystem: Combined Morphological and Molecular Approaches. PLoS ONE 9, e94110. https://doi.org/10.1371/journal.pone.0094110

Beamud, S.G., Karrasch, B., Pedrozo, F.L., Diaz, M.M., 2014. Utilisation of organic compounds by osmotrophic algae in an acidic lake of Patagonia (Argentina). Limnology 15, 163–172. https://doi.org/10.1007/s10201-014-0427-2

Bec, A., Martin-Creuzburg, D., Von Elert, E., 2006. Trophic upgrading of autotrophic picoplankton by the heterotrophic nanoflagellate *Paraphysomonas* sp. Limnol. Oceanogr. 51, 1699–1707. https://doi.org/10.4319/lo.2006.51.4.1699

Belkinova, D., Teneva, I., Basheva, D., Neykov, N., Moten, D., Gecheva, G., Apostolova, E., Naimov, S., 2021. Phytoplankton composition and ecological tolerance of the autotrophic picoplankton in Atanasovsko Lake (Black Sea coastal lagoon, Bulgaria). Appl. Ecol. Env. Res. 19, 849–866. https://doi.org/10.15666/aeer/1902_849866

Bemal, S., Anil, A.C., 2019. Picophytoplankton Synechococcus as food for nauplii of Amphibalanus amphitrite and Artemia salina. Hydrobiologia 835, 21–36. https://doi.org/10.1007/s10750-019-3923-x

Benner, I., Irwin, A.J., Finkel, Z.V., 2020. Capacity of the common Arctic picoeukaryote *Micromonas* to adapt to a warming ocean. Limnol Oceanogr Letters 5, 221–227. https://doi.org/10.1002/lol2.10133

Bergemann, M., 2004. Die Trübungszone in der Tideelbe - Beschreibung der räumlichen und zeitlichen Entwicklung [The turbidity zone in the tidal Elbe - Description of the spatial and temporal development].

Bergemann, M., Gaumert, T., 2010. Elbebericht 2008 [Elbe Report 2008]. FGG Elbe (Flussgebietsgemeinschaft Elbe/ Elbe River Basin Association).

Bergkemper, V., Weisse, T., 2018. Do current European lake monitoring programmes reliably estimate phytoplankton community changes? Hydrobiologia 824, 143–162. https://doi.org/10.1007/s10750-017-3426-6

Borges, A.V., Delille, B., Frankignoulle, M., 2005. Budgeting sinks and sources of CO_2 in the coastal ocean: Diversity of ecosystems counts: COASTAL CO_2 SINKS AND SOURCES. Geophys. Res. Lett. 32, n/a-n/a. https://doi.org/10.1029/2005GL023053

Boscolo-Galazzo, F., Crichton, K.A., Barker, S., Pearson, P.N., 2018. Temperature dependency of metabolic rates in the upper ocean: A positive feedback to global climate change? Global and Planetary Change 170, 201–212. https://doi.org/10.1016/j.gloplacha.2018.08.017

Calderini, M.L., Salmi, P., Rigaud, C., Peltomaa, E., Taipale, S.J., 2022. Metabolic plasticity of mixotrophic algae is key for their persistence in browning environments. Molecular Ecology 31, 4726–4738. https://doi.org/10.1111/mec.16619

Callahan, B.J., McMurdie, P.J., Rosen, M.J., Han, A.W., Johnson, A.J.A., Holmes, S.P., 2016. DADA2: High-resolution sample inference from Illumina amplicon data. Nat Methods 13, 581–583. https://doi.org/10.1038/nmeth.3869

Callieri, C., 2017. Synechococcus plasticity under environmental changes. FEMS Microbiology Letters 364. https://doi.org/10.1093/femsle/fnx229

Callieri, C., 2008. Picophytoplankton in Freshwater Ecosystems: The Importance of Small-Sized Phototrophs. Freshwater Reviews 1, 1–28. https://doi.org/10.1608/FRJ-1.1.1

Cerino, F., Zingone, A., 2006. A survey of cryptomonad diversity and seasonality at a coastal Mediterranean site. European Journal of Phycology 41, 363–378. https://doi.org/10.1080/09670260600839450

Charvet, S., Vincent, W.F., Lovejoy, C., 2012. Chrysophytes and other protists in High Arctic lakes: molecular gene surveys, pigment signatures and microscopy. Polar Biol 35, 733–748. https://doi.org/10.1007/s00300-011-1118-7

Chen, T., Zhang, Y., Song, S., Liu, Y., Sun, X., Li, C., 2022. Diversity and seasonal variation of marine phytoplankton in Jiaozhou Bay, China revealed by morphological observation and metabarcoding. J. Ocean. Limnol. 40, 577–591. https://doi.org/10.1007/s00343-021-0457-7

Chu, R., Ma, J., Zhou, C., Liu, D., Wang, G., Ruan, R., Lu, Y., Yan, X., Cheng, P., 2022. Improved growth of bait microalgae Isochrysis and aquacultural wastewater treatment with mixotrophic culture. Bioprocess Biosyst Eng 45, 589–597. https://doi.org/10.1007/s00449-021-02681-w

Coe, A., Biller, S.J., Thomas, E., Boulias, K., Bliem, C., Arellano, A., Dooley, K., Rasmussen, A.N., LeGault, K., O'Keefe, T.J., Stover, S., Greer, E.L., Chisholm, S.W., 2021. Coping with darkness: The adaptive response of marine picocyanobacteria to repeated light energy deprivation. Limnology & Oceanography 66, 3300–3312. https://doi.org/10.1002/lno.11880

Coello-Camba, A., Agustí, S., 2021. Picophytoplankton Niche Partitioning in the Warmest Oligotrophic Sea. Front. Mar. Sci. 8, 651877. https://doi.org/10.3389/fmars.2021.651877

Coyne, K.J., Salvitti, L.R., Mangum, A.M., Ozbay, G., Main, C.R., Kouhanestani, Z.M., Warner, M.E., 2021. Interactive effects of light, CO2 and temperature on growth and resource partitioning by the mixotrophic dinoflagellate, Karlodinium veneficum. PLoS ONE 16, e0259161. https://doi.org/10.1371/journal.pone.0259161

Crosbie, N., Teubner, K., Weisse, T., 2003. Flow-cytometric mapping provides novel insights into the seasonal and vertical distributions of freshwater autotrophic picoplankton. Aquat. Microb.

Ecol. 33, 53–66. https://doi.org/10.3354/ame033053

deNoyelles, F., Smith, V., Kastens, J., Bennett, L., Lomas, J., Knapp, C., Bergin, S., Dewey, S., Chapin, B., Graham, D., 2016. A 21-year record of vertically migrating subepilimnetic populations of Cryptomonas spp. IW 6, 173–184. https://doi.org/10.5268/IW-6.2.930

Dobbertin da Costa, M., Gast, R.J., Millette, N.C., 2024. Temporal and spatial variability of constitutive mixotroph abundance and proportion. FEMS Microbiology Ecology 100, fiae015. https://doi.org/10.1093/femsec/fiae015

Drebes, D., Kühn, S.F., Gmelch, A., Schnepf, E., 1996. Cryothecomonas aesfivalis sp. nov., a colourless nanoflagellate feeding on the marine centric diatom Guinardia delicatula (Cleve) Hasle. Helgoländer Meeresuntersuchungen 50, 497–515.

Dubelaar, G.B.J., Jonker, R.R., 2000. Flow cytometry as a tool for the study of phytoplankton. Sci. Mar. 64, 135–156. https://doi.org/10.3989/scimar.2000.64n2135

Dutta, M.K., Kumar, S., Mukherjee, R., Sharma, N., Bhushan, R., Sanyal, P., Paul, M., Mukhopadhyay, S.K., 2021. Carbon Biogeochemistry of Two Contrasting Tropical Estuarine Ecosystems During Premonsoon. Estuaries and Coasts 44, 1916–1930. https://doi.org/10.1007/s12237-021-00908-3

Estrada, M., Henriksen, P., Gasol, J.M., Casamayor, E.O., PedrÃ³s-AliÃ³, C., 2004. Diversity of planktonic photoautotrophic microorganisms along a salinity gradient as depicted by microscopy, flow cytometry, pigment analysis and DNA-based methods. FEMS Microbiology Ecology 49, 281–293. https://doi.org/10.1016/j.femsec.2004.04.002

Fabrin, T.M.C., Stabile, B.H.M., Da Silva, M.V., Jati, S., Rodrigues, L., De Oliveira, A.V., 2020. Cyanobacteria in an urban lake: hidden diversity revealed by metabarcoding. Aquat Ecol 54, 671–675. https://doi.org/10.1007/s10452-020-09763-z

Fast, T., 1993. Zur Dynamic von Biomasse und Primärproduktion des Phytoplanktons im Elbe-Ästuar [About the dynamic of biomass and primary production of the phytoplankton in the Elbe estuary]. PhD thesis available in the library of the University of Hamburg.

Fawley, M.W., Fawley, K.P., 2004. A simple and rapid technique for the isolation of DNA from Microalgae: DNA isolation technique. Journal of Phycology 40, 223–225. https://doi.org/10.1111/j.0022-3646.2004.03-081.x

Fernandes, L.F., Correr-Da-Silva, F., 2020. Diversity and distribution of nanoplanktonic *Minidiscus* (Bacillariophyta) in shelf waters of the Southwest Atlantic Ocean. Diatom Research 35, 327–338. https://doi.org/10.1080/0269249X.2020.1845807

FGG Elbe, 2024. FGG Elbe database (Flussgebietsgemeinschaft Elbe/ Elbe River Basin Association).

Field, C.B., Behrenfeld, M.J., Randerson, J.T., Falkowski, P., 1998. Primary Production of the Biosphere: Integrating Terrestrial and Oceanic Components. Science 281, 237–240. https://doi.org/10.1126/science.281.5374.237

Flombaum, P., Martiny, A.C., 2021a. Diverse but uncertain responses of picophytoplankton lineages to future climate change. Limnology & Oceanography 66, 4171–4181. https://doi.org/10.1002/lno.11951

Flombaum, P., Martiny, A.C., 2021b. Diverse but uncertain responses of picophytoplankton lineages to future climate change. Limnology & Oceanography 66, 4171–4181. https://doi.org/10.1002/lno.11951

Flynn, K.J., Stoecker, D.K., Mitra, A., Raven, J.A., Glibert, P.M., Hansen, P.J., Granéli, E., Burkholder, J.M., 2013. Misuse of the phytoplankton–zooplankton dichotomy: the need to assign organisms as mixotrophs within plankton functional types. Journal of Plankton Research 35, 3–11. https://doi.org/10.1093/plankt/fbs062

Foflonker, F., Ananyev, G., Qiu, H., Morrison, A., Palenik, B., Dismukes, G.C., Bhattacharya, D., 2016. The unexpected extremophile: Tolerance to fluctuating salinity in the green alga Picochlorum. Algal Research 16, 465–472. https://doi.org/10.1016/j.algal.2016.04.003

Foresi, N., Caló, G., Del Castello, F., Nejamkin, A., Salerno, G., Lamattina, L., Martínez-Noël, G., Correa-Aragunde, N., 2022. Arginine as the sole nitrogen source for Ostreococcus tauri growth: Insights on nitric oxide synthase enzyme. Front. Mar. Sci. 9, 1064077. https://doi.org/10.3389/fmars.2022.1064077

Forsström, L., Roiha, T., Rautio, M., 2013. Responses of microbial food web to increased allochthonous DOM in an oligotrophic subarctic lake. Aquat. Microb. Ecol. 68, 171–184. https://doi.org/10.3354/ame01614

Fragoso, G.M., Poulton, A.J., Pratt, N.J., Johnsen, G., Purdie, D.A., 2019. Trait-based analysis of subpolar North Atlantic phytoplankton and plastidic ciliate communities using automated flow cytometer. Limnology & Oceanography 64, 1763–1778. https://doi.org/10.1002/lno.11189

Franke, S., Hildebrandt, S., Schwarzbauer, J., Link, M., Francke, W., 1995. Organic compounds as contaminants of the Elbe River and its tributaries: Part II: GC/MS screening for contaminants of the Elbe water. Fresenius J Anal Chem 353, 39–49. https://doi.org/10.1007/BF00322888

Gaulke, A.K., Wetz, M.S., Paerl, H.W., 2010. Picophytoplankton: A major contributor to planktonic biomass and primary production in a eutrophic, river-dominated estuary. Estuarine, Coastal and Shelf Science 90, 45–54. https://doi.org/10.1016/j.ecss.2010.08.006

Gaumert, T., Bergemann, M., 2007. Sauerstoffgehalt der Tideelbe [Oxygen concentration in the tidal Elbe]. FGG Elbe (Flussgebietsgemeinschaft Elbe/ Elbe River Basin Association).

Geerts, L., Cox, T.J.S., Maris, T., Wolfstein, K., Meire, P., Soetaert, K., 2017. Substrate origin and morphology differentially determine oxygen dynamics in two major European estuaries, the Elbe and the Schelde. Estuarine, Coastal and Shelf Science 191, 157–170. https://doi.org/10.1016/j.ecss.2017.04.009

Ger, K.A., Urrutia-Cordero, P., Frost, P.C., Hansson, L.-A., Sarnelle, O., Wilson, A.E., Lürling, M., 2016. The interaction between cyanobacteria and zooplankton in a more eutrophic world. Harmful

Algae 54, 128–144. https://doi.org/10.1016/j.hal.2015.12.005

Gieskes, W.W.C., Kraay, G.W., 1983. Dominance of Cryptophyceae during the phytoplankton spring bloom in the central North Sea detected by HPLC analysis of pigments. Mar. Biol. 75, 179–185. https://doi.org/10.1007/BF00406000

Godhe, A., Asplund, M.E., Härnström, K., Saravanan, V., Tyagi, A., Karunasagar, I., 2008. Quantification of Diatom and Dinoflagellate Biomasses in Coastal Marine Seawater Samples by Real-Time PCR. Appl Environ Microbiol 74, 7174–7182. https://doi.org/10.1128/AEM.01298-08

Godrijan, J., Drapeau, D., Balch, W.M., 2020. Mixotrophic uptake of organic compounds by coccolithophores. Limnology & Oceanography 65, 1410–1421. https://doi.org/10.1002/lno.11396

Godrijan, J., Drapeau, D.T., Balch, W.M., 2022. Osmotrophy of dissolved organic carbon by coccolithophores in darkness. New Phytologist 233, 781–794. https://doi.org/10.1111/nph.17819

Gong, W., Marchetti, A., 2019. Estimation of 18S Gene Copy Number in Marine Eukaryotic Plankton Using a Next-Generation Sequencing Approach. Front. Mar. Sci. 6, 219. https://doi.org/10.3389/fmars.2019.00219

Gonzalez, L.M., Proulx, S.R., Moeller, H.V., 2022. Modeling the metabolic evolution of mixotrophic phytoplankton in response to rising ocean surface temperatures. BMC Ecol Evo 22, 136. https://doi.org/10.1186/s12862-022-02092-9

Gran-Stadniczeñko, S., Egge, E., Hostyeva, V., Logares, R., Eikrem, W., Edvardsen, B., 2019. Protist Diversity and Seasonal Dynamics in Skagerrak Plankton Communities as Revealed by Metabarcoding and Microscopy. J Eukaryotic Microbiology 66, 494–513. https://doi.org/10.1111/jeu.12700

Grob, C., Ulloa, O., Li, W., Alarcón, G., Fukasawa, M., Watanabe, S., 2007. Picoplankton abundance and biomass across the eastern South Pacific Ocean along latitude 32.5°S. Mar. Ecol. Prog. Ser. 332, 53–62. https://doi.org/10.3354/meps332053

Guillou, L., Bachar, D., Audic, S., Bass, D., Berney, C., Bittner, L., Boutte, C., Burgaud, G., De Vargas, C., Decelle, J., Del Campo, J., Dolan, J.R., Dunthorn, M., Edvardsen, B., Holzmann, M., Kooistra, W.H.C.F., Lara, E., Le Bescot, N., Logares, R., Mahé, F., Massana, R., Montresor, M., Morard, R., Not, F., Pawlowski, J., Probert, I., Sauvadet, A.-L., Siano, R., Stoeck, T., Vaulot, D., Zimmermann, P., Christen, R., 2012. The Protist Ribosomal Reference database (PR2): a catalog of unicellular eukaryote Small Sub-Unit rRNA sequences with curated taxonomy. Nucleic Acids Research 41, D597–D604. https://doi.org/10.1093/nar/gks1160

Hammer, A., Pitchford, J., 2006. Mixotrophy, allelopathy and the population dynamics of phagotrophic algae (cryptophytes) in the Darss Zingst Bodden estuary, southern Baltic. Mar. Ecol. Prog. Ser. 328, 105–115. https://doi.org/10.3354/meps328105

Hanžek, N., Gligora Udovič, M., Kajan, K., Borics, G., Várbíró, G., Stoeck, T., Orlić, S., Stanković, I., 2023. Comparative identification of phytoplankton taxonomic and functional group approach

in karst lakes using classical microscopy and eDNA metabarcoding for ecological status assessment. Hydrobiologia. https://doi.org/10.1007/s10750-023-05344-x

Hattich, G.S.I., Listmann, L., Raab, J., Ozod-Seradj, D., Reusch, T.B.H., Matthiessen, B., 2017. Inter- and intraspecific phenotypic plasticity of three phytoplankton species in response to ocean acidification. Biol. Lett. 13, 20160774. https://doi.org/10.1098/rsbl.2016.0774

Hernández-Fariñas, T., Soudant, D., Barillé, L., Belin, C., Lefebvre, A., Bacher, C., 2014. Temporal changes in the phytoplankton community along the French coast of the eastern English Channel and the southern Bight of the North Sea. ICES Journal of Marine Science 71, 821–833. https://doi.org/10.1093/icesjms/fst192

Holfeld, H., 2000. Infection of the single-celled diatom *Stephanodiscus alpinus* by the chytrid *Zygorhizidium* : Parasite distribution within host population, changes in host cell size, and host–parasite size relationship. Limnology & Oceanography 45, 1440–1444. https://doi.org/10.4319/lo.2000.45.6.1440

Hossain, Md.A., Aktar, S., Qin, J.G., 2016. Salinity stress response in estuarine fishes from the Murray Estuary and Coorong, South Australia. Fish Physiol Biochem 42, 1571–1580. https://doi.org/10.1007/s10695-016-0241-3

HU, 2023. Monitoring data HU (Institut für Hygiene und Umwelt Hamburg) - Phytoplankton taxa and biovolume (via personal communication).

Hu, Y.O.O., Karlson, B., Charvet, S., Andersson, A.F., 2016. Diversity of Pico- to Mesoplankton along the 2000 km Salinity Gradient of the Baltic Sea. Front. Microbiol. 7. https://doi.org/10.3389/fmicb.2016.00679

Huo, S., Li, X., Xi, B., Zhang, H., Ma, C., He, Z., 2020. Combining morphological and metabarcoding approaches reveals the freshwater eukaryotic phytoplankton community. Environ Sci Eur 32, 37. https://doi.org/10.1186/s12302-020-00321-w

Hutchings, J.A., Bianchi, T.S., Najjar, R.G., Herrmann, M., Kemp, W.M., Hinson, A.L., Feagin, R.A., 2020. Carbon Deposition and Burial in Estuarine Sediments of the Contiguous United States. Global Biogeochemical Cycles 34, e2019GB006376. https://doi.org/10.1029/2019GB006376

Jansen, S., Riser, C.W., Wassmann, P., Bathmann, U., 2006. Copepod feeding behaviour and egg production during a dinoflagellate bloom in the North Sea. Harmful Algae 5, 102–112. https://doi.org/10.1016/j.hal.2005.06.006

Jewson, D., Kuwata, A., Cros, L., Fortuño, J.M., Estrada, M., 2016. Morphological adaptations to small size in the marine diatom Minidiscus comicus. Sci. Mar. 80, 89–96. https://doi.org/10.3989/scimar.04331.06C

Jones, H., Cockell, C.S., Goodson, C., Price, N., Simpson, A., Thomas, B., 2009. Experiments on Mixotrophic Protists and Catastrophic Darkness. Astrobiology 9, 563–571. https://doi.org/10.1089/ast.2008.0283

Kaneko, H., Blanc-Mathieu, R., Endo, H., Chaffron, S., Delmont, T.O., Gaia, M., Henry, N.,

Hernández-Velázquez, R., Nguyen, C.H., Mamitsuka, H., Forterre, P., Jaillon, O., De Vargas, C., Sullivan, M.B., Suttle, C.A., Guidi, L., Ogata, H., 2021. Eukaryotic virus composition can predict the efficiency of carbon export in the global ocean. iScience 24, 102002. https://doi.org/10.1016/j.isci.2020.102002

Kang, R., Wang, J., Shi, D., Cong, W., Cai, Z., Ouyang, F., 2004. Interactions between organic and inorganic carbon sources during mixotrophic cultivation of Synechococcus sp. Biotechnology Letters 26, 1429–1432. https://doi.org/10.1023/B:BILE.0000045646.23832.a5

Kang, S., Kim, J.-H., Kim, D., Song, H., Ryu, J.-S., Ock, G., Shin, K.-H., 2019. Temporal variation in riverine organic carbon concentrations and fluxes in two contrasting estuary systems: Geum and Seomjin, South Korea. Environment International 133, 105126. https://doi.org/10.1016/j.envint.2019.105126

Kang, W., Anslan, S., Börner, N., Schwarz, A., Schmidt, R., Künzel, S., Rioual, P., Echeverría-Galindo, P., Vences, M., Wang, J., Schwalb, A., 2021. Diatom metabarcoding and microscopic analyses from sediment samples at Lake Nam Co, Tibet: The effect of sample-size and bioinformatics on the identified communities. Ecological Indicators 121, 107070. https://doi.org/10.1016/j.ecolind.2020.107070

Kappenberg, J., Fanger, H.-U., 2007. Sedimenttransportgeschehen in der tidebeeinflussten Elbe, der Deutschen Bucht und in der Nordsee [Sediment transport processes in the tidally influenced Elbe, the German Bight and in the North Sea] (GKSS 2007/20), wissen schafft nutzen.

Karrasch, B., Ullrich, S., Mehrens, M., Zimmermann-Timm, H., 2003. Free and Particle-associated Extracellular Enzyme Activity and Bacterial Production in the Lower Elbe Estuary, Germany. Acta hydrochim. hydrobiol. 31, 297–306. https://doi.org/10.1002/aheh.200300505

Katechakis, A., Haseneder, T., Kling, R., Stibor, H., 2005. Mixotrophic versus photoautotrophic specialist algae as food for zooplankton: The light : nutrient hypothesis might not hold for mixotrophs. Limnol. Oceanogr. 50, 1290–1299. https://doi.org/10.4319/lo.2005.50.4.1290

Kelly, R.P., Shelton, A.O., Gallego, R., 2019. Understanding PCR Processes to Draw Meaningful Conclusions from Environmental DNA Studies. Sci Rep 9, 12133. https://doi.org/10.1038/s41598-019-48546-x

Kerner, M., Yasseri, S., 1997. Utilization of phytoplankton in seston aggregates from the Elbe estuary, Germany, during early degradation processes. Mar. Ecol. Prog. Ser. 158, 87–102. https://doi.org/10.3354/meps158087

Kezlya, E., Tseplik, N., Kulikovskiy, M., 2023. Genetic Markers for Metabarcoding of Freshwater Microalgae: Review. Biology 12, 1038. https://doi.org/10.3390/biology12071038

Kim, D., Sung, J.W., Kim, T.-H., Cho, H.-M., Kim, J., Park, H.J., 2023. Comparative seasonality of phytoplankton community in two contrasting temperate estuaries on the western coast of Korea. Front. Mar. Sci. 10, 1257904. https://doi.org/10.3389/fmars.2023.1257904

Klöpper, S., Scharek, R., Gerdts, G., 2003. Diarrhetic shellfish toxicity in relation to the abundance of Dinophysis spp. in the German Bight near Helgoland. Mar. Ecol. Prog. Ser. 259, 93–102.

https://doi.org/10.3354/meps259093

Kolda, A., Ljubešić, Z., Gavrilović, A., Jug-Dujaković, J., Pikelj, K., Kapetanović, D., 2020. Metabarcoding Cyanobacteria in coastal waters and sediment in central and southern Adriatic Sea. Acta bot. Croat. (Online) 79, 157–169. https://doi.org/10.37427/botcro-2020-021

Koppelle, S., López-Escardó, D., Brussaard, C.P.D., Huisman, J., Philippart, C.J.M., Massana, R., Wilken, S., 2022. Mixotrophy in the bloom-forming genus Phaeocystis and other haptophytes. Harmful Algae 117, 102292. https://doi.org/10.1016/j.hal.2022.102292

Krienitz, L., Bock, C., Dadheech, P.K., Pröschold, T., 2011. Taxonomic reassessment of the genus *Mychonastes* (Chlorophyceae, Chlorophyta) including the description of eight new species. Phycologia 50, 89–106. https://doi.org/10.2216/10-15.1

Labbé, M., Raymond, F., Lévesque, A., Thaler, M., Mohit, V., Audet, M., Corbeil, J., Culley, A., 2018. Communities of Phytoplankton Viruses across the Transition Zone of the St. Lawrence Estuary. Viruses 10, 672. https://doi.org/10.3390/v10120672

Lancelot, C., Muylaert, K., 2011. Trends in Estuarine Phytoplankton Ecology, in: Treatise on Estuarine and Coastal Science. Elsevier, pp. 5–15. https://doi.org/10.1016/B978-0-12-374711-2.00703-8

Lane, C.E., Archibald, J.M., 2008. NEW MARINE MEMBERS OF THE GENUS *HEMISELMIS* (CRYPTOMONADALES, CRYPTOPHYCEAE). Journal of Phycology 44, 439–450. https://doi.org/10.1111/j.1529-8817.2008.00486.x

Laufkötter, C., Vogt, M., Gruber, N., Aita-Noguchi, M., Aumont, O., Bopp, L., Buitenhuis, E., Doney, S.C., Dunne, J., Hashioka, T., Hauck, J., Hirata, T., John, J., Le Quéré, C., Lima, I.D., Nakano, H., Seferian, R., Totterdell, I., Vichi, M., Völker, C., 2015. Drivers and uncertainties of future global marine primary production in marine ecosystem models. Biogeosciences 12, 6955–6984. https://doi.org/10.5194/bg-12-6955-2015

Leblanc, K., Quéguiner, B., Diaz, F., Cornet, V., Michel-Rodriguez, M., Durrieu De Madron, X., Bowler, C., Malviya, S., Thyssen, M., Grégori, G., Rembauville, M., Grosso, O., Poulain, J., De Vargas, C., Pujo-Pay, M., Conan, P., 2018. Nanoplanktonic diatoms are globally overlooked but play a role in spring blooms and carbon export. Nat Commun 9, 953. https://doi.org/10.1038/s41467-018-03376-9

Lee, D., Keller, D., Crump, B., Hood, R., 2012. Community metabolism and energy transfer in the Chesapeake Bay estuarine turbidity maximum. Mar. Ecol. Prog. Ser. 449, 65–82. https://doi.org/10.3354/meps09543

Lepori-Bui, M., Paight, C., Eberhard, E., Mertz, C.M., Moeller, H.V., 2022. Evidence for evolutionary adaptation of mixotrophic nanoflagellates to warmer temperatures. Global Change Biology 28, 7094–7107. https://doi.org/DOI: 10.1111/gcb.16431

Levin, L.A., Boesch, D.F., Covich, A., Dahm, C., Erséus, C., Ewel, K.C., Kneib, R.T., Moldenke, A., Palmer, M.A., Snelgrove, P., Strayer, D., Weslawski, J.M., 2001. The Function of Marine Critical

Transition Zones and the Importance of Sediment Biodiversity. Ecosystems 4, 430–451. https://doi.org/10.1007/s10021-001-0021-4

Li, M., Chen, Y., Zhang, F., Song, Y., Glibert, P.M., Stoecker, D.K., 2022. A three-dimensional mixotrophic model of Karlodinium veneficum blooms for a eutrophic estuary. Harmful Algae 113, 102203. https://doi.org/10.1016/j.hal.2022.102203

Li, Q., Dong, K., Wang, Y., Edwards, K.F., 2024. Relative importance of bacterivorous mixotrophs in an estuary-coast environment. Limnol Oceanogr Letters 9, 81–91. https://doi.org/10.1002/lol2.10362

Listmann, L., Kerl, F., Martens, N., Schaum, C.-E., 2021. Differences in Carbon Acquisition Could Explain Adaptive Responses in a Baltic Sea Pico-Phytoplankton. Front. Mar. Sci. 8, 740763. https://doi.org/10.3389/fmars.2021.740763

Liu, X., Duan, S., Li, A., Xu, N., Cai, Z., Hu, Z., 2009. Effects of organic carbon sources on growth, photosynthesis, and respiration of Phaeodactylum tricornutum. J Appl Phycol 21, 239–246. https://doi.org/10.1007/s10811-008-9355-z

Malinsky-Rushansky, N., 2002. Physiological characteristics of picophytoplankton, isolated from Lake Kinneret: responses to light and temperature. Journal of Plankton Research 24, 1173–1183. https://doi.org/10.1093/plankt/24.11.1173

Markina, Zh.V., 2019. Flow Cytometry as a Method to Study Marine Unicellular Algae: Development, Problems, and Prospects. Russ J Mar Biol 45, 333–340. https://doi.org/10.1134/S1063074019050079

Martens, N., Ehlert, E., Putri, W., Sibbertsen, M., Schaum, C.-E., 2024a. Organic compounds drive growth in phytoplankton taxa from different functional groups. Proc. R. Soc. B 291. https://doi.org/10.1098/rspb.2023.2713

Martens, N., Russnak, V., Woodhouse, J., Grossart, H.-P., Schaum, C.-E., 2024b. Metabarcoding reveals potentially mixotrophic flagellates and picophytoplankton as key groups of phytoplankton in the Elbe estuary. Environmental Research 252. https://doi.org/10.1016/j.envres.2024.119126

Martin, J.L., Santi, I., Pitta, P., John, U., Gypens, N., 2022. Towards quantitative metabarcoding of eukaryotic plankton: an approach to improve 18S rRNA gene copy number bias. MBMG 6, e85794. https://doi.org/10.3897/mbmg.6.85794

Massana, R., 2011. Eukaryotic Picoplankton in Surface Oceans. Annu. Rev. Microbiol. 65, 91–110. https://doi.org/10.1146/annurev-micro-090110-102903

McKindles, K.M., McKay, R.M.L., Bullerjahn, G.S., Frenken, T., 2023. Interactions between chytrids cause variable infection strategies on harmful algal bloom forming species. Harmful Algae 122, 102381. https://doi.org/10.1016/j.hal.2023.102381

Medlin, L.K., Piwosz, K., Metfies, K., 2017. Uncovering hidden biodiversity in the cryptophyta: clone library studies at the Helgoland time series site in the southern German bight identifies the

cryptophycean clade potentially responsible for the majority of its genetic diversity during the spring bloom. Vie Milieu 67, 27–32.

Millette, N., Da Costa, M., Mora, J., Gast, R., 2021. Temporal and spatial variability of phytoplankton and mixotrophs in a temperate estuary. Mar. Ecol. Prog. Ser. 677, 17–31. https://doi.org/10.3354/meps13850

Millette, N.C., Gast, R.J., Luo, J.Y., Moeller, H.V., Stamieszkin, K., Andersen, K.H., Brownlee, E.F., Cohen, N.R., Duhamel, S., Dutkiewicz, S., Glibert, P.M., Johnson, M.D., Leles, S.G., Maloney, A.E., Mcmanus, G.B., Poulton, N., Princiotta, S.D., Sanders, R.W., Wilken, S., 2023. Mixoplankton and mixotrophy: future research priorities. Journal of Plankton Research 45, 576–596. https://doi.org/10.1093/plankt/fbad020

Millette, N.C., Pierson, J.J., Aceves, A., Stoecker, D.K., 2017. Mixotrophy in *Heterocapsa rotundata* : A mechanism for dominating the winter phytoplankton. Limnol. Oceanogr. 62, 836–845. https://doi.org/10.1002/lno.10470

Mitbavkar, S., Rath, A.R., Anil, A.C., 2021. Picophytoplankton community dynamics in a tropical river estuary and adjacent semi-enclosed water body. Aquat Sci 83, 61. https://doi.org/10.1007/s00027-021-00813-8

Mitra, A., Flynn, K.J., Burkholder, J.M., Berge, T., Calbet, A., Raven, J.A., Granéli, E., Glibert, P.M., Hansen, P.J., Stoecker, D.K., Thingstad, F., Tillmann, U., Våge, S., Wilken, S., Zubkov, M.V., 2014. The role of mixotrophic protists in the biological carbon pump. Biogeosciences 11, 995–1005. https://doi.org/10.5194/bg-11-995-2014

Modéran, J., David, V., Bouvais, P., Richard, P., Fichet, D., 2012. Organic matter exploitation in a highly turbid environment: Planktonic food web in the Charente estuary, France. Estuarine, Coastal and Shelf Science 98, 126–137. https://doi.org/10.1016/j.ecss.2011.12.018

Montoya, N., Akselman, R., Carignan, M., Carreto, J., 2006. Pigment profile and toxin composition during a red tide of *Gymnodinium catenatum* Graham and *Myrionecta rubra* (Lohman) Jankowski in coastal waters off Mar del Plata, Argentina. African Journal of Marine Science 28, 199–202. https://doi.org/10.2989/18142320609504147

Mora, D., Abarca, N., Proft, S., Grau, J.H., Enke, N., Carmona, J., Skibbe, O., Jahn, R., Zimmermann, J., 2019. Morphology and metabarcoding: a test with stream diatoms from Mexico highlights the complementarity of identification methods. Freshwater Science 38, 448–464. https://doi.org/10.1086/704827

Moreira-Turcq, P.F., Cauwet, G., Martin, J.M., 2001. Contribution of flow cytometry to estimate picoplankton biomass in estuarine systems. Hydrobiologia 462, 157–168.

Muñoz-Marín, M.C., Gómez-Baena, G., López-Lozano, A., Moreno-Cabezuelo, J.A., Díez, J., García-Fernández, J.M., 2020. Mixotrophy in marine picocyanobacteria: use of organic compounds by Prochlorococcus and Synechococcus. ISME J 14, 1065–1073. https://doi.org/10.1038/s41396-020-0603-9

Murrell, M.C., Lores, E.M., 2004. Phytoplankton and zooplankton seasonal dynamics in a subtropical

estuary: importance of cyanobacteria. Journal of Plankton Research 26, 371–382. https://doi.org/10.1093/plankt/fbh038

Muylaert, K., Sabbe, K., 1999. Spring phytoplankton assemblages in and around the maximum turbidity zone of the estuaries of the Elbe (Germany), the Schelde (Belgium/ The Netherlands) and the Gironde (France).

Naselli-Flores, L., Barone, R., 2019. Mixotrophic phytoplankton dynamics in a shallow Mediterranean water body: how to make a virtue out of necessity. Hydrobiologia 831, 33–41. https://doi.org/10.1007/s10750-018-3507-1

Ning, M., Li, H., Xu, Z., Chen, L., He, Y., 2021. Picophytoplankton identification by flow cytometry and high-throughput sequencing in a clean reservoir. Ecotoxicology and Environmental Safety 216, 112216. https://doi.org/10.1016/j.ecoenv.2021.112216

Nishino, H., Hodoki, Y., Thottathil, S.D., Ohbayashi, K., Takao, Y., Nakano, S., 2015. Identification of species and genotypic compositions of Cryptomonas (Cryptophyceae) populations in the eutrophic Lake Hira, Japan, using single-cell PCR. Aquat Ecol 49, 263–272. https://doi.org/10.1007/s10452-015-9520-9

NLWKN, 2023. Monitoring data NLWKN (Niedersächsischer Landesbetrieb für Wasserwirtschaft, Küsten- und Naturschutz) - Phytoplankton taxa and biovolume (via personal communication).

Oliveira, C.Y.B., Nader, C., Silva, M.F.O., Fracalossi, D.M., Gálvez, A.O., Lopes, R.G., Derner, R.B., 2022. Integrated use of microalgal biomass of Choricystis minor var. minor: a promising model for production of biodiesel and aquafeeds. Biomass Conv. Bioref. 12, 1565–1573. https://doi.org/10.1007/s13399-020-01091-4

Otero-Ferrer, J.L., Cermeño, P., Bode, A., Fernández-Castro, B., Gasol, J.M., Morán, X.A.G., Marañon, E., Moreira-Coello, V., Varela, M.M., Villamaña, M., Mouriño-Carballido, B., 2018. Factors controlling the community structure of picoplankton in contrasting marine environments. Biogeosciences 15, 6199–6220. https://doi.org/10.5194/bg-15-6199-2018

Padfield, D., Yvon-Durocher, Genevieve, Buckling, A., Jennings, S., Yvon-Durocher, Gabriel, 2016. Rapid evolution of metabolic traits explains thermal adaptation in phytoplankton. Ecol Lett 19, 133–142. https://doi.org/10.1111/ele.12545

Paerl, R.W., Venezia, R.E., Sanchez, J.J., Paerl, H.W., 2020. Picophytoplankton dynamics in a large temperate estuary and impacts of extreme storm events. Sci Rep 10, 22026. https://doi.org/10.1038/s41598-020-79157-6

Pang, M., Liu, K., Liu, H., 2022. Evidence for mixotrophy in pico-chlorophytes from a new Picochlorum (Trebouxiophyceae) strain. J. Phycol. 58, 80–91. https://doi.org/10.1111/jpy.13218

Park, J.S., Jung, S.W., Ki, J.-S., Guo, R., Kim, H.J., Lee, K.-W., Lee, J.H., 2017. Transfer of the small diatoms Thalassiosira proschkinae and T. spinulata to the genus Minidiscus and their taxonomic re-description. PLoS ONE 12, e0181980. https://doi.org/10.1371/journal.pone.0181980

Patnaik, R., Mallick, N., 2020. Individual and combined supplementation of carbon sources for growth augmentation and enrichment of lipids in the green microalga Tetradesmus obliquus. J Appl Phycol 32, 205–219. https://doi.org/10.1007/s10811-019-01979-3

Pattanaik, S., Chanda, A., Sahoo, R.K., Swain, S., Satapathy, D.R., Panda, C.R., Choudhury, S.B., Mohapatra, P.K., 2020. Contrasting intra-annual inorganic carbon dynamics and air–water CO2 exchange in Dhamra and Mahanadi Estuaries of northern Bay of Bengal, India. Limnology 21, 129–138. https://doi.org/10.1007/s10201-019-00592-0

Petersen, W., Schroeder, F., Bockelmann, F.-D., 2011. FerryBox - Application of continuous water quality observations along transects in the North Sea. Ocean Dynamics 61, 1541–1554. https://doi.org/10.1007/s10236-011-0445-0

Piredda, R., Claverie, J.-M., Decelle, J., De Vargas, C., Dunthorn, M., Edvardsen, B., Eikrem, W., Forster, D., Kooistra, W.H.C.F., Logares, R., Massana, R., Montresor, M., Not, F., Ogata, H., Pawlowski, J., Romac, S., Sarno, D., Stoeck, T., Zingone, A., 2018. Diatom diversity through HTS-metabarcoding in coastal European seas. Sci Rep 8, 18059. https://doi.org/10.1038/s41598-018-36345-9

Piwosz, K., Całkiewicz, J., Gołębiewski, M., Creer, S., 2018. Diversity and community composition of pico- and nanoplanktonic protists in the Vistula River estuary (Gulf of Gdańsk, Baltic Sea). Estuarine, Coastal and Shelf Science 207, 242–249. https://doi.org/10.1016/j.ecss.2018.04.013

Princiotta, S.D., Hendricks, S.P., White, D.S., 2019. Production of Cyanotoxins by Microcystis aeruginosa Mediates Interactions with the Mixotrophic Flagellate Cryptomonas. Toxins 11, 223. https://doi.org/10.3390/toxins11040223

Puigcorbé, V., Benitez-Nelson, C.R., Masqué, P., Verdeny, E., White, A.E., Popp, B.N., Prahl, F.G., Lam, P.J., 2015. Small phytoplankton drive high summertime carbon and nutrient export in the Gulf of California and Eastern Tropical North Pacific. Global Biogeochemical Cycles 29, 1309–1332. https://doi.org/10.1002/2015GB005134

Purcell-Meyerink, D., Fortune, J., Butler, E.C.V., 2017. Productivity dominated by picoplankton in a macro-tidal tropical estuary, Darwin Harbour. New Zealand Journal of Botany 55, 47–63. https://doi.org/10.1080/0028825X.2016.1231125

Raven, J.A., 1998. The twelfth Tansley Lecture. Small is beautiful: the picophytoplankton: Picophyto-plankton. Functional Ecology 12, 503–513. https://doi.org/10.1046/j.1365-2435.1998.00233.x

Read, Daniel.S., Bowes, M.J., Newbold, L.K., Whiteley, A.S., 2014. Weekly flow cytometric analysis of riverine phytoplankton to determine seasonal bloom dynamics. Environ. Sci.: Processes Impacts 16, 594. https://doi.org/10.1039/c3em00657c

Reinl, K.L., Harris, T.D., Elfferich, I., Coker, A., Zhan, Q., De Senerpont Domis, L.N., Morales-Williams, A.M., Bhattacharya, R., Grossart, H.-P., North, R.L., Sweetman, J.N., 2022. The role of organic nutrients in structuring freshwater phytoplankton communities in a rapidly changing world.

Water Research 219, 118573. https://doi.org/10.1016/j.watres.2022.118573

Ren, L., Jensen, K., Porada, P., Mueller, P., 2022. Biota-mediated carbon cycling—A synthesis of biotic-interaction controls on blue carbon. Ecology Letters 25, 521–540. https://doi.org/10.1111/ele.13940

Richard, M., Bec, B., Bergeon, L., Hébert, M., Mablouké, C., Lagarde, F., 2022. Are mussels and oysters capable of reducing the abundances of Picochlorum sp., responsible for a massive green algae bloom in Thau lagoon, France? Journal of Experimental Marine Biology and Ecology 556, 151797. https://doi.org/10.1016/j.jembe.2022.151797

Rynearson, T.A., Flickinger, S.A., Fontaine, D.N., 2020. Metabarcoding Reveals Temporal Patterns of Community Composition and Realized Thermal Niches of Thalassiosira Spp. (Bacillariophyceae) from the Narragansett Bay Long-Term Plankton Time Series. Biology 9, 19. https://doi.org/10.3390/biology9010019

Salmi, P., Mäki, A., Mikkonen, A., Puupponen, V.-M., Vuorio, K., Tiirola, M., 2021. Comparison of epifluorescence microscopy and flow cytometry in counting freshwater picophytoplankton. BOREAL ENVIRONMENT RESEARCH 26, 17–27.

Santi, I., Kasapidis, P., Karakassis, I., Pitta, P., 2021. A Comparison of DNA Metabarcoding and Microscopy Methodologies for the Study of Aquatic Microbial Eukaryotes. Diversity 13, 180. https://doi.org/10.3390/d13050180

Santoferrara, L.F., 2019. Current practice in plankton metabarcoding: optimization and error management. Journal of Plankton Research 41, 571–582. https://doi.org/10.1093/plankt/fbz041

Sassenhagen, I., Langenheder, S., Lindström, E.S., 2023. Infection strategies of different chytrids in a diatom spring bloom. Freshwater Biology 68, 972–986. https://doi.org/10.1111/fwb.14079

Sathicq, M.B., Unrein, F., Gómez, N., 2020. Recurrent pattern of picophytoplankton dynamics in estuaries around the world: The case of Río de la Plata. Marine Environmental Research 161, 105136. https://doi.org/10.1016/j.marenvres.2020.105136

Schaum, C.-E., Rost, B., Collins, S., 2016. Environmental stability affects phenotypic evolution in a globally distributed marine picoplankton. The ISME Journal 10, 75–84.

Schlüter, M.H., Kraberg, A., Wiltshire, K.H., 2012. Long-term changes in the seasonality of selected diatoms related to grazers and environmental conditions. Journal of Sea Research 67, 91–97. https://doi.org/10.1016/j.seares.2011.11.001

Schöl, A., Blohm, W., Becker, A., Fischer, H., 2009. Untersuchungen zum Rückgang hoher Algenbiomassen im limnischen Abschnitt der Tideelbe [Investigations concerning the decline of high algal biomass in the limnic part of the tidal Elbe].

Seto, K., Van Den Wyngaert, S., Degawa, Y., Kagami, M., 2020. Taxonomic revision of the genus *Zygorhizidium* : *Zygorhizidiales* and *Zygophlyctidales ord. nov.* (*Chytridiomycetes* , *Chytridiomycota*). Fungal Systematics and Evolution 5, 17–38.

https://doi.org/10.3114/fuse.2020.05.02

Sew, G., Todd, P., 2020. Effects of Salinity and Suspended Solids on Tropical Phytoplankton Mesocosm Communities. Tropical Conservation Science 13, 194008292093976. https://doi.org/10.1177/1940082920939760

Sim, Z.Y., Goh, K.C., He, Y., Gin, K.Y.H., 2023. Present and future potential role of toxin-producing Synechococcus in the tropical region. Science of The Total Environment 896, 165230. https://doi.org/10.1016/j.scitotenv.2023.165230

Sime-Ngando, T., 2012. Phytoplankton Chytridiomycosis: Fungal Parasites of Phytoplankton and Their Imprints on the Food Web Dynamics. Front. Microbio. 3. https://doi.org/10.3389/fmicb.2012.00361

Smith, R.T., Bangert, K., Wilkinson, S.J., Gilmour, D.J., 2015. Synergistic carbon metabolism in a fast growing mixotrophic freshwater microalgal species Micractinium inermum. Biomass and Bioenergy 82, 73–86. https://doi.org/10.1016/j.biombioe.2015.04.023

Somogyi, B., Felföldi, T., Boros, E., Szabó, A., Vörös, L., 2022. Where the Little Ones Play the Main Role—Picophytoplankton Predominance in the Soda and Hypersaline Lakes of the Carpathian Basin. Microorganisms 10, 818. https://doi.org/10.3390/microorganisms10040818

Somogyi, B., Felföldi, T., Tóth, L.G., Bernát, G., Vörös, L., 2020. Photoautotrophic picoplankton – a review on their occurrence, role and diversity in Lake Balaton. BIOLOGIA FUTURA 71, 371–382. https://doi.org/10.1007/s42977-020-00030-8

Somogyi, B., Pálffy, K., V. -Balogh, K., Botta-Dukát, Z., Vörös, L., 2017. Unusual behaviour of phototrophic picoplankton in turbid waters. PLoS ONE 12, e0174316. https://doi.org/10.1371/journal.pone.0174316

Sonntag, B., Posch, T., Psenner, R., 2000. Comparison of three methods for determining flagellate abundance, cell size, and biovolume in cultures and natural freshwater samples. fal 149, 337–351. https://doi.org/10.1127/archiv-hydrobiol/149/2000/337

Soulier, N., Walters, K., Laremore, T.N., Shen, G., Golbeck, J.H., Bryant, D.A., 2022. Acclimation of the photosynthetic apparatus to low light in a thermophilic Synechococcus sp. strain. Photosynth Res 153, 21–42. https://doi.org/10.1007/s11120-022-00918-7

Stat, M., Huggett, M.J., Bernasconi, R., DiBattista, J.D., Berry, T.E., Newman, S.J., Harvey, E.S., Bunce, M., 2017. Ecosystem biomonitoring with eDNA: metabarcoding across the tree of life in a tropical marine environment. Sci Rep 7, 12240. https://doi.org/10.1038/s41598-017-12501-5

Steidle, L., Vennell, R., 2024. Phytoplankton retention mechanisms in estuaries: a case study of the Elbe estuary. Nonlin. Processes Geophys. 31, 151–164. https://doi.org/10.5194/npg-31-151-2024

Stomp, M., Van Dijk, M.A., Van Overzee, H.M.J., Wortel, M.T., Sigon, C.A.M., Egas, M., Hoogveld, H., Gons, H.J., Huisman, J., 2008. The Timescale of Phenotypic Plasticity and Its Impact on Competition in Fluctuating Environments. The American Naturalist 172, E169–E185.

https://doi.org/10.1086/591680

Stukel, M.R., Décima, M., Selph, K.E., Taniguchi, D.A.A., Landry, M.R., 2013. The role of Synechococcus in vertical flux in the Costa Rica upwelling dome. Progress in Oceanography 112–113, 49–59. https://doi.org/10.1016/j.pocean.2013.04.003

Subramaniam, A., Yager, P.L., Carpenter, E.J., Mahaffey, C., Björkman, K., Cooley, S., Kustka, A.B., Montoya, J.P., Sañudo-Wilhelmy, S.A., Shipe, R., Capone, D.G., 2008. Amazon River enhances diazotrophy and carbon sequestration in the tropical North Atlantic Ocean. Proc. Natl. Acad. Sci. U.S.A. 105, 10460–10465. https://doi.org/10.1073/pnas.0710279105

Sutherland, D.L., Ralph, P.J., 2021. Differing growth responses in four related microalgal genera grown under autotrophic, mixotrophic and heterotrophic conditions. J Appl Phycol 33, 3539–3553. https://doi.org/10.1007/s10811-021-02593-y

Tagliapietra, D., Sigovini, M., Ghirardini, A.V., 2009. A review of terms and definitions to categorise estuaries, lagoons and associated environments. Mar. Freshwater Res. 60, 497. https://doi.org/10.1071/MF08088

Takasu, H., Ikeda, M., Miyahara, K., Shiragaki, T., 2023. High contribution of picophytoplankton to phytoplankton biomass in a shallow, eutrophic coastal sea. Marine Environmental Research 184, 105852. https://doi.org/10.1016/j.marenvres.2022.105852

Tan, Y.-H., Poong, S.-W., Yang, C.-H., Lim, P.-E., John, B., Pai, T.-W., Phang, S.-M., 2022. Transcriptomic analysis reveals distinct mechanisms of adaptation of a polar picophytoplankter under ocean acidification conditions. Marine Environmental Research 182, 105782. https://doi.org/10.1016/j.marenvres.2022.105782

Thyssen, M., Grégori, G., Créach, V., Lahbib, S., Dugenne, M., Aardema, H.M., Artigas, L.-F., Huang, B., Barani, A., Beaugeard, L., Bellaaj-Zouari, A., Beran, A., Casotti, R., Del Amo, Y., Denis, M., Dubelaar, G.B.J., Endres, S., Haraguchi, L., Karlson, B., Lambert, C., Louchart, A., Marie, D., Moncoiffé, G., Pecqueur, D., Ribalet, F., Rijkeboer, M., Silovic, T., Silva, R., Marro, S., Sosik, H.M., Sourisseau, M., Tarran, G., Van Oostende, N., Zhao, L., Zheng, S., 2022. Interoperable vocabulary for marine microbial flow cytometry. Front. Mar. Sci. 9, 975877. https://doi.org/10.3389/fmars.2022.975877

Tillmann, U., Hesse, K.-J., Tillmann, A., 1999. Large-scale parasitic infection of diatoms in the Northfrisian Wadden Sea. Journal of Sea Research 42, 255–261. https://doi.org/10.1016/S1385-1101(99)00029-5

Traboni, C., Calbet, A., Saiz, E., 2021. Mixotrophy upgrades food quality for marine calanoid copepods. Limnology & Oceanography 66, 4125–4139. https://doi.org/10.1002/lno.11948

Tragin, M., Vaulot, D., 2019. Novel diversity within marine Mamiellophyceae (Chlorophyta) unveiled by metabarcoding. Sci Rep 9, 5190. https://doi.org/10.1038/s41598-019-41680-6

Trask, B.J., Van Den Engh, G.J., Elgershuizen, J.H.B.W., 2005. Analysis of phytoplankton by flow cytometry. Cytometry 2, 258–264. https://doi.org/10.1002/cyto.990020410

Trigueros, J.M., 2000. Tidally driven distribution of phytoplankton blooms in a shallow, macrotidal estuary. Journal of Plankton Research 22, 969–986. https://doi.org/10.1093/plankt/22.5.969

Tuchman, N.C., Schollett, M.A., Rier, S.T., Geddes, P., 2006. Differential Heterotrophic Utilization of Organic Compounds by Diatoms and Bacteria under Light and Dark Conditions. Hydrobiologia 561, 167–177. https://doi.org/10.1007/s10750-005-1612-4

Umanskaya, M.V., Gorbunov, M.Yu., Bykova, S.V., Tarasova, N.G., 2023. Diversity and Transformation of the Community of Planktonic Freshwater Protists in the Estuarine Tributary Zone of a Large Plainland Reservoir: Metabarcoding of the 18S Ribosomal RNA Gene. Biol Bull Russ Acad Sci 50, 707–723. https://doi.org/10.1134/S1062359022602804

Urabe, J., Gurung, T.B., Yoshida, T., Sekino, T., Nakanishi, M., Maruo, M., Nakayama, E., 2000. Diel changes in phagotrophy by Cryptomonas in Lake Biwa. Limnol. Oceanogr 45, 1558–1563. https://doi.org/10.4319/lo.2000.45.7.1558

Van Maren, D.S., Van Kessel, T., Cronin, K., Sittoni, L., 2015. The impact of channel deepening and dredging on estuarine sediment concentration. Continental Shelf Research 95, 1–14. https://doi.org/10.1016/j.csr.2014.12.010

Vasselon, V., Bouchez, A., Rimet, F., Jacquet, S., Trobajo, R., Corniquel, M., Tapolczai, K., Domaizon, I., 2018. Avoiding quantification bias in metabarcoding: Application of a cell biovolume correction factor in diatom molecular biomonitoring. Methods Ecol Evol 9, 1060–1069. https://doi.org/10.1111/2041-210X.12960

Veldhuis, M., Kraay, G., 1990. Vertical distribution and pigment composition of a picoplanktonic prochlorophyte in the subtropical North Atlantic:a combined study of HPLC-analysis of pigments and flow cytometry. Mar. Ecol. Prog. Ser. 68, 121–127. https://doi.org/10.3354/meps068121

Villanova, V., Spetea, C., 2021. Mixotrophy in diatoms: Molecular mechanism and industrial potential. Physiologia Plantarum 173, 603–611. https://doi.org/10.1111/ppl.13471

Vörös, L., Mózes, A., Somogyi, B., 2009. A five-year study of autotrophic winter picoplankton in Lake Balaton, Hungary. Aquat Ecol 43, 727–734. https://doi.org/10.1007/s10452-009-9272-5

Walter, B., 2017. Hydrobiologische Untersuchung zur spatio-temporären Verteilung des Phyto-und Zooplanktons im Hansahafen und in der Norderelbe sowie ergänzende Laborexperimente zur Abschätzung der Primärproduktion und der Grazing-Effekte [Hydrobiological investigations about the spatiotemporal distribution of phyto- and zooplankton in the Hansahafen and in the Norderelbe as well as additional laboratory experiments to estimate primary production and grazing effects].

Ward, B.A., Follows, M.J., 2016. Marine mixotrophy increases trophic transfer efficiency, mean organism size, and vertical carbon flux. Proc. Natl. Acad. Sci. U.S.A. 113, 2958–2963. https://doi.org/10.1073/pnas.1517118113

Weston, K., Greenwood, N., Fernand, L., Pearce, D.J., Sivyer, D.B., 2008. Environmental controls on phytoplankton community composition in the Thames plume, U.K. Journal of Sea Research

60, 246–254. https://doi.org/10.1016/j.seares.2008.09.003

Wetz, M., Paerl, H., Taylor, J., Leonard, J., 2011. Environmental controls upon picophytoplankton growth and biomass in a eutrophic estuary. Aquat. Microb. Ecol. 63, 133–143. https://doi.org/10.3354/ame01488

Wieczynski, D.J., Moeller, H.V., Gibert, J.P., 2023. Mixotrophic microbes create carbon tipping points under warming. Functional Ecology 37, 1774–1786. https://doi.org/10.1111/1365-2435.14350

Wilson, S., Steinberg, D., 2010. Autotrophic picoplankton in mesozooplankton guts: evidence of aggregate feeding in the mesopelagic zone and export of small phytoplankton. Mar. Ecol. Prog. Ser. 412, 11–27. https://doi.org/10.3354/meps08648

Wirth, C., Limberger, R., Weisse, T., 2019. Temperature × light interaction and tolerance of high water temperature in the planktonic freshwater flagellates *Cryptomonas* (Cryptophyceae) and *Dinobryon* (Chrysophyceae). Journal of Phycology 55, 404–414. https://doi.org/10.1111/jpy.12826

Wolfstein, K., 1996. Untersuchungen zur Bedeutung des Phytoplanktons als Bestandteil der Schwebstoffe für das Ökosystem Tide-Elbe [Investigations about the significance of phytoplankton as a component of suspended matter for the tidal Elbe ecosystem] (Dissertation). University of Hamburg, Germany.

Wolfstein, K., 1990. Aufnahme organischer Kohlenstoffverbindungen durch das Phytoplankton in der Elbe [Uptake of organic carbon compounds by phytoplankton in the Elbe]. Diploma thesis available in the library of the University of Hamburg.

Wu, Y., Guo, P., Su, H., Zhang, Y., Deng, J., Wang, M., Sun, Y., Li, Y., Zhang, X., 2022. Seasonal and spatial variations in the phytoplankton community and their correlation with environmental factors in the Jinjiang River Estuary in Quanzhou, China. Environ Monit Assess 194, 44. https://doi.org/10.1007/s10661-021-09697-5

Xia, S., 2013. Improved Methodology for Identification of Cryptomonads: Combining Light Microscopy and PCR Amplification. J. Microbiol. Biotechnol. 23, 289–296. https://doi.org/10.4014/jmb.1203.03057

Xu, S., Li, G., He, C., Huang, Y., Yu, D., Deng, H., Tong, Z., Wang, Y., Dupuy, C., Huang, B., Shen, Z., Xu, J., Gong, J., 2023. Diversity, community structure, and quantity of eukaryotic phytoplankton revealed using 18S rRNA and plastid 16S rRNA genes and pigment markers: a case study of the Pearl River Estuary. Mar Life Sci Technol 5, 415–430. https://doi.org/10.1007/s42995-023-00186-x

Yao, S., Lyu, S., An, Y., Lu, J., Gjermansen, C., Schramm, A., 2019. Microalgae-bacteria symbiosis in microalgal growth and biofuel production: a review. J Appl Microbiol 126, 359–368. https://doi.org/10.1111/jam.14095

Zamora-Terol, S., Novotny, A., Winder, M., 2020. Reconstructing marine plankton food web interactions using DNA metabarcoding. Molecular Ecology 29, 3380–3395.

https://doi.org/10.1111/mec.15555

Zhang, F., He, J., Lin, L., Jin, H., 2015. Dominance of picophytoplankton in the newly open surface water of the central Arctic Ocean. Polar Biol 38, 1081–1089. https://doi.org/10.1007/s00300-015-1662-7

Zhao, Y.T., Zhao, P., Li, T., Wang, L., Yu, X.Y., 2013. The Influence of Glucose on Growth and Lipid Production under Heterotrophic and Mixotrophic Conditions for Monoraphidium sp. FXY-10. AMR 864–867, 49–55. https://doi.org/10.4028/www.scientific.net/AMR.864-867.49

Zimmermann, J., Glöckner, G., Jahn, R., Enke, N., Gemeinholzer, B., 2015. Metabarcoding vs. morphological identification to assess diatom diversity in environmental studies. Mol Ecol Resour 15, 526–542. https://doi.org/10.1111/1755-0998.12336

Zimmermann-Timm, H., Holst, H., Müller, S., Muller, S., 1998. Seasonal Dynamics of Aggregates and Their Typical Biocoenosis in the Elbe Estuary. Estuaries 21, 613. https://doi.org/10.2307/1353299

Znachor, P., Nedoma, J., 2010. Importance of dissolved organic carbon for phytoplankton nutrition in a eutrophic reservoir. Journal of Plankton Research 32, 367–376. https://doi.org/10.1093/plankt/fbp129

Supplementary material

Note that this supplementary material is condensed to show the most important information and to fit in A4 format. The complete material is available online together with the published versions of the different chapters, and this is noted accordingly where relevant.

Supplementary tables

Tab. S2.1: Metadata sampling. LP = Research Vessel Ludwig Prandtl. This table was condensed for clarity, the full table is available online with the publication https://doi.org/10.1016/j.envres.2024.119126 (there named tab. S1).

Season	**Station**	**Date**	**Cruise**	**Comparative dataset monitoring** (NLWKN 2023, HU 2023)
Spring 2021	609 & 633 km	2021-05-07	LP210503	Sampling 2021-05-03 (586 km, 599 km, 629 km, 646 km)
	692 & 713 km	2021-05-08		none
Summer 2021	609 km	2021-07-29	From pier	Sampling 2021-08-09 (586 km, 599 km, 629 km, 646 km)
	633 km	2021-07-30	LP210725	
	692 & 713 km			none
Winter 2022	609, 633 & 651 km	2022-02-28	LP220228	Sampling 2022-03-09 (599 km, 629 km)
	665, 692 & 713 km			none
Spring 2022	609, 633 & 651 km	2022-05-22	LP220522	Sampling 2022-06-01 (586 km, 599 km, 629 km, 646 km)
	665 km			none
	692 km			
	713 km			
Summer 2022	609, 633 & 651 km	2022-06-20	LP220613	Sampling 2022-07-04 (586 km, 599 km, 646 km)
	665, 692 & 713 km			none

Tab. S2.2: Assignment of classes to the genera from the monitoring data. Please find this supplementary material online, published with the publication https://doi.org/10.1016/j.envres.2024.119126 (there named tab. S2).

Tab. S2.3: r and p values from spearman rank correlation. Please find this supplementary material online, published with the publication https://doi.org/10.1016/j.envres.2024.119126 (there named tab. S3).

Tab. S2.4: Comparisons of the contributions of key genera & classes along areas (t-test), defined as upper (609 & 633 km), mid (651 & 665 km) and lower (692 & 713 km).

Group	Area 1	Area 2	p	Mean (Area 1)	Mean (Area 2)
Chlorophyceae	upper	lower	0.0347262111	19.24	3.84
Chlorophyceae	upper	mid	0.3864300477	19.24	12.97
Chlorophyceae	lower	mid	0.0391011685	3.84	12.97
Chrysophyceae	upper	lower	0.590988949	9.48	7.54
Chrysophyceae	upper	mid	0.3891365823	9.48	13.55
Chrysophyceae	lower	mid	0.1912338101	7.54	13.55
Cryptophyceae	upper	lower	0.0105250579	9.87	21.68
Cryptophyceae	upper	mid	0.0005440104	9.87	26.75
Cryptophyceae	lower	mid	0.2697179668	21.68	26.75
Dinophyceae	upper	lower	0.0501332008	0.78	11.68
Dinophyceae	upper	mid	0.1364700576	0.78	0.06
Dinophyceae	lower	mid	0.0390254657	11.68	0.06
Mediophyceae	upper	lower	0.0037783017	57.73	33.82
Mediophyceae	upper	mid	0.0400698211	57.73	40.55
Mediophyceae	lower	mid	0.2466075529	33.82	40.55
Coscinodiscophyceae	upper	lower	0.0723372395	0.19	10.92
Coscinodiscophyceae	upper	mid	0.7032318014	0.19	0.11
Coscinodiscophyceae	lower	mid	0.0704835322	10.92	0.11
Coelastrum	upper	lower	0.1083652554	6.59	0.21
Coelastrum	upper	mid	0.3159818754	6.59	2.6
Coelastrum	lower	mid	0.1219044334	0.21	2.6
Cyclotella	upper	lower	0.2072373979	9.03	2.09
Cyclotella	upper	mid	0.1585033823	9.03	1.24
Cyclotella	lower	mid	0.388019729	2.09	1.24

Tab. S2.4 (continued)					
Group	**Area 1**	**Area 2**	**p**	**Mean (Area 1)**	**Mean (Area 2)**
Mychonastes	upper	lower	0.1090359985	4.19	0.81
Mychonastes	upper	mid	0.951479519	4.19	4.36
Mychonastes	lower	mid	0.1459713132	0.81	4.36
Skeletonema	upper	lower	0.9550378352	4.71	4.49
Skeletonema	upper	mid	0.7261618121	4.71	3.41
Skeletonema	lower	mid	0.5394700955	4.49	3.41
Stephanodiscus	upper	lower	0.005141533	34.64	3.22
Stephanodiscus	upper	mid	0.0100005069	34.64	6.61
Stephanodiscus	lower	mid	0.2681092124	3.22	6.61
Thalassiosira	upper	lower	0.0010161455	2.98	11.01
Thalassiosira	upper	mid	0.2454429894	2.98	9.28
Thalassiosira	lower	mid	0.7364862639	11.01	9.28
Minidiscus	upper	lower	0.0002424473	0.49	9.74
Minidiscus	upper	mid	0.0955408734	0.49	4.41
Minidiscus	lower	mid	0.0548868968	9.74	4.41
Cryptomonas	upper	lower	0.5599407441	5.54	3.65
Cryptomonas	upper	mid	0.0309967804	5.54	14.48
Cryptomonas	lower	mid	0.0179663395	3.65	14.48
Guinardia	upper	lower	0.0904315974	0	10.1
Guinardia	upper	mid	0.3632174676	0	0.03
Guinardia	lower	mid	0.0913352887	10.1	0.03
Hemiselmis	upper	lower	0.0378849592	0	3.04
Hemiselmis	upper	mid	0.3632174676	0	0.05
Hemiselmis	lower	mid	0.0407181402	3.04	0.05

Tab. S2.5: Species identified *via* metabarcoding. Note that species identification remains uncertain due to short ca. 300 - 350 bp amplicons. This table was condensed for clarity, showing only the four most dominant genotypes of each genus, or less, where less than four genotypes appeared. The full table is available online with the publication https://doi.org/10.1016/j.envres.2024.119126 (there named tab. S5).

Genus	Geno-type	Species	Average contribution to genus reads across seasons & stations [%]
Coelastrum	1	*NA*	100
Cryptomonas	1	*Cryptomonas curvata*	45.81
Cryptomonas	2	*Cryptomonas curvata*	40.02
Cryptomonas	3	*Cryptomonas pyrenoidifera*	9.39
Cryptomonas	4	*Cryptomonas pyrenoidifera*	2.23
Cyclotella	1	*Cyclotella meneghiniana*	32.3
Cyclotella	2	*NA*	26.71
Cyclotella	3	*Cyclotella meneghiniana*	21.14
Cyclotella	4	*Cyclotella meneghiniana*	3.53
Guinardia	1	*Guinardia delicatula*	99.3
Guinardia	2	*Guinardia delicatula*	0.43
Guinardia	3	*Guinardia flaccida*	0.21
Guinardia	4	*Guinardia delicatula*	0.06
Hemiselmis	1	*Hemiselmis andersenii*	90.85
Hemiselmis	2	*Hemiselmis andersenii*	4.99
Hemiselmis	3	*Hemiselmis andersenii*	4.1
Hemiselmis	4	*Hemiselmis cryptochromatica*	0.06
Minidiscus	1	*Minidiscus spinulatus*	48.97
Minidiscus	2	*Minidiscus spinulatus*	28.37
Minidiscus	3	*Minidiscus comicus*	18.71
Minidiscus	4	*Minidiscus variabilis*	2.39

Tab. S2.5 (continued)			
Genus	**Geno-type**	**Species**	**Average contribution to genus reads across seasons & stations**
Mychonastes	1	*NA*	82.38
Mychonastes	2	*NA*	14.5
Mychonastes	3	*Mychonastes homosphaera*	2.93
Mychonastes	4	*NA*	0.19
Skeletonema	1	*Skeletonema subsalsum*	91.92
Skeletonema	2	*Skeletonema marinoi*	6.64
Skeletonema	3	*Skeletonema subsalsum*	1.44
Stephanodiscus	1	*Stephanodiscus hantzschii*	50.72
Stephanodiscus	2	*Stephanodiscus hantzschii*	25.23
Stephanodiscus	3	*NA*	21.84
Stephanodiscus	4	*NA*	1.43
Thalassiosira	1	*Thalassiosira guillardii*	49.88
Thalassiosira	2	*Thalassiosira pseudonana*	15.6
Thalassiosira	3	*NA*	12.7
Thalassiosira	4	*NA*	9.73

Tab. S3.1: Metadata flow cytometry. The sample volume describes the sample taken from the water. These samples were then mixed before an aliquot of 20 µL per replicate was used for the flow cytometric measurement.

Station (km)	Date	Included in dataset(s):	Technical replicates	Type of sampling	Cruise number	Sampling method	Water sample volume	Storage times (cold)
609	2022-06-21	spatial	5	Prandtl (Ship)	LP220613	Ferrybox	500 mL	ca. 14 - 22 h
633	2022-06-21	spatial + seasonal	5	Prandtl (Ship)	LP220613	Ferrybox	500 mL	ca. 14 - 22 h
651	2022-06-21	spatial	5	Prandtl (Ship)	LP220613	Ferrybox	500 mL	ca. 14 - 22 h
665	2022-06-21	spatial	5	Prandtl (Ship)	LP220613	Ferrybox	500 mL	ca. 14 - 22 h
692	2022-06-21	spatial	5	Prandtl (Ship)	LP220613	Ferrybox	500 mL	ca. 14 - 22 h
713	2022-06-21	spatial	5	Prandtl (Ship)	LP220613	Ferrybox	500 mL	ca. 14 - 22 h
609	2022-05-22	spatial	5	Prandtl (Ship)	LP220522	Ferrybox	500 mL	ca. 7 - 13 h
633	2022-05-22	spatial + seasonal	5	Prandtl (Ship)	LP220522	Ferrybox	500 mL	ca. 7 - 13 h
651	2022-05-22	spatial	5	Prandtl (Ship)	LP220522	Ferrybox	500 mL	ca. 7 - 13 h
665	2022-05-22	spatial	5	Prandtl (Ship)	LP220522	Ferrybox	500 mL	ca. 7 - 13 h
692	2022-05-22	spatial	5	Prandtl (Ship)	LP220522	Ferrybox	500 mL	ca. 7 - 13 h
713	2022-05-22	spatial	5	Prandtl (Ship)	LP220522	Ferrybox	500 mL	ca. 7 - 13 h
629	2022-04-28	seasonal	5	Longterm (Pier)	NA	Bucket/ tube	15 mL	7 h
629	2022-04-13	seasonal	5	Longterm (Pier)	NA	Bucket/ tube	15 mL	6 h
629	2022-04-01	seasonal	5	Longterm (Pier)	NA	Bucket/ tube	15 mL	4 h
633	2022-03-12	seasonal	10 (5 each)	Ostetal (Ship)	NA	Bucket/ tube	2 x 15 mL (ebb & flood)	ca. 1 d
629	2022-03-02	seasonal	5	Longterm (Pier)	NA	Bucket/ tube	15 mL	28 h

Tab. S3.1 (continued)

Station (km)	Date	Included in dataset(s):	Technical replicates	Type of sampling	Cruise number	Sampling method	Water sample volume	Storage times (cold)
609	2022-02-28	spatial	5	Prandtl (Ship)	LP220228	Ferrybox	500 mL	ca. 4 - 13 h
633	2022-02-28	spatial + seasonal	5	Prandtl (Ship)	LP220228	Ferrybox	500 mL	ca. 4 - 13 h
651	2022-02-28	spatial	5	Prandtl (Ship)	LP220228	Ferrybox	500 mL	ca. 4 - 13 h
665	2022-02-28	spatial	5	Prandtl (Ship)	LP220228	Ferrybox	500 mL	ca. 4 - 13 h
692	2022-02-28	spatial	5	Prandtl (Ship)	LP220228	Ferrybox	500 mL	ca. 4 - 13 h
713	2022-02-28	spatial	5	Prandtl (Ship)	LP220228	Ferrybox	500 mL	ca. 4 - 13 h
629	2022-02-03	seasonal	5	Longterm (Pier)	NA	Bucket/ tube	15 mL	5 h
629	2022-01-20	seasonal	5	Longterm (Pier)	NA	Bucket/ tube	15 mL	5 h
629	2021-12-16	seasonal	5	Longterm (Pier)	NA	Bucket/ tube	15 mL	30 h
629	2021-12-02	seasonal	5	Longterm (Pier)	NA	Bucket/ tube	15 mL	9 h
629	2021-11-22	seasonal	5	Prandtl substitute (Pier)	NA	Bucket/ tube	15 mL	3 h
629	2021-11-18	seasonal	5	Longterm (Pier)	NA	Bucket/ tube	15 mL	7 h
629	2021-11-03	seasonal	5	Longterm (Pier)	NA	Bucket/ tube	15 mL	27 h
623	2021-10-21	seasonal	5	Dockland (Pier)	none	Bucket/ tube	15 mL	< 1 h
629	2021-10-21	seasonal	5	Longterm (Pier)	NA	Bucket/ tube	15 mL	3 h
623	2021-10-14	seasonal	5	Dockland (Pier)	none	Bucket/ tube	15 mL	< 1 h
623	2021-10-13	seasonal	5	Dockland (Pier)	none	Bucket/ tube	15 mL	< 1 h
623	2021-10-06	seasonal	5	Dockland (Pier)	none	Bucket/ tube	15 mL	< 1 h
629	2021-10-06	seasonal	5	Longterm (Pier)	NA	Bucket/ tube	15 mL	26 h

Tab. S3.1 (continued)

Station (km)	Date	Included in dataset(s):	Technical replicates	Type of sampling	Cruise number	Sampling method	Water sample volume	Storage times (cold)
633	2021-08-29	seasonal	18 (3 each)	Ostetal (Ship)	NA	Bucket/ tube	6 x 15 mL (3x ebb, 3x flood)	up to 14 h
633	2021-07-30	spatial + seasonal	3	Prandtl (Ship)	LP210725	Ferrybox	2 L	13 h
665	2021-07-30	spatial	3	Prandtl (Ship)	LP210725	Ferrybox	2 L	10 h
692	2021-07-30	spatial	3	Prandtl (Ship)	LP210725	Ferrybox	2 L	8 h
713	2021-07-30	spatial	3	Prandtl (Ship)	LP210725	Ferrybox	2 L	6 h
609	2021-07-29	spatial	3	Prandtl (Ship)	LP210725	Ferrybox	2 L	10 h
623	2021-07-23	seasonal	3	Dockland (Pier)	NA	Bucket/ tube	15 mL	< 1 h
692	2021-05-08	spatial	3	Prandtl (Ship)	LP210503	Ferrybox	2 L	ca. 11 h
713	2021-05-08	spatial	3	Prandtl (Ship)	LP210503	Ferrybox	2 L	ca. 9 h
609	2021-05-07	spatial	3	Prandtl (Ship)	LP210503	Ferrybox	2 L	ca. 36 h
633	2021-05-07	spatial + seasonal	3	Prandtl (Ship)	LP210503	Ferrybox	2 L	ca. 34 h
651	2021-05-07	spatial	3	Prandtl (Ship)	LP210503	Ferrybox	2 L	ca. 34 h
665	2021-05-07	spatial	3	Prandtl (Ship)	LP210503	Ferrybox	2 L	ca. 32 h

Tab. S3.2: Results from ANOVA and Tukey test for assessment of spatial patterns (spatial dataset)

Picophytoplankton group	Compared areas	p	F	Direction
Picophytoplankton cells	Upper (609 km) vs. mid to lower (633 - 713 km)	6.0×10^{-11}	51.6	609 km > other
Picoeukaryotes cells		2.1×10^{-10}	48.2	
Picocyanobacteria cells		3.7×10^{-6}	23.5	
Picophytoplankton % of phytoplankton	Upper (609 km) vs. mid (633-692 km)	0.009	5.26	mid > upper
	Upper (609 km) vs. lower (713 km)	0.610		not relevant
	Mid (633-692 km) vs. lower (713 km)	0.171		not relevant
Picoeukaryotes % of phytoplankton	Upper (609 km) vs. mid (633-692 km)	0.031	4.42	mid > upper
	Upper (609 km) vs. lower (713 km)	0.891		not relevant
	Mid (633-692 km) vs. lower (713 km)	0.118		not relevant

Tab. S3.3: GAM fitting. For the spatial data (fig. 3.2), we tested all possible k values (3 - 6), for seasonal data (fig. 3.3, S3.4) we tested k values from 10 - 20. In all cases we selected the k with the lowest AIC for in the figures. For clarity, only a selection of the tested k values and their AIC are shown here.

Figure	k	AIC	Comment
2a (Picophytoplankton cell counts ~ station)	4	1096.92	
	5	**1096.86**	Chosen for figure
	6	1097.1	
2b (Picophytoplankton as % of phytoplankton ~ station)	**3**	**1009.9**	Chosen for figure
	4	1010.3	
2c (Picoeukaryotes as % of phytoplankton ~ station)	**3**	**969.4**	Chosen for figure
	4	970.0	

Tab. S3.3 (continued)			
Figure	**k**	**AIC**	**Comment**
3.3a (Picoeukaryotes cell counts ~ date)	10	784.2	
	17	**651.7**	Chosen for figure
	20	655.6	
3.3b (Picocyanobacteria cell counts ~ date)	10	509.3	
	15	**470.1**	Chosen for figure
	20	471.4	
3.3c (Picophytoplankton as % of phytoplankton ~ date)	10	922.7	
	15	906.8	
	20	**878.8**	Chosen for figure
3.3d (Picoeukaryotes as % of picophytoplankton ~ date)	10	881.5	
	15	**819.9**	Chosen for figure
	20	820.8	
S3.4a (Picophytoplankton cell counts ~ date)	10	787.5	
	15	**710.2**	Chosen for figure
	20	713.6	
S3.4b (Picoeukaryotes as % of phytoplankton ~ date)	10	933.4	
	15	893.8	
	20	**880.8**	Chosen for figure
S3.4c (Picocyanobacteria as % of phytoplankton ~ date)	10	841.2	
	15	784.9	
	20	**781.1**	Chosen for figure

Tab. S3.4: r and p values from spearman rank correlation (for abbreviations and units see fig. 3.4)

Var1	Var2	p	r
Temp_spatial	*Mychonastes*	0.2698	0.27
Salinity	*Mychonastes*	< 0.0001	-0.83
Turbidity	*Mychonastes*	0.6013	-0.13
NO3	*Mychonastes*	0.1206	-0.37
PO4	*Mychonastes*	0.0757	-0.42
Temp_spatial	*Nannochloropsis*	0.0097	-0.58
Salinity	*Nannochloropsis*	0.3887	-0.21
Turbidity	*Nannochloropsis*	0.6328	0.12
NO3	*Nannochloropsis*	0.3708	-0.22
PO4	*Nannochloropsis*	0.0216	-0.52
Temp_spatial	*Minidiscus*	0.7259	0.09
Salinity	*Minidiscus*	0.0001	0.77
Turbidity	*Minidiscus*	0.9488	-0.02
NO3	*Minidiscus*	0.1671	0.33
PO4	*Minidiscus*	0.0096	0.58
Temp_spatial	*Choricystis*	0.6446	-0.11
Salinity	*Choricystis*	0.2049	0.30
Turbidity	*Choricystis*	0.0517	0.45
NO3	*Choricystis*	0.0068	0.60
PO4	*Choricystis*	0.0150	0.55
Temp_seasonal	Pico [cells/ mL]	< 0.0001	0.53
Temp_spatial	Pico [cells/ mL]	< 0.0001	0.59
Salinity	Pico [cells/ mL]	0.2712	0.100
Turbidity	Pico [cells/ mL]	0.0291	-0.2
NO3	Pico [cells/ mL]	< 0.0001	-0.48

Tab. S3.4 (continued)

Var1	Var2	p	r
PO4	Pico [cells/ mL]	0.1310	-0.14
Temp_seasonal	Pico [% of phyto]	0.3255	-0.09
Temp_spatial	Pico [% of phyto]	0.9793	~ 0
Salinity	Pico [% of phyto]	0.0397	-0.19
Turbidity	Pico [% of phyto]	< 0.0001	0.42
NO3	Pico [% of phyto]	< 0.0001	0.5
PO4	Pico [% of phyto]	0.0010	0.29
Temp_seasonal	Picoeuk [cells/ mL]	< 0.0001	0.47
Temp_spatial	Picoeuk [cells/ mL]	< 0.0001	0.54
Salinity	Picoeuk [cells/ mL]	0.3039	0.09
Turbidity	Picoeuk [cells/ mL]	0.0254	-0.20
NO3	Picoeuk [cells/ mL]	< 0.0001	-0.50
PO4	Picoeuk [cells/ mL]	0.0368	-0.19
Temp_seasonal	Picoeuk [% of phyto]	< 0.0001	-0.48
Temp_spatial	Picoeuk [% of phyto]	0.0012	-0.29
Salinity	Picoeuk [% of phyto]	0.2404	-0.11
Turbidity	Picoeuk [% of phyto]	< 0.0001	0.37
NO3	Picoeuk [% of phyto]	0.0032	0.26
PO4	Picoeuk [% of phyto]	0.5694	-0.05
Temp_seasonal	Picocyano [cells/ mL]	< 0.0001	0.70
Temp_spatial	Picocyano [cells/ mL]	< 0.0001	0.63
Salinity	Picocyano [cells/ mL]	0.2698	0.10
Turbidity	Picocyano [cells/ mL]	0.0067	-0.24
NO3	Picocyano [cells/ mL]	< 0.0001	-0.41
PO4	Picocyano [cells/ mL]	0.3389	-0.09

Tab. S3.4 (continued)			
Var1	**Var2**	**p**	**r**
Temp_seasonal	Picocyano [% of phyto]	< 0.0001	0.42
Temp_spatial	Picocyano [% of phyto]	0.1551	0.13
Salinity	Picocyano [% of phyto]	0.2590	-0.10
Turbidity	Picocyano [% of phyto]	0.0019	0.28
NO3	Picocyano [% of phyto]	< 0.0001	0.52
PO4	Picocyano [% of phyto]	< 0.0001	0.40

Tab. S4.1: Metadata strains. This table was condensed for clarity, the full table is available online with the publication https://doi.org/10.1098/rspb.2023.2713 (there named tab. S1). Note that origin was corrected (609 & 692 km = 610 & 690 km in the published version).

Internal strain ID	Group	Genus	Origin	Season	Temperature	
					Incubation	Origin
N1	Nano green algae	*Micractinium*	609 km	May 21	12 °C	10 °C
N2		*Monoraphidium*	609 km	March 21	15 °C	5 °C
N3		*Tetradesmus*	609 km	May 21	12 °C	10 °C
N4		*Chlorella*-like	609 km	March 21	15 °C	5 °C
N7		*Monoraphidium*	692 km	May 21	12 °C	10 °C
N8		*Monoraphidium*	609 km	May 21	12 °C	10 °C
P1	Pico green algae	*Mychonastes*	609 km	July 21	18 °C	22 °C
P2		*Chlorella*	692 km	Feb 22	12 °C	5 °C
P3		*Choricystis*	634 km	Feb 22	12 °C	5 °C
P4		*Mychonastes*	692 km	May 21	12 °C	10 °C
P5		unidentified	609 km	Feb 22	12 °C	5 °C
P6		*Mychonastes*	634 km	May 21	12 °C	10 °C
P9		unidentified	609 km	July 21	18 °C	22 °C
D1	Diatoms	Thalassiosirales	634 km	Feb 22	12 °C	5 °C
C1	Cyano-bacteria	Synechococcales	609 km	July 21	18 °C	22 °C
C6						
C9						

Tab. S4.2: Metadata EcoPlates™. Please find this supplementary material online, published with the publication https://doi.org/10.1098/rspb.2023.2713 (there named tab. S2).

Tab. S4.3: p values t-test. The t-test was carried out to compare different treatments (e.g. organic carbon, ampicillin) with the respective controls. Please find this supplementary material online, published with the publication https://doi.org/10.1098/rspb.2023.2713 (there named tab. S3).

Tab. S4.4: Test of strain homogeneity. Please find this supplementary material online, published with the publication https://doi.org/10.1098/rspb.2023.2713 (there named tab. S4).

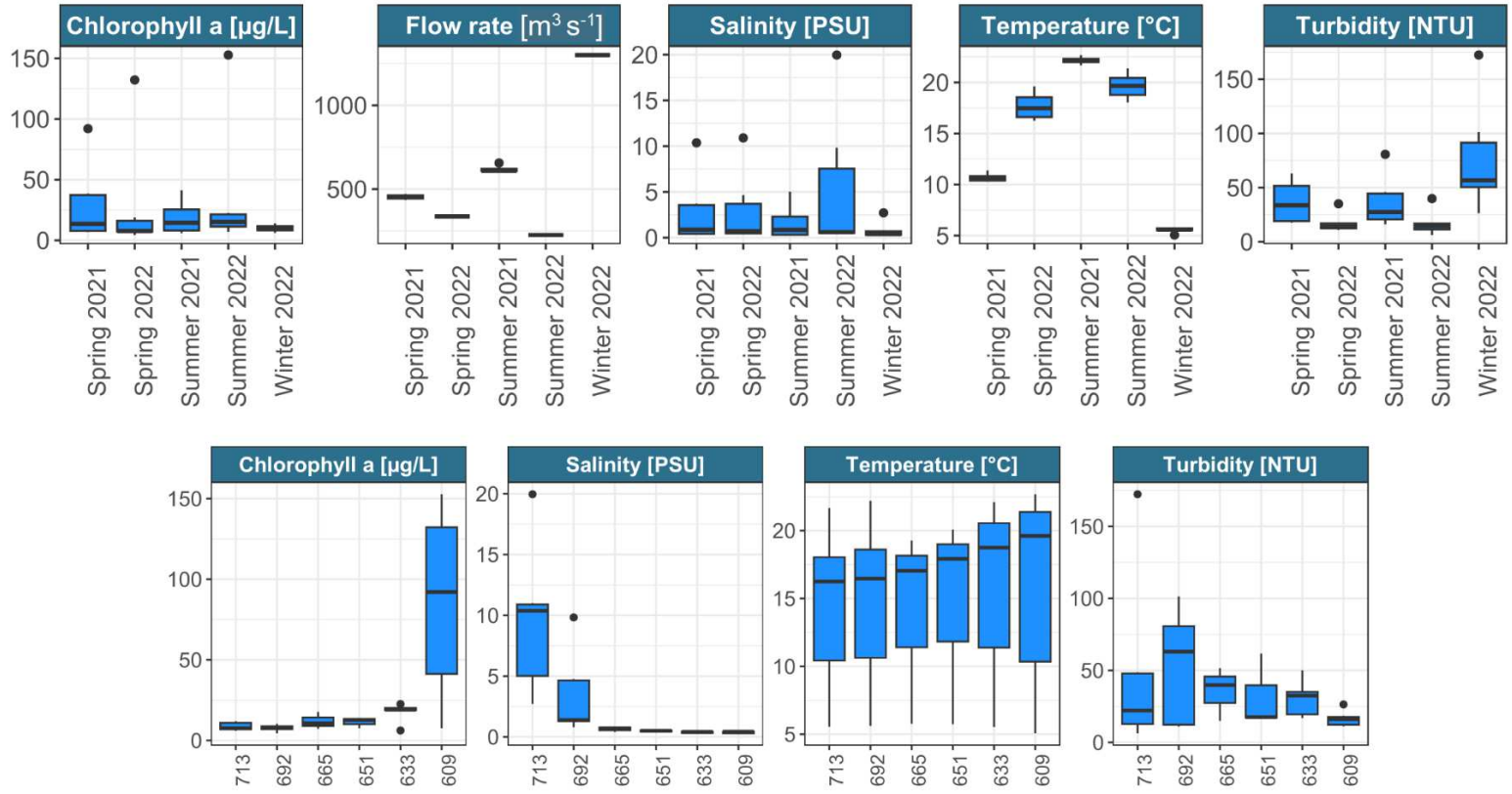

Fig. S2.1: Abiotic conditions and chlorophyll a along seasons (top row; across stations) and along stations (bottom row; across seasons) in the Elbe estuary. Flow rate is obtained from the FGG database (FGG Elbe, 2024) and refers to a fixed station in the upper Elbe (Neu Darchau, at ca. 536 km). Where samples were taken at different dates within a season, flow rate is shown for these different dates (spring 2021, summer 2021). Note that the stations 651 km and 665 km only include data from 2022 and data from spring and summer 2021 does not include data from those stations. All values are additionally shown in the online version of tab. S2.1. Note that the unit referring to each vertical axis is shown in the panel header.

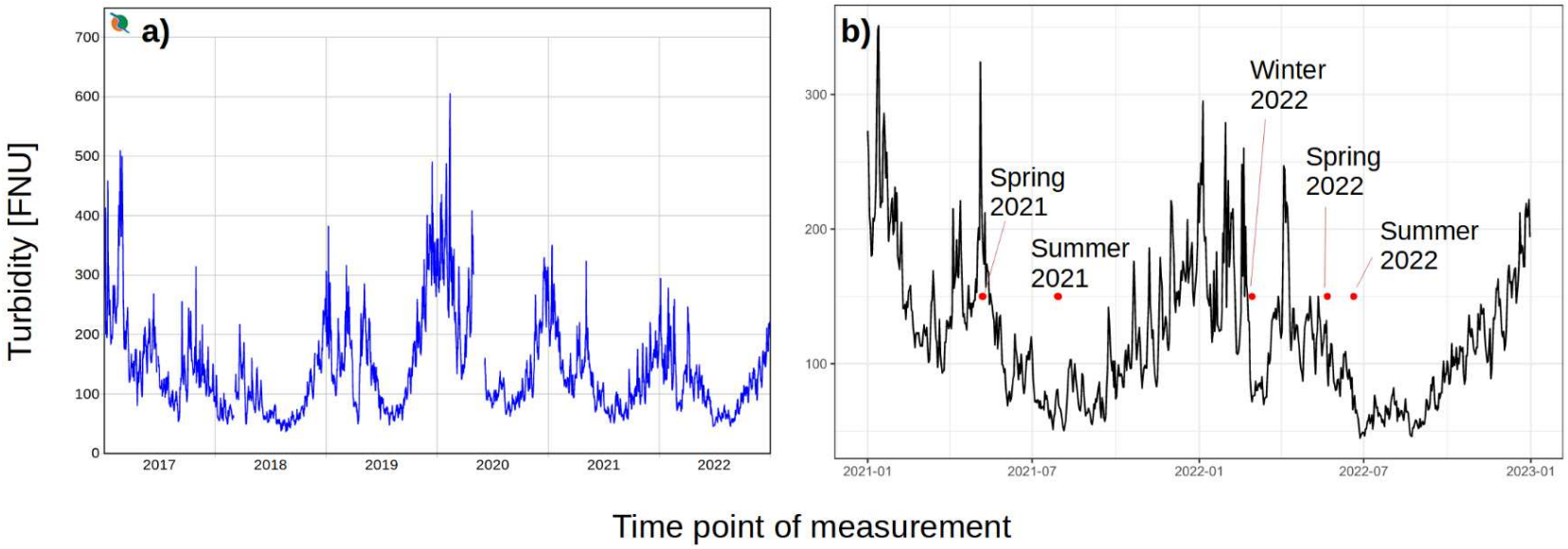

Fig. S2.2: Average daily turbidity (FNU) at the station Grauerort (ca. 661 km) in the Elbe estuary based on data from the FGG Elbe database (a) from 2017 - 2022 and (b) zoomed in for 2021 – 2022 (FGG Elbe, 2024). Panel (a) was obtained directly from the FGG database, but modified by removing German texts. It is added to show that turbidity was specifically high in winter across years. Panel (b) was generated based on the FGG database data and additionally shows the days when our samples were taken as red dots at a random vertical height.

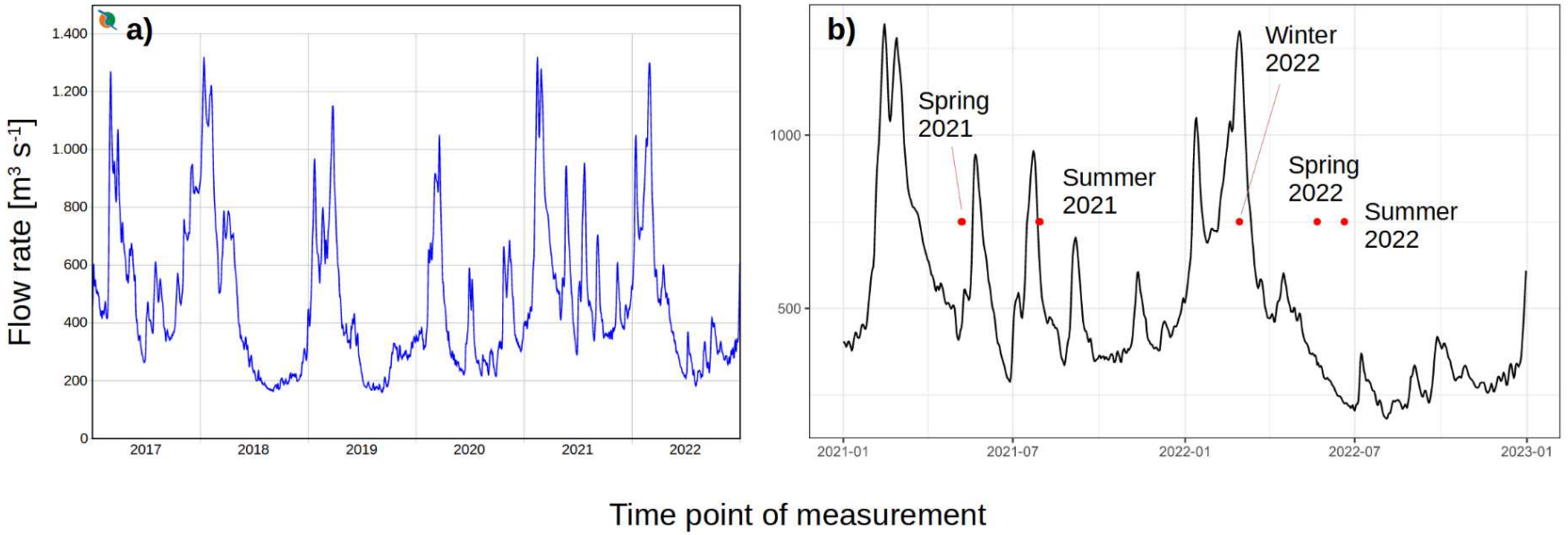

Fig. S2.3: Average daily flow rate (m3 s^{-1}) at the station Neu Darchau (ca. 536 km) in the Elbe river based on data from the FGG Elbe database (a) from 2017 - 2022 and (b) zoomed in for 2021 – 2022 (FGG Elbe, 2024). Panel (a) was obtained directly from the FGG database, but modified by removing German texts. It is added to show that the flow rate was specifically high in earlier seasons. Panel (b) was generated based on the FGG database data and additionally shows the days when our samples were taken as red dots at a random vertical height.

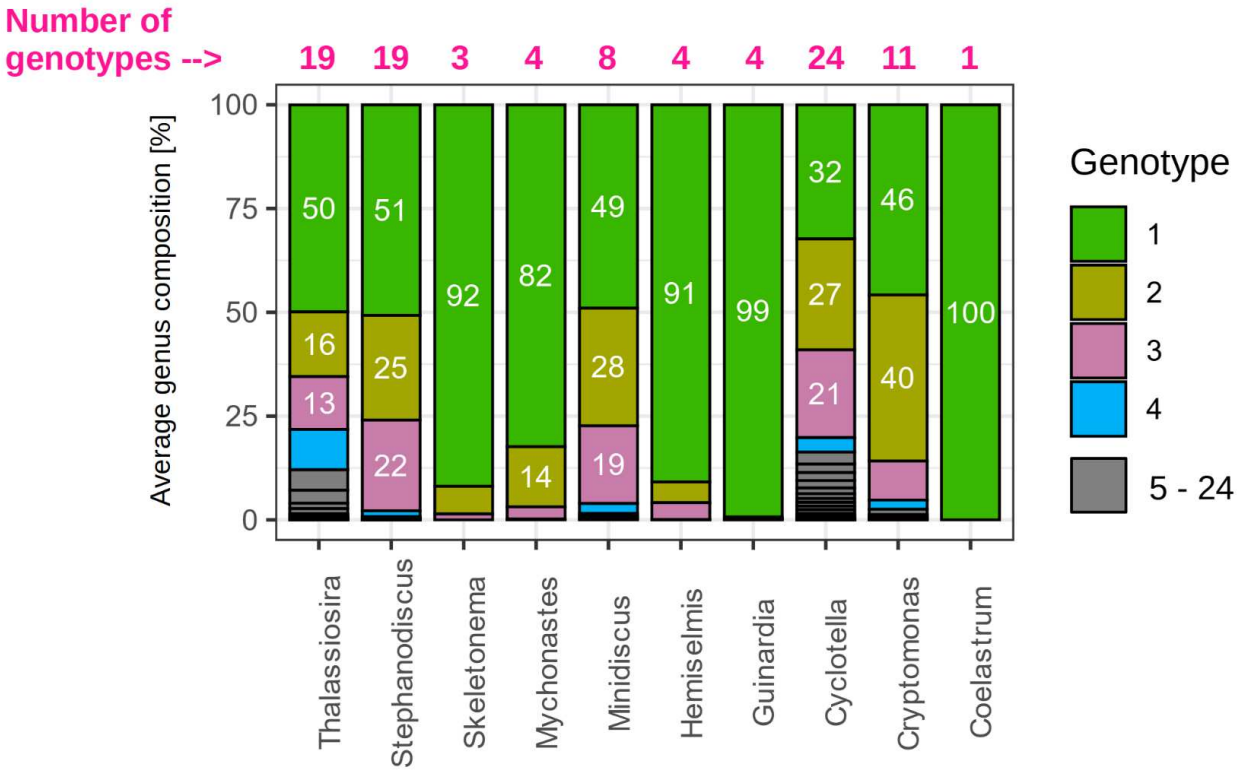

Fig. S2.4: Average genotype composition of key genera across seasons and stations in the Elbe estuary (based on metabarcoding). Genotypes are named by sequential numbers ordered by their dominance (% of genus). For clarity, only the most dominant genotypes 1 – 4 are shown as different colors. Average contributions are calculated from the relative contributions of the genotype to the genus contributions across seasons and stations (differences in absolute abundances between samples are not included). Labels are shown where contribution was ≥ 10 %.

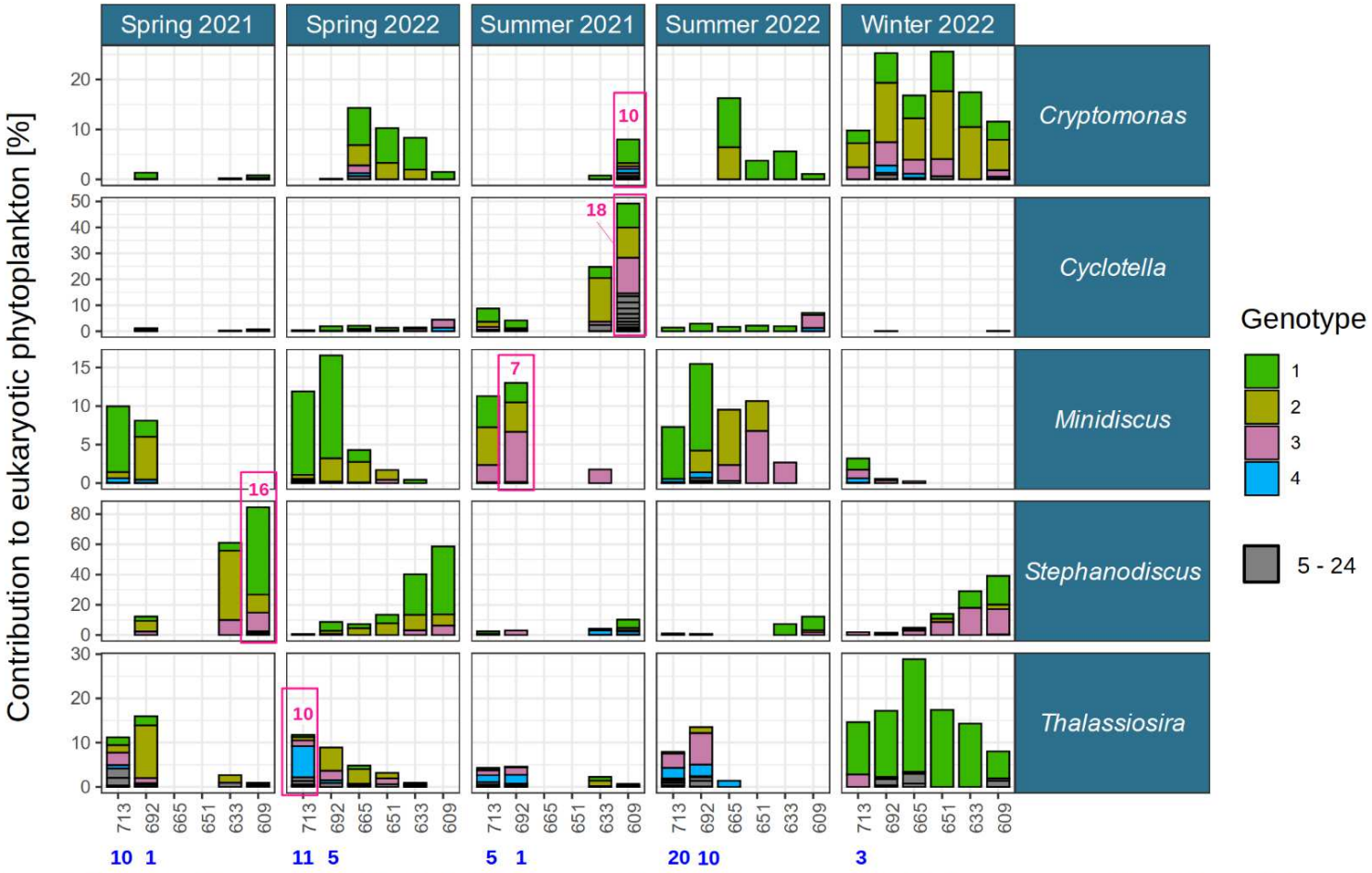

Fig. S2.5: Contributions of genotypes of selected key genera to the eukaryotic phytoplankton communities along stations of the Elbe estuary in different seasons (based on metabarcoding). Here we only included the data of key genera that were not mostly (defined as ≥ 80 %) represented by a single genotype (see also fig. S2.4). Genotypes are named by sequential numbers ordered by their dominance (% of genus, see fig. S4). For clarity, only the most dominant genotypes 1 – 4 are shown as different colors. Note that 651 km and 665 km were not included in 2021. Pink frames highlight the samples with the highest genotype diversity of each genus and the number shows the respective number of genotypes. Blue numbers show approximate salinity where > 1 PSU (see also online version of tab. S2.1).

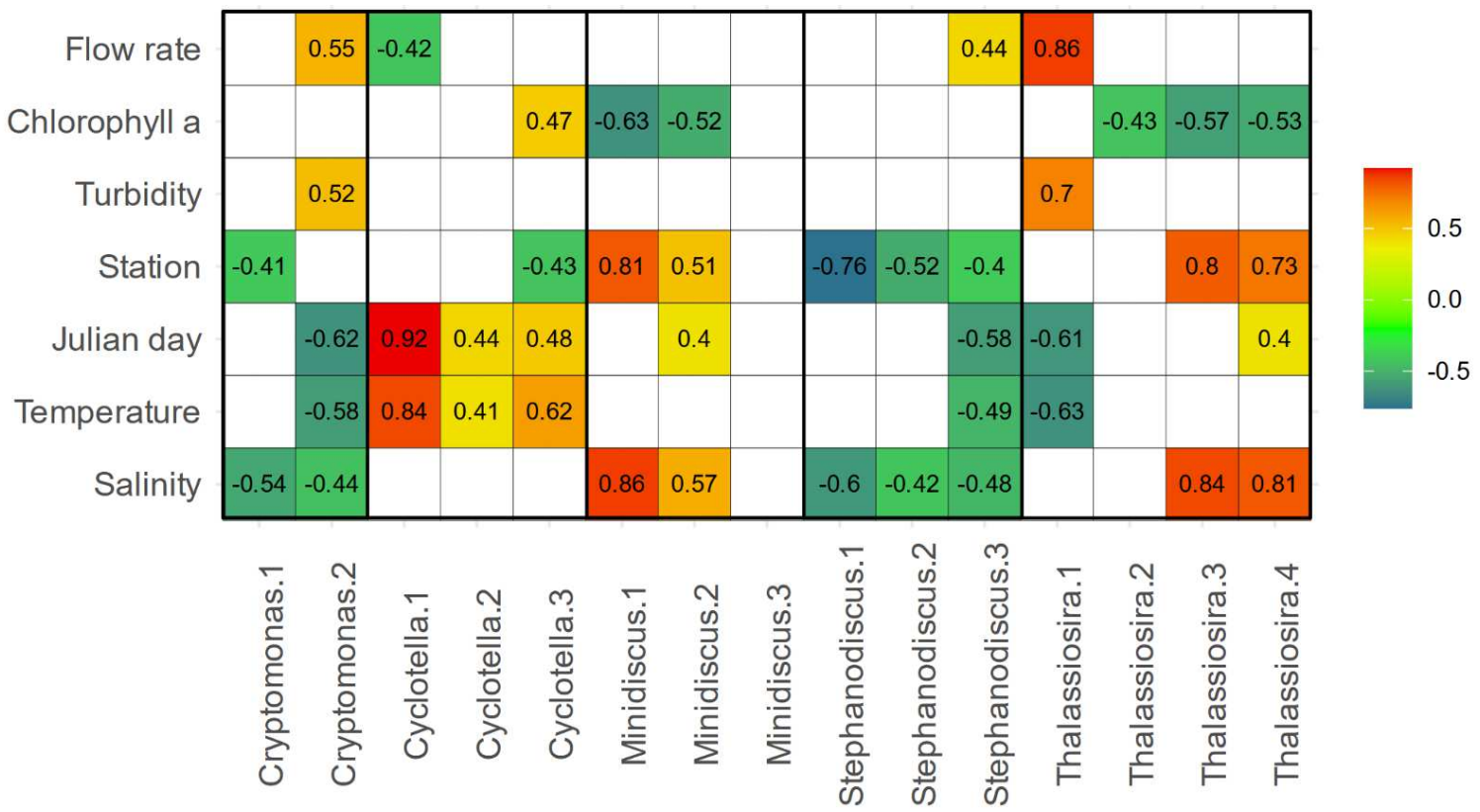

Fig. S2.6: Relationship between the contributions of phytoplankton (genotypes of key genera) and station, season as well as other environmental parameters (based on metabarcoding). Here we only included the data of key genera that were *not* mostly (defined as ≥ 80 %) represented by a single genotype (see also fig. S2.4). Genotypes are named by sequential numbers ordered by their average dominance across seasons (% of genus, see fig. S2.4). We here only included genotypes that contributed at least 5 % to the eukaryotic phytoplankton in at least one sample (i.e. at one station in one season; see also fig. S2.5). The number behind the genus indicates the assigned genotype (e.g. Cryptomonas.1 = Cryptomonas genotype 1). Numbers in the heatmap and color scheme show the correlation coefficient r calculated with spearman rank correlation. Numbers are shown if the relationship is significant ($p \leq 0.05$). All p-values and r-values are shown in the supplementary data (available online, see notes with respect to tab. S2.3). Flow rate is obtained from the FGG database (FGG Elbe 2024) and refers to a fixed station in the upper Elbe (Neu Darchau, at ca. 536 km). Units for environmental parameters are shown in the online version of supplementary tab. S2.1.

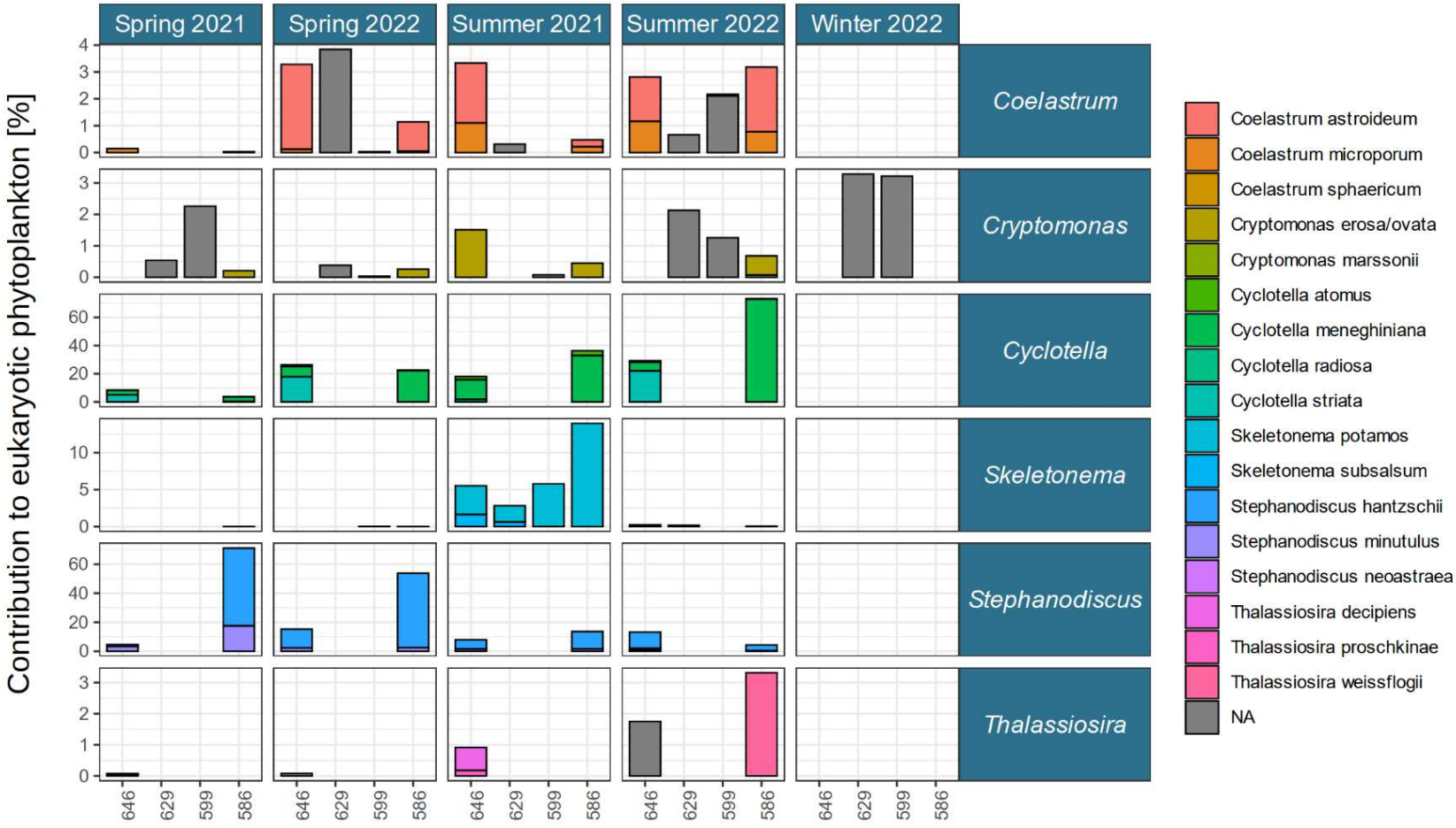

Fig. S2.7 (part 1 of 2): Contributions of species of key genera to the eukaryotic phytoplankton communities along stations in the upper to mid Elbe estuary in different seasons (based on microscopy/ biovolume) (NLWKN 2023, HU 2023). Note that centric diatoms were largely not classified further at 629 km and 599 km, hence data for genera such as e.g. *Stephanodiscus* are missing at those stations. Also, winter data are not available from 586 km and 646 km.

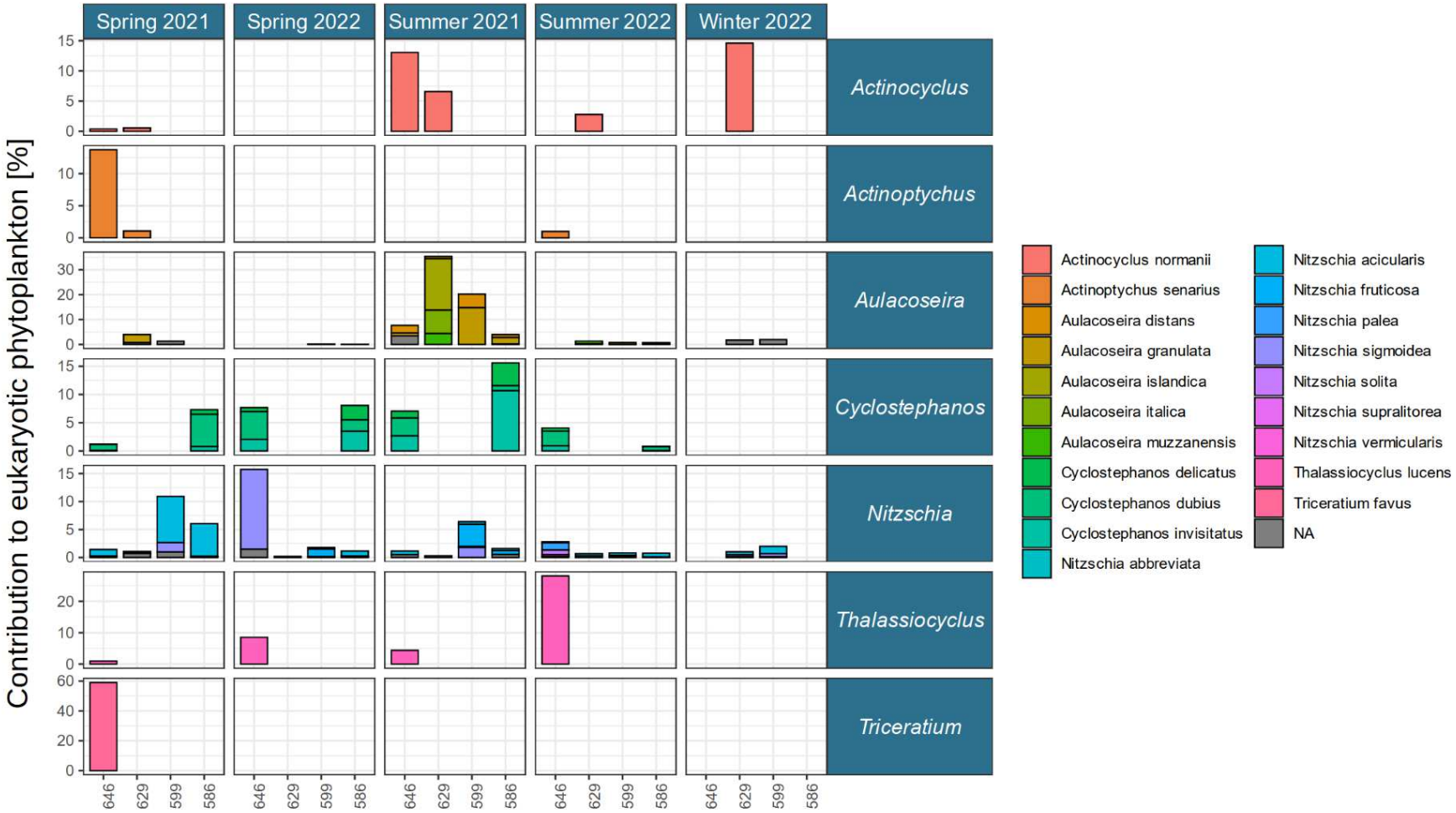

Fig. S2.7 (part 2 of 2): Contributions of species of key genera to the eukaryotic phytoplankton communities along stations in the upper to mid Elbe estuary in different seasons (based on microscopy/ biovolume) (NLWKN 2023, HU 2023). Note that centric diatoms were largely not classified further at 629 km and 599 km, hence data for genera such as e.g. *Thalassiocyclus* are missing at those stations. Also, winter data are not available from 586 km and 646 km.

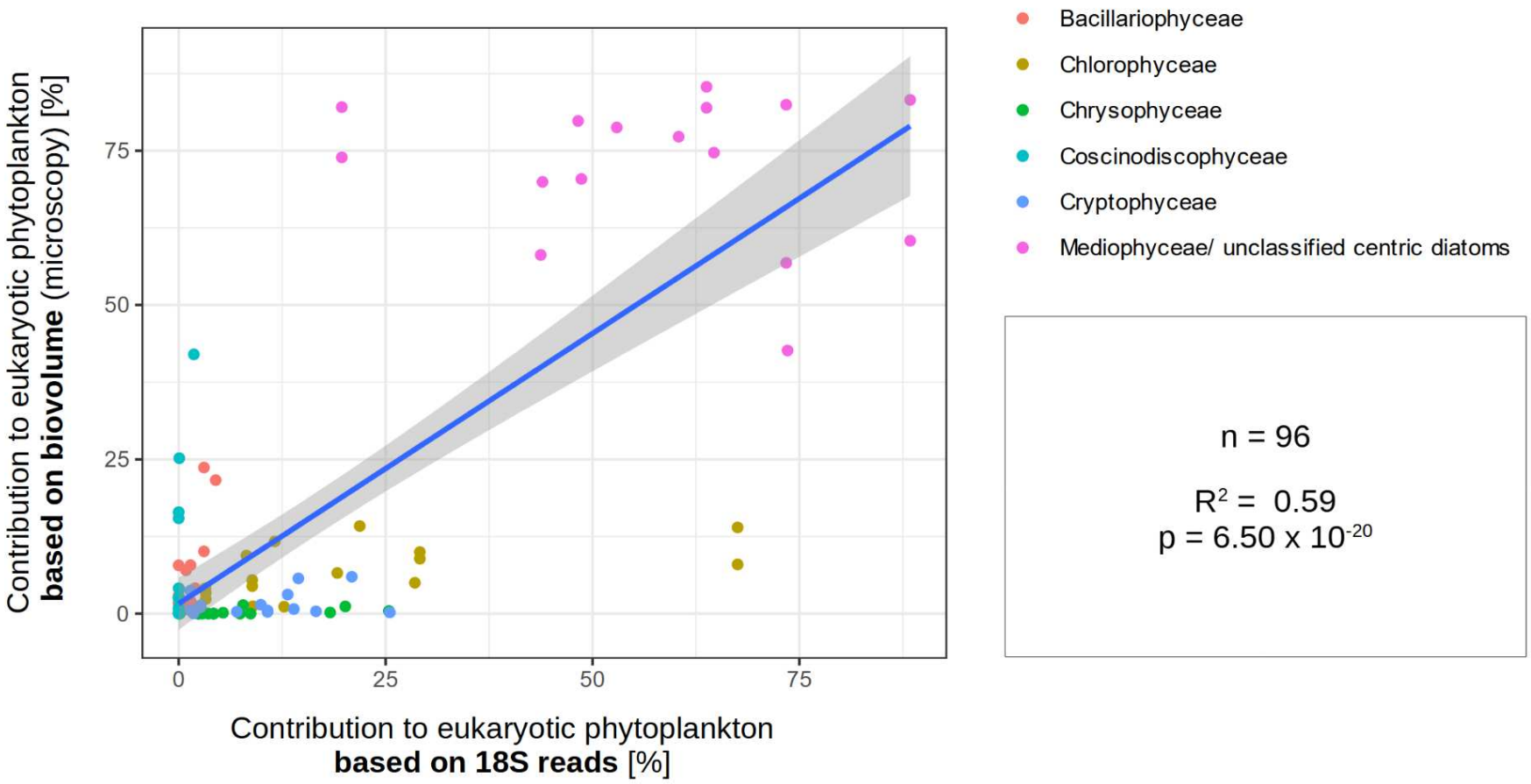

Fig. S2.8a: Contributions of key classes to the eukaryotic phytoplankton communities based on metabarcoding reads and microscopy biovolumes (NLWKN 2023, HU 2023). Note that the comparability is affected by actual ecological differences between the samples (different sampling time points and stations). To allow statistical analysis, we here paired microscopy and metabarcoding stations (see fig. 2.1) in the following way: 586 km and 599 km were each compared with 609 km, 629 km was compared with 633 km and 646 km was compared with 651 km. Sampling dates were grouped as shown in tab. S2.1. R2 and p are based on a pearson correlation. Note that data from 646 km in 2021 and from 651 km in winter 2022 are not included because data from the respective comparative station (i.e. 651 km in 2021 and 646 in winter 2022) are missing.

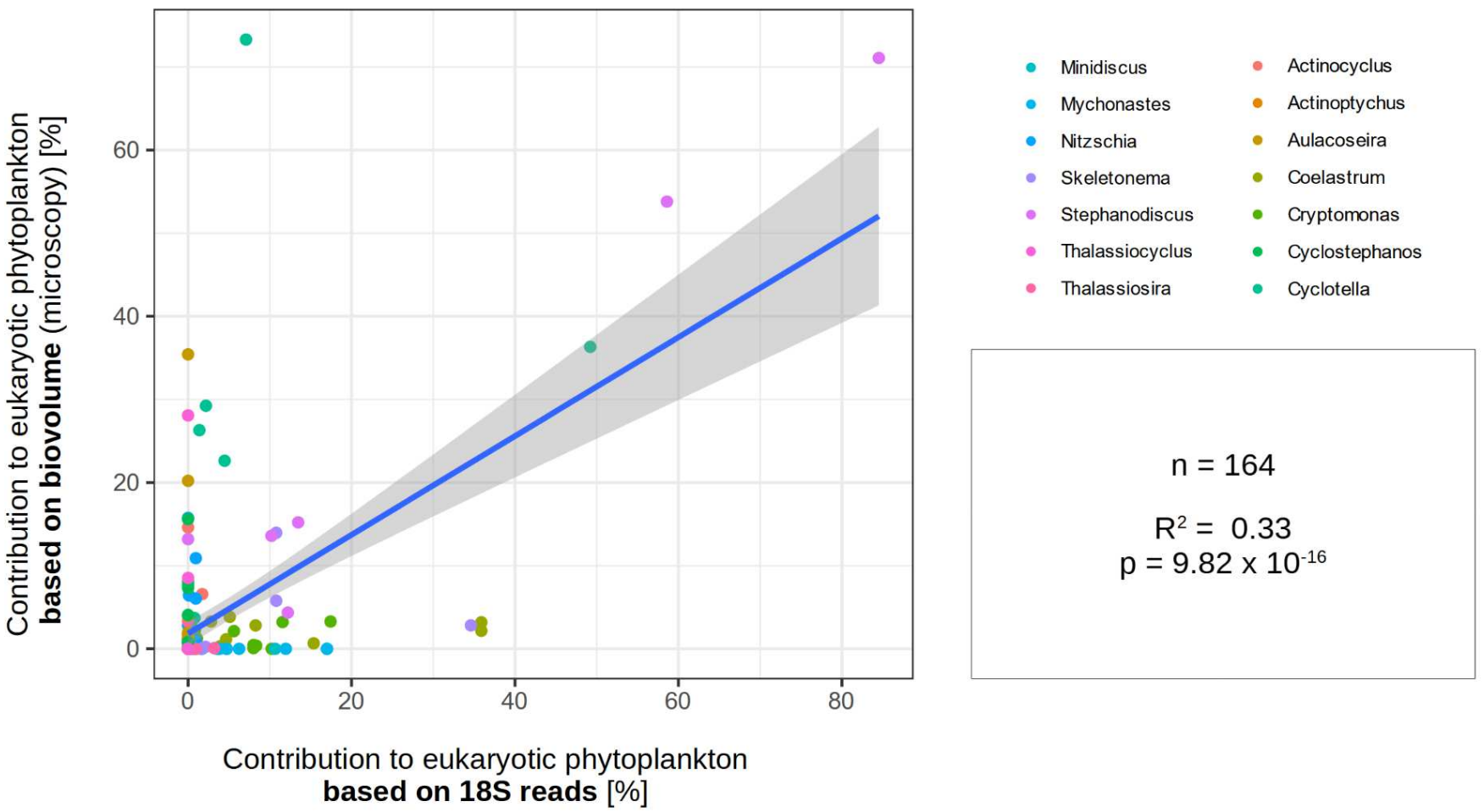

Fig. S2.8b: Contributions of key genera to the eukaryotic phytoplankton communities based on metabarcoding reads and microscopy biovolumes (NLWKN 2023, HU 2023). Note that the comparability is affected by actual ecological differences between the samples (different sampling time points and stations). To allow statistical analysis, we here paired microscopy and metabarcoding stations (see fig. 2.1) in the following way: 586 km and 599 km were each compared with 609 km, 629 km was compared with 633 km and 646 km was compared with 651 km. Sampling dates were grouped as shown in tab. S2.1. Note that data from 646 km in 2021 and from 651 km in winter 2022 are not included because data from the respective comparative station (i.e. 651 km in 2021 and 646 in winter 2022) are missing. Therefore, also the key genus *Triceratium* is not included, as it only appeared at 646 km in spring 2021.

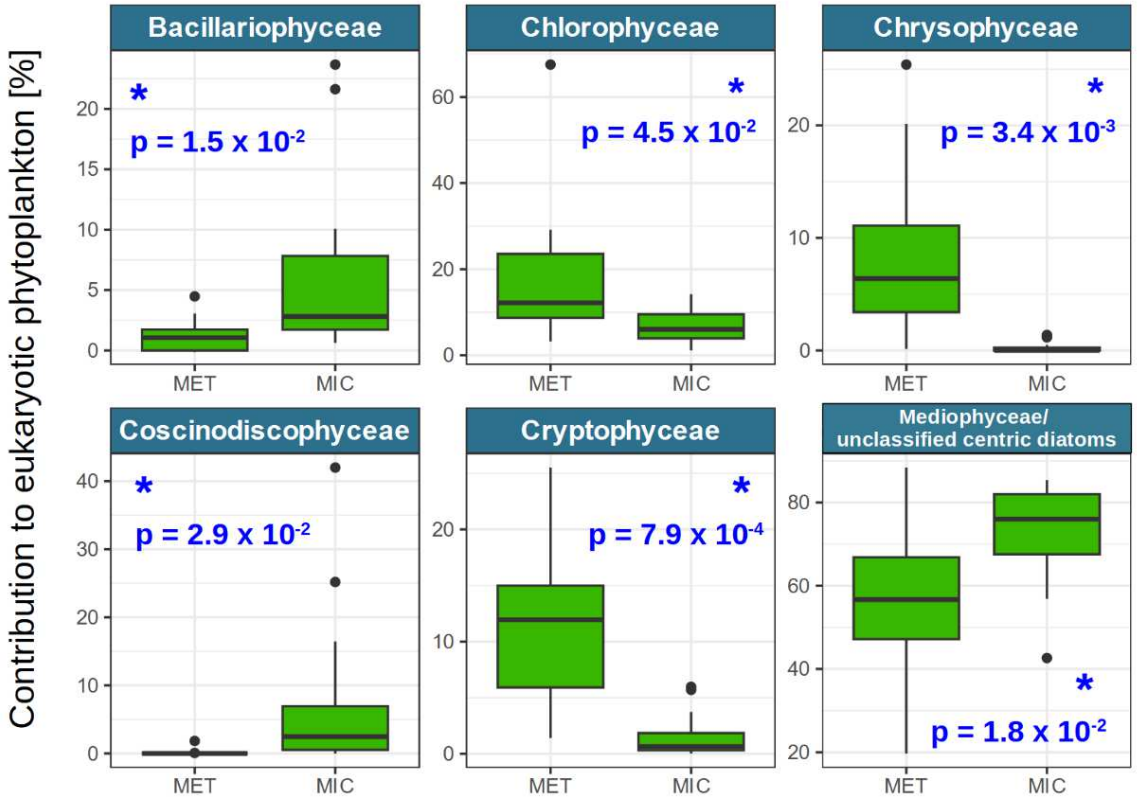

Fig. S2.9a: Contributions of key classes to the eukaryotic phytoplankton communities based on metabarcoding reads (MET) and microscopy biovolumes (MIC) (NLWKN 2023, HU 2023) across seasons (tab. S2.1) and stations in the upper to mid area (586 – 651 km). Note that the comparability is affected by actual ecological differences between the samples (different sampling time points and stations; tab. S2.1, fig. 2.1). * indicate significant differences between the results of the two methods based on a t-test ($p \leq 0.05$). Note that data from 646 km in 2021 and from 651 km in winter 2022 are not included because data from the respective comparative station (i.e. 651 km in 2021 and 646 in winter 2022) are missing.

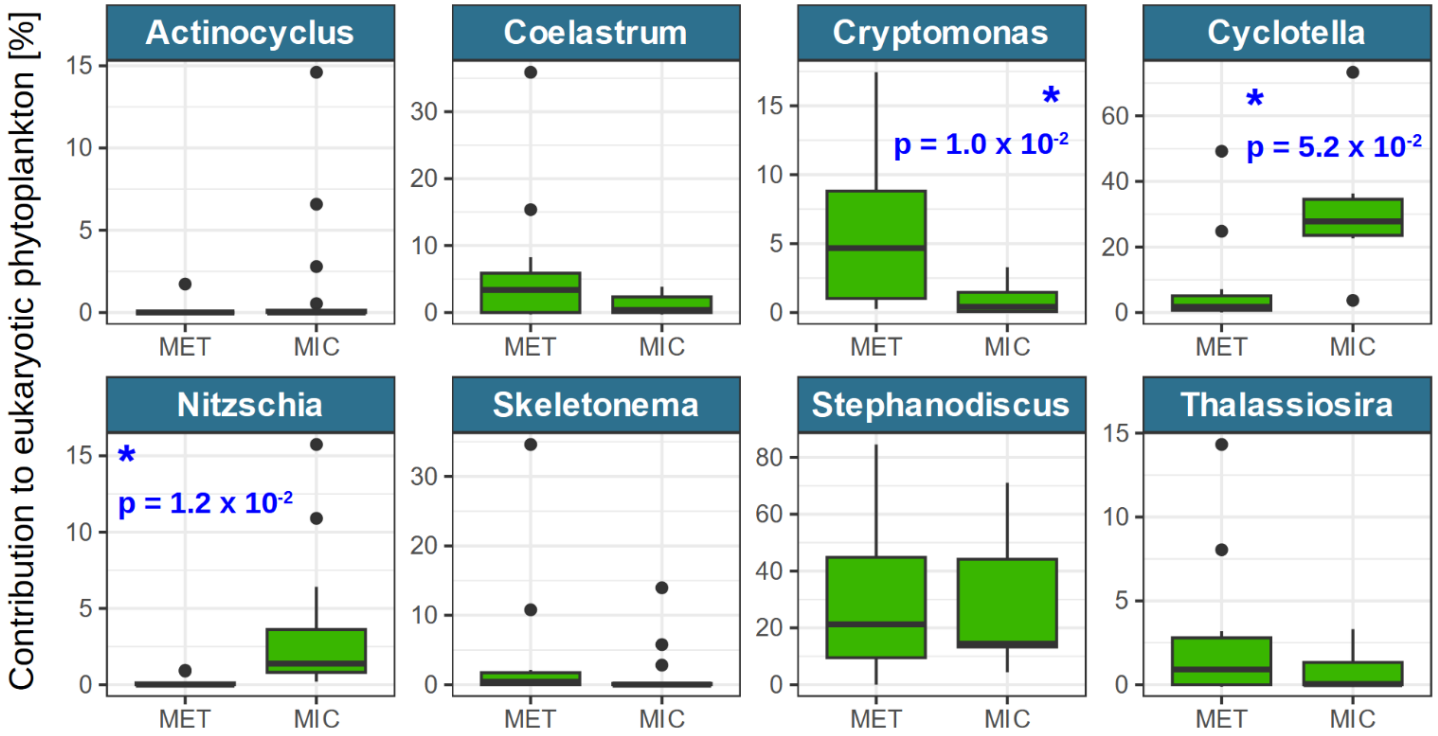

Fig. S2.9b: Contributions of key genera to the eukaryotic phytoplankton communities based on metabarcoding reads (MET) and microscopy biovolumes (MIC) (NLWKN 2023, HU 2023) across seasons (tab. S2.1) and stations in the upper to mid area (586 – 651 km). *Actinoptychus*, *Aulacoseira*, *Cyclostephanos*, *Thalassiocyclus*, *Triceratium*, *Minidiscus* and *Mychonastes* only appear either in microscopy or metabarcoding and are hence not included. Note that the comparability is affected by actual ecological differences between the samples (different sampling time points and stations; tab. S2.1, fig. 2.1). * indicate significant differences between the results of the two methods based on a t-test ($p \leq 0.05$). Note that data from 646 km in 2021 and from 651 km in winter 2022 are not included because data from the respective comparative station (i.e. 651 km in 2021 and 646 in winter 2022) are missing.

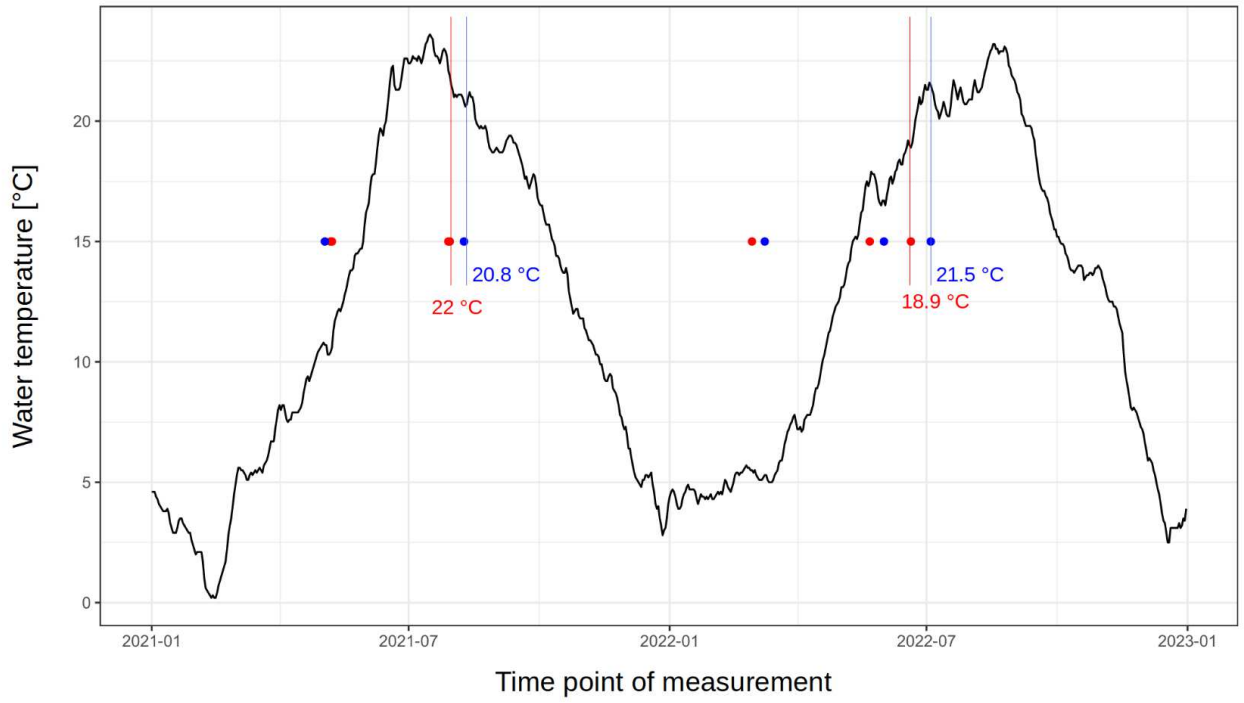

Fig. S2.10: Average daily water temperatures (°C) at the station Grauerort (ca. 661 km) in the Elbe river based on data from the FGG Elbe database from 2021 – 2022 (FGG Elbe, 2024). Red dots show the sampling dates of this study at a random vertical height. Blue dots show the respective sampling dates from the comparative monitoring dataset used in this study. The notes/ vertical lines exemplary show the temperature differences between the metabarcoding and monitoring samplings in summer 2021 and summer 2022. Temperature was particularly different in summer 2022 (18.9 °C vs. 21.5 °C) which might explain part of the differences found in terms of phytoplankton community composition.

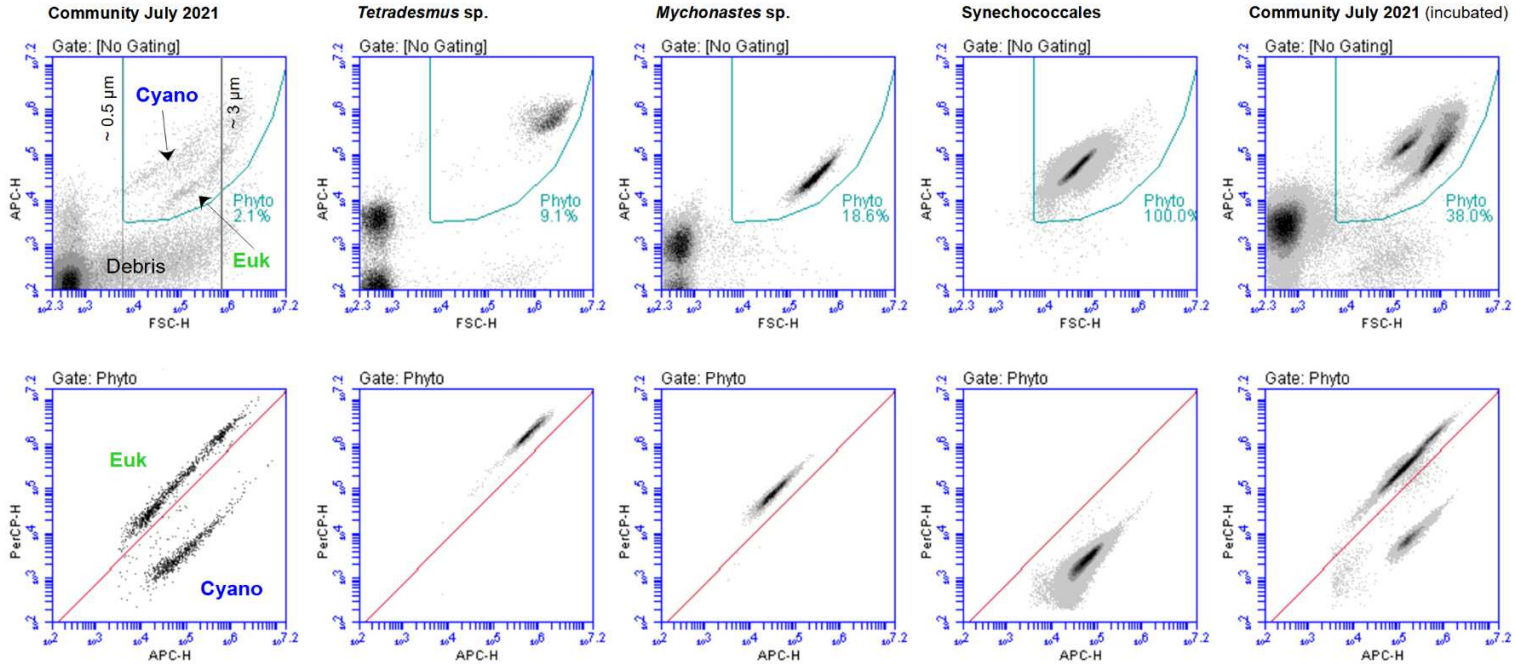

Fig. S3.1: Cytogram examples of communities and single strains of phytoplankton isolated from the Elbe estuary. We used approximately 40 different samples (isolated taxa and laboratory incubated communities) from the Elbe estuary to determine the borders between phytoplankton and other suspended matter (e.g. bacteria, debris) and between eukaryotes and phycocyanin-rich cyanobacteria based on the flow cytometric properties. The gating of phytoplankton (phyto; upper panels) was based on forward scatter (FSC ; ~ size) and APC (allophycocyanin fluorescence; red fluorescence, filter 675 nm, laser 640 nm). Here we also set a lower size border of around 0.5 µm which was proxied in between the FSC values of 0.12 and 1 µm beads. The gating of eukaryotes (euk) and cyanobacteria (cyano) (lower panels) was done based on the ratio of APC and PerCP (peridinin-chlorophyll-protein complex fluorescence; red fluorescence, filter 670 nm, laser 488 nm). Lastly, we defined the picophytoplankton threshold based on 3 µm beads.

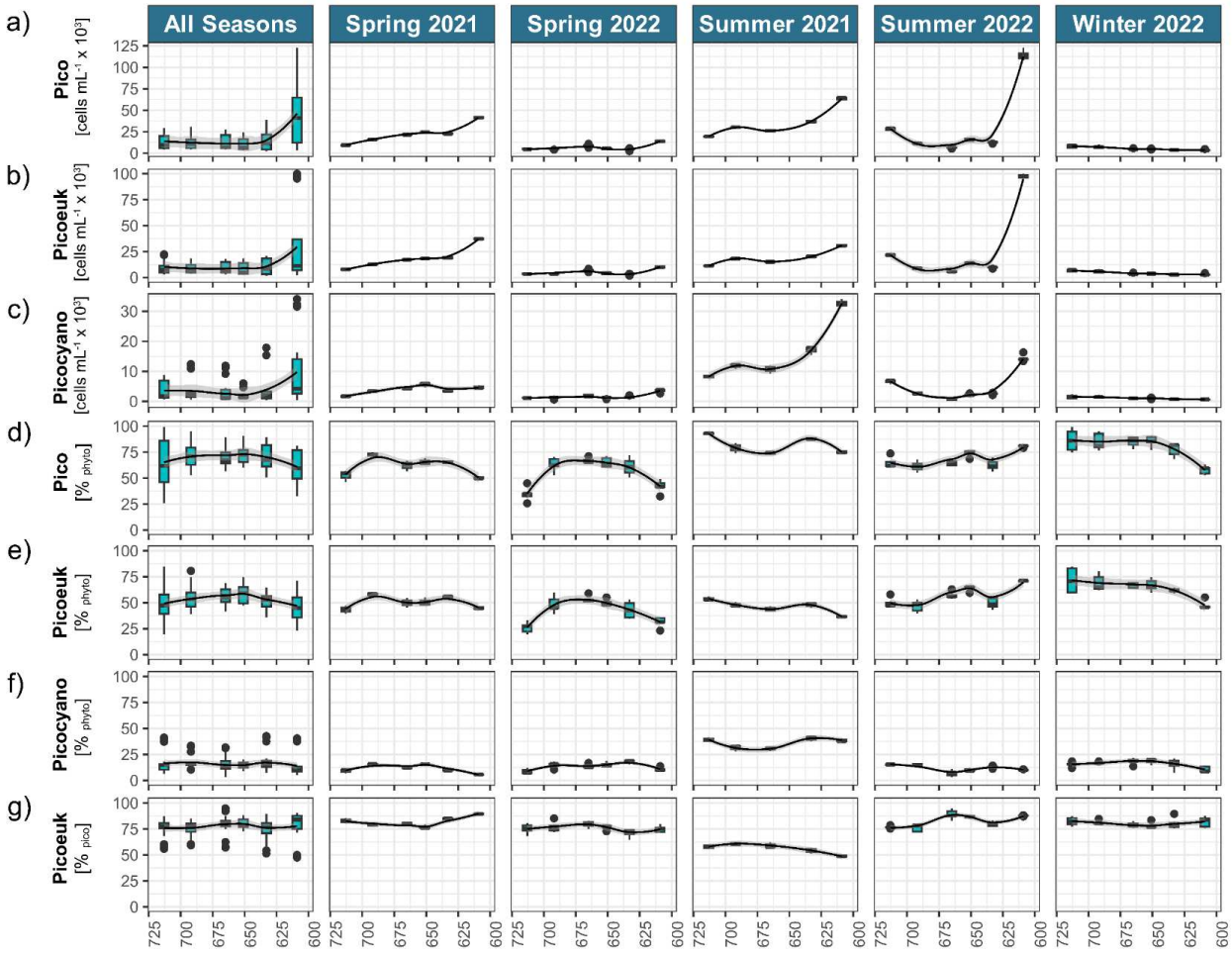

Fig. S3.2: Spatial distribution of different picophytoplankton groups along different stations (stream km; fig. 3.1) and different seasons. Contributions of cyanobacteria to picophytoplankton can be obtained from c) ("picocyanobacteria = 1 - picoeukaryotes"). Regression lines were added with geom_smooth() from ggplot2 and the method "loess" as visual support. For clarity we use the following abbreviations: Pico = picophytoplankton, picoeuk = picoeukaryotes, phyto = phytoplankton. Note that 651 km was not sampled in July 2021.

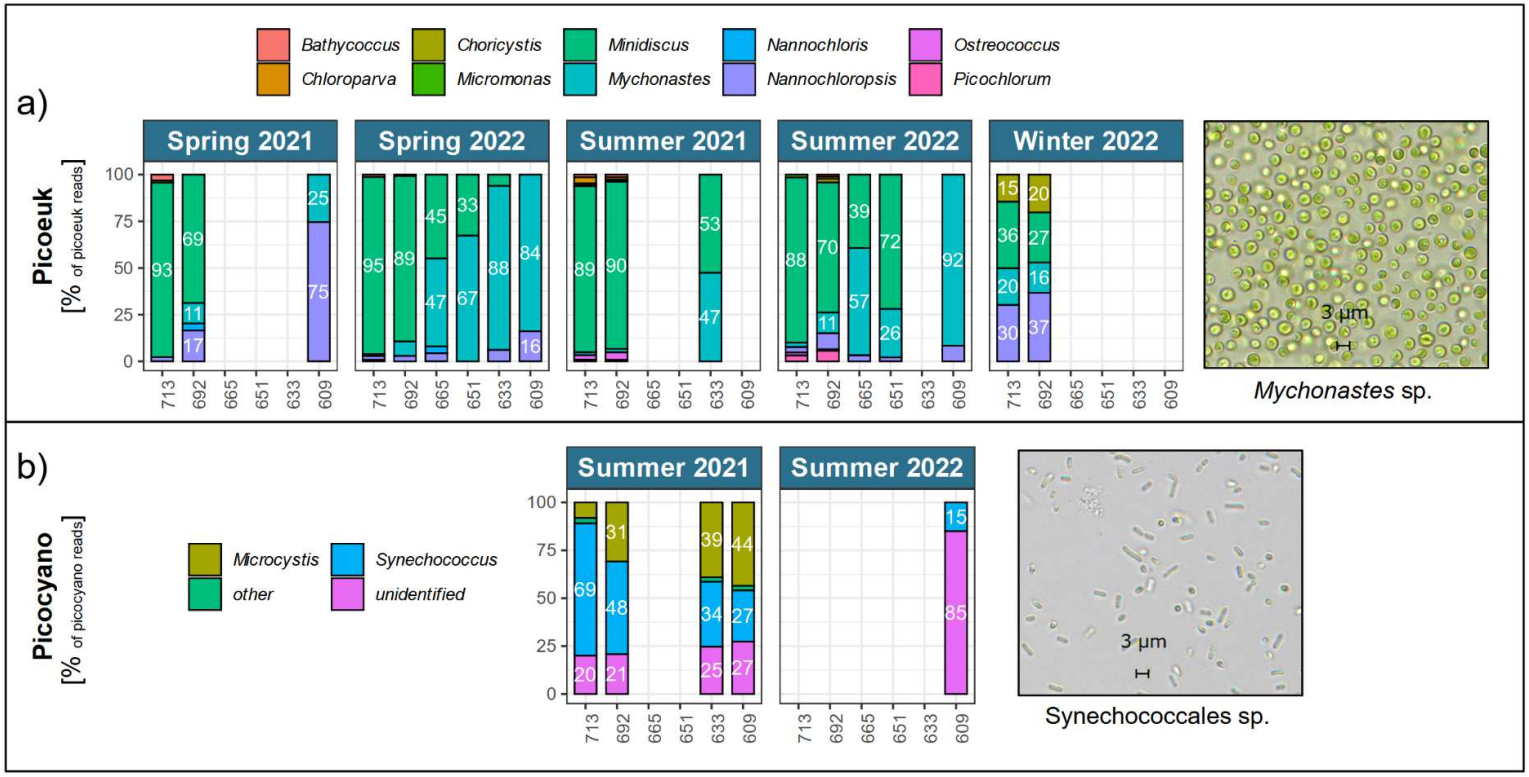

Fig. S3.3: Spatial contributions of picoeukaryote genera to picoeukaryote 18S rRNA reads (a) and picocyanobacteria genera to picocyanobacteria 16S rRNA reads (b). Labels are shown where contribution was at least 10 %. Station is used as a factor (i.e. bars have the same distance independent of the actual location). Note that in each a) and b) we selected different taxa that *can* be or are *usually* understood as picophytoplankton (< 3 µm). Cells of these taxa however *can* sometimes be larger than 3 µm or form colonies and some unidentified cyanobacteria might not be < 3 µm. Moreover, the number of reads can depend on cell size (Godhe et al., 2008). Hence, the selection in this plot does not necessarily accurately represent the picophytoplankton obtained from flow cytometry, where the definition is based on their actual cell size and abundance (see also fig. 3.1b). Where bars are missing - or in case of picocyanobacteria even complete panels - metabarcoding was either not carried out (651 - 665 km in 2021) or data was removed due to low number of picocyanobacteria or picoeukaryotes reads (< 100) (all other cases). Photos show examples of picophytoplankton strains isolated from the Elbe estuary (Martens et al., 2024a). For clarity we use the following abbreviations: Picocyano = picocyanobacteria, picoeuk = picoeukaroytes.

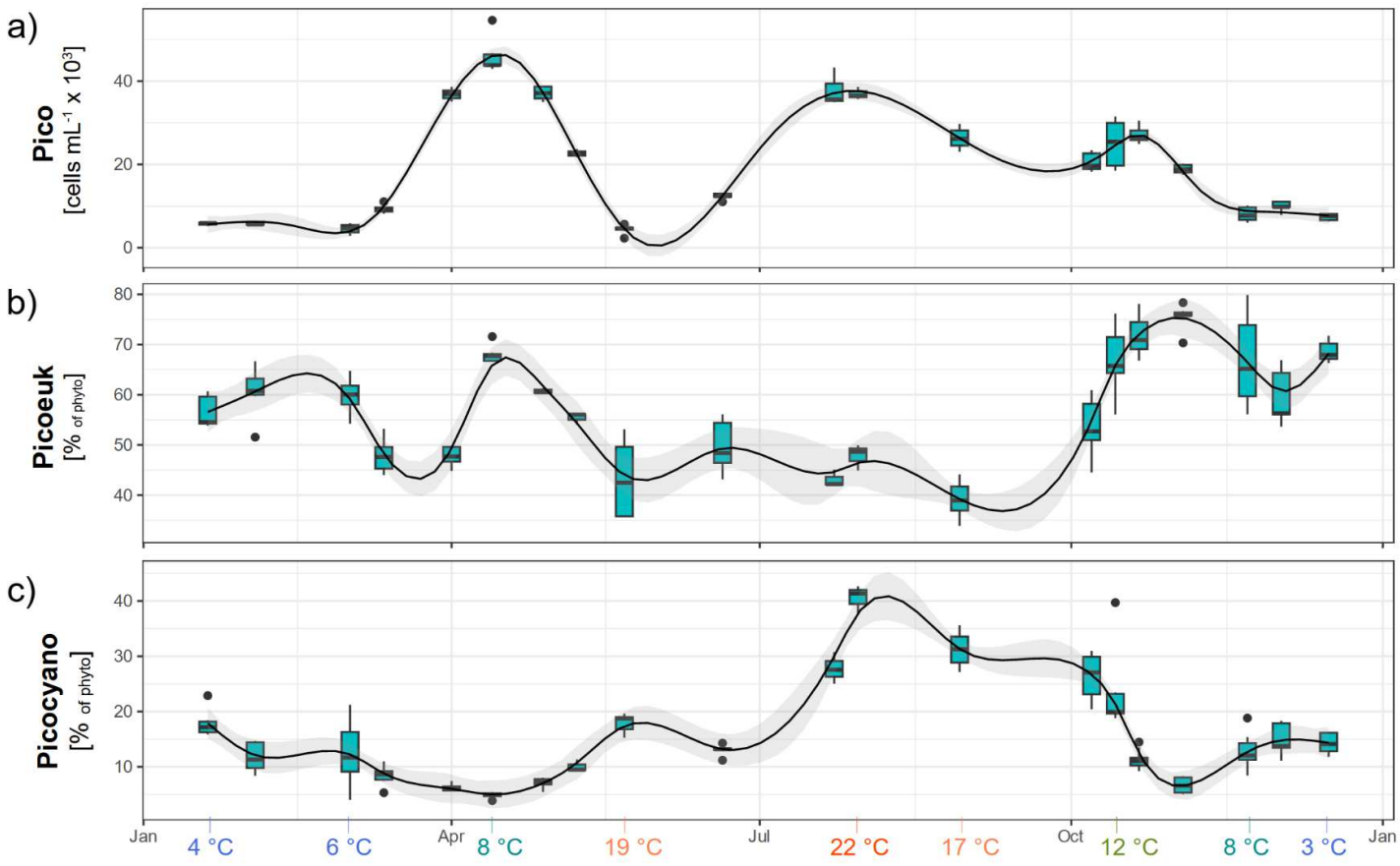

Fig. S3.4: Seasonal distribution of different picophytoplankton groups in the area around Hamburg (approx. 623 - 633 km). Horizontal scales show the sampling date independent of the year, i.e. day of the month. Data was merged when sampling was carried out < 5 days apart. Contributions of cyanobacteria to picophytoplankton can be obtained from the picoeukaryotes contribution in c) ("picocyanobacteria = 1 - picoeukaryotes"). Regression lines were added with geom_smooth() from ggplot2 and the method "gam" (see also tab. S3.3). For clarity we use the following abbreviations: Pico = picophytoplankton, picoeuk = eukaryotes, phyto = phytoplankton. On the bottom we show the temperatures at certain time points (see further details in fig. S3.6).

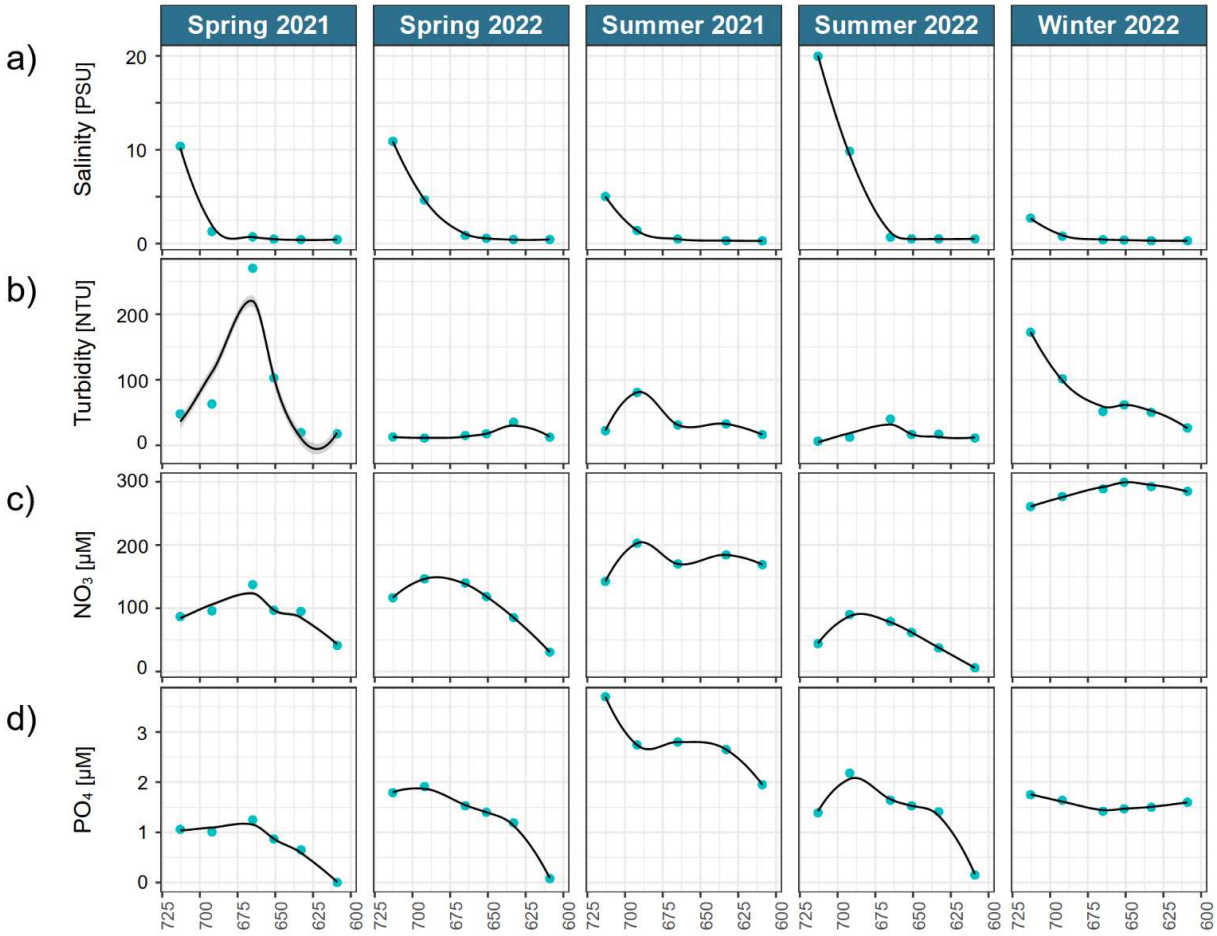

Fig. S3.5: Abiotic conditions at the different stations and seasons of the spatial dataset. Regression lines were added with geom_smooth() from ggplot2 and the method "loess" as visual support. Note that one missing value of turbidity on 2021-07-29 (summer 2021) at 609 km was replaced by a value from 2021-07-26 at 609 km.

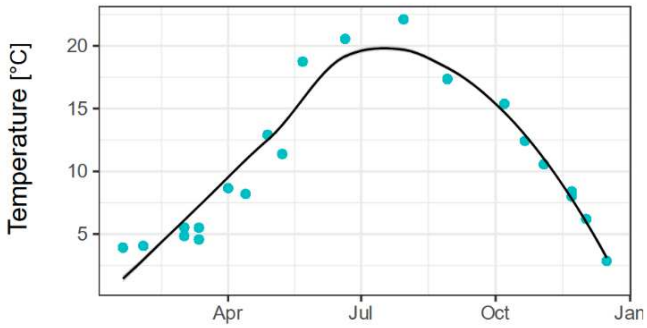

Fig. S3.6: Water temperature along seasons in the seasonal dataset. Regression line was added with geom_smooth() from ggplot2 and the method "loess" as visual support.

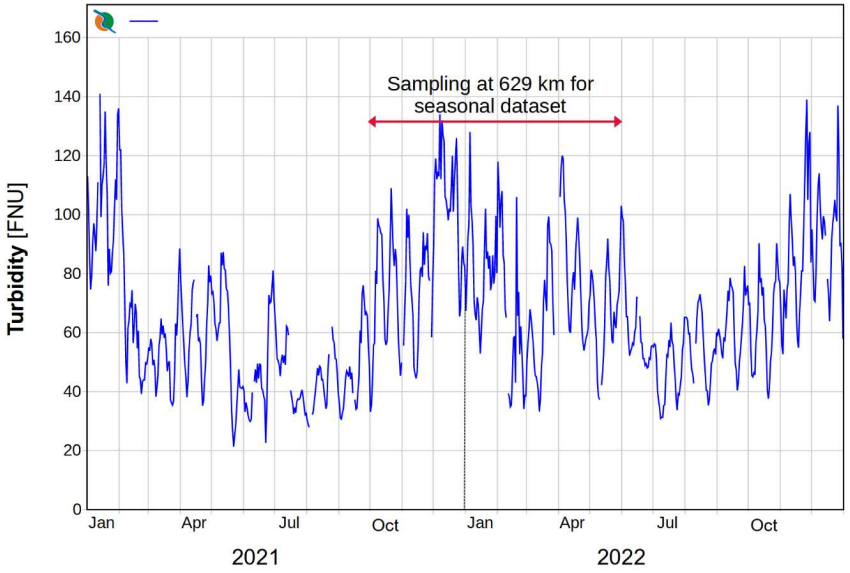

Fig. S3.7: Average daily turbidity (FNU) at the station Seemannshöft (ca. 629 km) in the Elbe estuary based on data from the FGG Elbe database from 2021 - 2022 (FGG Elbe, 2024). Figure was obtained directly from the FGG database, but modified by removing German texts.

Fig. S4.1.1-S4.1.24: Cell counts of different strains after 24 h exposure to organic compounds in the EcoPlates™ under different light conditions. Please find this supplementary material online, published with the publication https://doi.org/10.1098/rspb.2023.2713 (there named fig. S1.1-S1.24).

Fig. S4.2: Casual tracking of cell counts of different strain cultures used for the EcoPlates™. Please find this supplementary material online, published with the publication https://doi.org/10.1098/rspb.2023.2713 (there named fig. S2).

Fig. S4.3.1-S4.3.10: Number of significantly positive and negative effects across strain densities and further detailed information about the respective results of selected strains. Please find this supplementary material online, published with the publication https://doi.org/10.1098/rspb.2023.2713 (there named fig. S3.1-S3.10).